CHARACTERISTICS AND POTENTIAL OF ANTRIM SHALE FOR IN SITU ENERGY PRODUCTION

BY

MOHAMMED SAID ABUBAKR

A DISSERTATION

Submitted To
Michigan State University
In Partial Fulfillment Of The Requirements
For The Degree Of

DOCTOR OF PHILOSOPHY

Department of Chemical Engineering

1982

ABSTRACT

CHARACTERISTICS AND POTENTIAL OF ANTRIM SHALE
FOR IN SITU ENERGY PRODUCTION

By

Mohammed Said Abubakr

Antrim shale contains energy more than 1000 times the annual petroleum production of the United States.

Recovery of this energy involves heating the shale to 900°F at which temperature combustible material is evolved. This may be accomplished either aboveground after mining or underground. At 1500 feet depth, mining would be expensive, and true in situ processing would be advantageous if economically feasible.

A mathematical model was studied based on heat conduction into the formation from a hot well fueled by effluent gas and air. The model showed that the net energy production does not justify the process economically. Improvements on this model by higher temperature driving force for conduction, and by making a larger surface area accessible to combustion zone were investigated. Another mechanism considered was diffusion or forcing of air into the rock, followed by combustion of residual carbon deposited within the spent shale.

Laboratory experiments simulating in situ energy production under a variety of conditions were performed to investigate these possibilities.

Experiments showed that when shale is heated to about 1800°F glazing occurs blocking gas flow in or out of the rock.

The compressibility of retorted shale, containing porosity of 20%, was only 1.6%. Thus the porosity formed is of little use in producing space or fractures.

The opening of horizontal cracks during retorting under atmospheric pressure provided an important mechanism for the release of organic matter and the penetration of air into them. This was evident by the disappearance of carbonaceous residue along the cracks' surface. However, experiments performed under simulated overburden pressure showed no cracks and, therefore, this mechanism would be eliminated for true in situ energy production from Antrim.

In situ energy production from Antrim utilizing heat transfer is therefore not economically feasible. To make it feasible, an entirely different mechanism has to be found.

In situ energy production from other richer shales may be economically feasible if they occur at shallow depths, and produce more porous and compressible spent shale.

ACKNOWLEDGMENT

I wish to express my deepest appreciation for the assistance, guidance, encouragement and caring of my dissertation advisor, Professor Carl Cooper. Working under the supervision of Professor Cooper taught me not only about engineering and science, but also about life and friendship.

Furthermore, I would like to thank the members of my guidance committee: Dr. Charles Petty, Dr. Bruce Wilkinson, and Dr. Charles St. Clair. A special thanks to Dr. Donald Anderson, Chairman of the Chemical Engineering Department for the opportunity to teach in the department.

Appreciation is extended to Yormouk University of Jordan for the scholarship which enabled me to carry out my education.

I am also grateful to Don Child and co-workers from the machine shop for the construction of my equipment.

Finally, I would like to thank my family and friends for their moral support.

To my mother, Um-Maher,

who dedicated her life to her children.

TABLE OF CONTENTS

LIST OF TABLES

LIST OF FIGURES

CHAPTER ONE

INTRODUCTION

Nature of shale

Shale is rock formed through geologic ages by consolidation under pressure of silt, mud, or clay deposited in ancient streams, lakes or other marine environments. Most shale therefore contains some organic matter formed from the remains of the minute plant and animal life which made up the plankton of these environments (110). Shales vary widely in the quantity and in the chemical form of this organic content (35, 78, 80).

In general it contains carbon and hydrogen plus some oxygen and other elements, with the atomic ratio of hydrogen to carbon somewhere between 1 and 2 (57, 98). The compounds present are of very high molecular weight and are therefore non-volatile, as might be expected considering their retention in the rock over millions of years. When heated to temperatures in the range of 550^{o} to 1150^{o}F, however, these high molecular weight compounds crack and produce gas, condensible vapors, and carbonaceous residue (39).

Kerogen (i.e., wax forming) is the name generally given to the macromolecular mixture of organics which, on heating, yields these predominantly hydrocarbon products. The process of heating shale, decomposing its kerogen content, and distilling over a liquid product, is generally referred to as retorting. The liquid produced is called

shale oil. Shales which produce significant quantities of shale oil are called oil shales. It should be noted again at this point that kerogen is neither a single chemical compound nor is it a mixture of well-defined and well characterized compounds. Rather it is a highly variable mixture of transformed residues (80).

Origin and distribution of fossil fuels

Both the oxygen in the earth's atmosphere and the fossil carbon in the earth's crust were formed from carbon dioxide in ages past by the same photosynthetic biological processes. The stoichiometric equivalence between these quantities suggests a total world fossil fuel supply equivalent to 500 trillion tons carbon or 2900 trillion barrels of petroleum (See Appendix C). A large fraction of this total fossil carbon is believed to be in the form of shale kerogen. Michigan's Antrim shale alone is believed to contain about a trillion tons of fossil carbon which according to Leffert (45) could yield over three trillion barrels of Fischer assayable shale oil. Duncan and Swanson estimated a worldwide resource of 2100 trillion barrels of shale oil. Of this, they estimate that less than 10% is recoverable (23).

Another large fraction of the world's fossil carbon supply is in the form of coal, which has been formed by the consolidation of ancient trees, plants, and other vegetation. Petroleum represents only a small fraction of the world's fossil carbon. It is believed to have been formed by shale kerogen decomposition with the resulting liquid migrating into the pores of adjacent sandstone formations. Natural gas represents a similarly small fraction of our total fossil carbon, with much smaller fractions represented by tar sands, asphalt beds, and so on.

The relative economic importance of petroleum and natural gas among fossil fuels is due to their ease of production from the ground, ease of refining, and ease of conversion to useful products. Coal, as a solid, requires more mechanical effort than petroleum to remove it from the ground, and more complex equipment and effort to utilize it. Shale, like coal, is a solid, and its mining requires considerable mechanical effort. In addition it contains much more inorganic matter than coal, produces much less energy per ton mined, and presents far greater problems in disposing of the residue. The cost of mining shale per ton should be no less in money, machinery, energy, and manpower than the cost of mining coal. Yet the energy content of a ton of shale is typically only 10 to 20% the energy content of a ton of coal.

In situ production

The problems of handling and disposing of solids might be eliminated if shale retorting or coal conversion could be carried out underground, with the production above ground of only the gas and liquid products of the underground reactions. Energy produced in this manner is called production in situ (i.e., in place). Although the costs associated with solids handling are reduced, such processes have serious drawbacks related to our relative inability to monitor and control the process underground. Also these processes can be quite inefficient and the energy needed to make them work can represent a very high proportion of the energy recovered.

Perhaps the most serious problem of in situ production relates to the structure and permeability of the solid before, during, and after the process. Veins of relatively pure coal can burn away leaving holes into which the overburden can collapse in an unpredictable manner. With

shale however, the structural strength of the bed is typically not as drastically altered by retorting. However, this high strength is usually accompanied by low permeabiity which prevents gases and liquids from moving readily through the formation.

The ideal structure for in situ production would involve a coarse sandstone-like structure with both high permeability and high mechanical strength. Efforts have been made to mine a portion of the shale mechanically (about 20%), and rubblize the remainder of the bed with explosives, followed by retorting in situ. These combination processes are called modified in situ processes, in contradistinction to true in situ processes, in which mechanical mining, external retorting, and solids disposal are completely eliminated.

A sporadic industry

Rocks from organic-rich shale outcroppings have no doubt been used to fuel human kind fires since earliest times. The discovery that the evolved vapors could be condensed to liquid on cold surfaces must be nearly as old. When the Drake well came in at Titusville, Pennsylvania in 1859, there were already small shale oil plants in the United States and elsewhere in the world producing burning and lubricating oils as well as waxes in competition with products from coal, from vegetable oils, and from animal fats.

After the Drake discovery the petroleum industry developed very quickly, and the ready availability from that source of large quantities of all the products of oil shale quickly put the shale oil industry out of business. Shale oil production cannot compete economically in a free market where there is an abundant supply of petroleum. The cost per barrel of drilling a productive oil well and flowing or pumping

petroleum from the ground is only a fraction of the cost per barrel of mining shale, retorting it, and disposing of the residue.

Interest in shale oil during the past hundred years therefore has been sporadic, and a viable industry has existed only in isolated locations or in special situations where the cutoff of a nation's petroleum has either occurred or was threatened. In the United States there was a surge of oil shale activity during World War I, and again during World War II (86). In each case proponents of shale as a source of energy sought and obtained substantial government subsidies to build the industry. In each case active interest declined rapidly when the industry had to face the realities of economics and engineering problems in the absence of continued subsidy.

Recent activity in oil shale

The current surge of interest in U.S. oil shale is related not so much to the threat of war and blockade as it is to the monopolistic pricing policies of those who control our petroleum supplies. Investing in shale oil production facilities to compete with monopolistically priced petroleum is a hazardous enterprise for a private company. If the petroleum supplier cuts his profit margin by a small percentage, the shale oil supplier's profit can be completely eliminated. Where government policy seeks the establishment of a shale industry, it is up to government to provide the incentives needed to encourage private industry participation.

The generosity of the United States government during the past eight years has reached an all time high in providing subsidies aimed at developing a viable oil shale industry. These have taken the form of supporting research at academic and governmental institutions, awarding

contracts to design, construct and operate field and pilot plant installations, and supporting industrial oil shale enterprises with sales contracts and government guaranteed loans at the multibillion dollar level. During the past six months, however, it has become apparent that we are once more in a period of rapid decline in oil shale activity. The recent news item (See Appendix D), "Oil Shale Fiasco: The Death Knell for Synfuels?" (U.S. News and World Report 5-17-82) summarizes some current developments in the Western U.S. shale activities.

Although all the factors involved in these on-and-off decisions on oil shale are not clear at this time, it is apparent that they can be very costly to government and perhaps also to industry. Furthermore, one of these factors is certainly the economic potential of shale as a source of energy, and any contribution to our knowledge in this respect should result in better decision making.

Research Objectives

While the largest recent activities in oil shale involved Western shale, this thesis is principally a study of the potentialities of Michigan Antrim shale. The largest government subsidized contract in this respect was DOE contract 2346 awarded to Dow Chemical Company principally for field tests on in situ production of energy from the shale. The award was for approximately 14 million dollars and the contract was terminated after this amount was spent.

This investigation was begun in 1978 during the period in which the Dow field tests were in progress. The objective was to conduct bench scale simulations of in situ energy production for Antrim shale and to use the result with suitable modeling to determine the

feasibility of such a process. It was hoped at first that positive results would be obtained and that these would contribute to the development of an important industry. It was also recognized from the first that negative results could also be important in calling for different directions of attack in future work on Antrim shale development. Finally it was felt that the work might demonstrate that government sponsorship of continuing low cost investigations of this type could be a valuable tool in making sound decisions on the sponsorship of multimillion dollar projects.

A conclusion that the Dow field tests would not lead to a viable energy production process was reached by this investigation long before DOE decided to discontinue the project. Furthermore reaching this conclusion did not require any information resulting from the government's 14 million dollar expenditure. Descriptions of the experimentation and of the calculations involved are included as part of the thesis which follows.

CHAPTER TWO

THEORETICAL ANALYSIS

PART A. ANALYSIS OF ECONOMIC FEASIBILITY

Establishing the economic feasibility of in situ production of energy from Antrim shale is a task of considerable magnitude. Nothing less than an operating pilot plant or semi-commercial plant would be needed to establish such feasibility. On the other hand, if there is a lack of economic feasibility, it is much easier to establish that such a lack exists. The benefit to society of establishing a lack of feasibility is significant since it can be used by government to avoid some of its very considerable expenditures on energy development and to direct these expenditures into more fruitful channels.

The reasoning developed in this thesis to demonstrate the lack of feasibility for the in situ productin of energy from Antrim shale is as follows:

(1) A model for in situ production of energy from Antrim shale is chosen.

(2) Using this model along with certain simplifying assumptions, the net energy output is found not to justify the investment and operating cost.

(3) The model chosen is analyzed and shown to give a more favorable economic picture than other reasonably realistic models.

(4) Each of the simplifying assumptions is analyzed and shown to give a more favorable economic picture than actual production conditions.

The arguments developed above are based on mathematical analysis, on data obtained from the extensive literature on oil shale, and on the results of experimental work performed as part of the current research.

1. The model

The model chosen for this thesis consists of a single well drilled through 1500 feet of overburden and then through 200 feet of Antrim shale. The Antrim part of the hole is one foot in diameter and a fire is maintained in that 200 feet height by burning the gases and vapors evolved from the shale with air. The air is introduced through a central distributor with its rate, distribution and preheat temperature controlled to give a constant temperature at the wall of 1750^{o}F.

Heat penetrates into the formation from the cylindrical central cavity in a radial direction. Gases and vapors are evolved from the rock when it reaches retorting temperature. A portion of these are burned in the cavity to maintain the desired temperature. The rest are removed from the cavity at the top and are burned with additional air to produce flue gases to be used for power generation or some other beneficial purpose.

2. Energy output

The total energy output from the well during its useful life is calculated using the following simplistic assumptions:

(a) Ignition is instantaneous giving a constant wall temperature at all points and lasting as long as a net production is obtained.

(b) The wall temperature is 1750^{o}F.

(c) Heat transfer to the formation is by thermal conduction only.

(d) Heat capacity of the formation is constant at 0.3 Btu/lb^{o}F, density at 145 lb/ft^{3}, and thermal conductivity at 1.0 Btu/ft^{o}F hr.

(e) Retorting reaction of the shale is instantaneous when its temperature reaches 900^{o}F.

(f) Gases evolved have a high heating value of 1000 Btu per pound of shale.

(g) The value of the gases produced is $3 per million Btu.

The value for the total net energy production from the well as obtained in this manner is less than 10 million Btu, as shown in Table 2-3 and Figure 2-4 in this thesis. The total value of this energy is only $30. By comparison, the cost of drilling the well will be no less than $100,000.* The fact that the total return is less than 1/3000 of the investment makes it clear that in situ production of energy from Antrim shale will not pay unless the central cavity model proves to be an unrealistically pessimistic one.

---

* Cost per foot for drilling is given as $67.7 by IPAA (42).

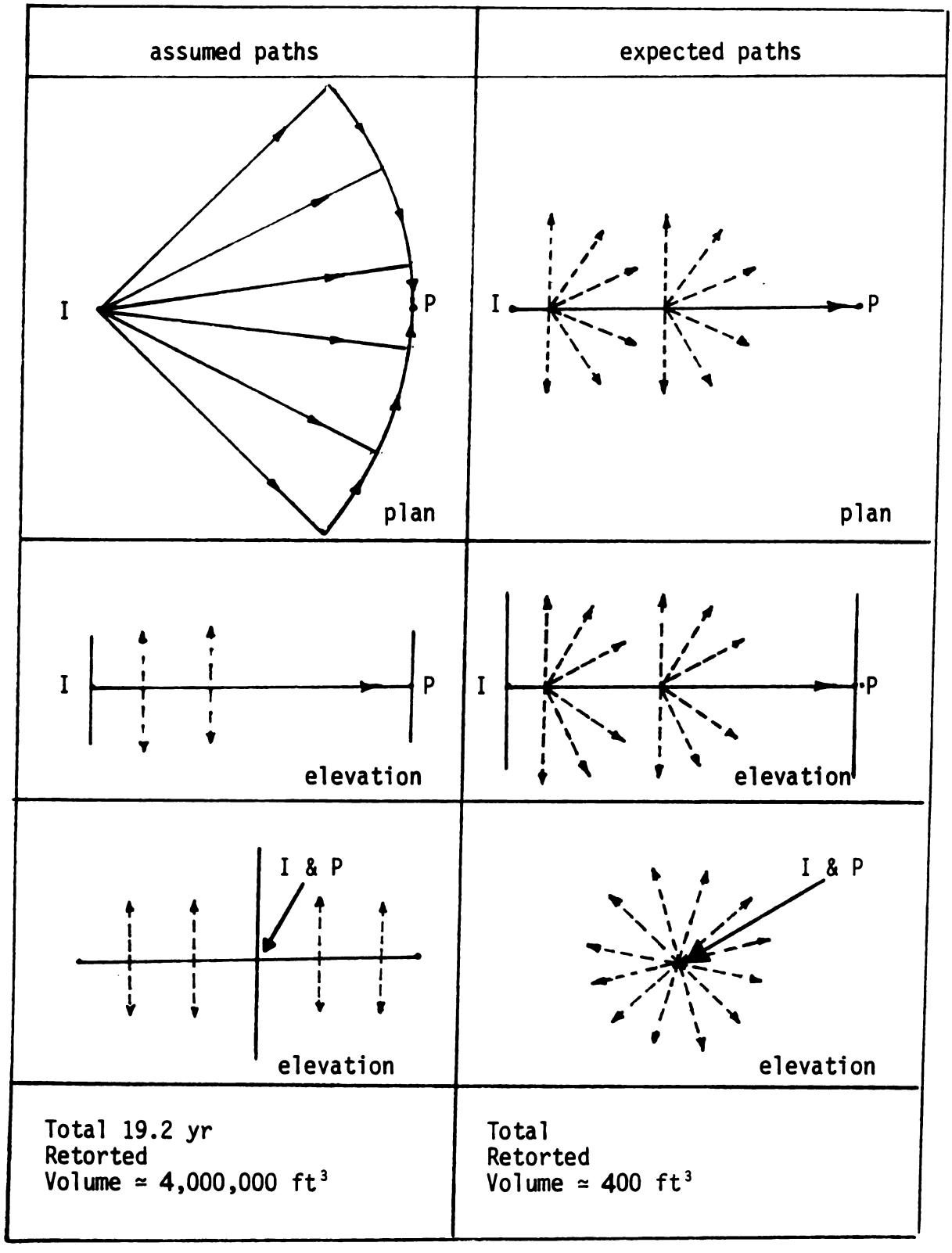

Figure 2-1. Thomas model (99). Assumed fluid (⟶) and heat (--→) paths from Injection to Production well. Also expected ones.

3. Comparison with reality and other models

The central cavity model was chosen as one giving a more optimistic economic picture than any reasonably expected real situation. It is, however, possible to hypothesize some unrealistic models which would give economic pictures which are much more optimistic even than the central cavity model.

The model proposed by Thomas (99) utilizes one injection well surrounded by four production wells to retort over a period of 19.2 years a body of rock 180 feet high with circular cross section reaching a maximum diameter of 200 feet at its mid-plane. The net energy production predicted with such a model for Antrim shale would be 250,000 million Btu or 50,000 million Btu per well. At $3 per million Btu, this comes to $150,000 per well which might possibly cover the cost of drilling it, outfitting it, and operating it for 19.2 years.

However, the model of Thomas includes some very unattainable assumptions. These include heating to 2000°F a horizontal crack intersecting all 5 wells. The temperature in the crack is assumed to be a step function beginning at the center well and proceeding outward until the 2000°F temperature covers the area enclosed by a circle through the other four wells. The contour of the crack between the injection well and any production well would then have to be such as to distribute the hot gas injected uniformly over the plan area shown in Figure 2-1. The possibility of producing such a crack by explosive fracturing is extremely remote and the model cannot, therefore, be considered realistic. More likely the hot gas would flow essentially in a straight line from injection well to production well and give a small heated zone.

Another unrealistic assumption of the Thomas model is that heat flows through the formation only in the vertical direction. The effect of such an assumption is illustrated in Figure 2-5, which shows the effect of heat flow direction on the energy input-output relation for Antrim shale. With both radial flow in spherical geometry and radial flow in cylindrical geometry there is a limit to the rock penetration at which a net energy production can be obtained. Thus, the 90 foot penetration calculated by Thomas was possible only by assuming liner geometry. With spherical or cylindrical geometry, penetration would have been less than one foot. Heat from a hot spot would normally be expected to flow in a spherical radial direction, and from a heated line to flow in a cylindrical radial direction. Linear flow from the area shown in Figure 2-1 could be expected only if the entire area could be held at a uniform high temperature throughout the time of operation. Thomas did not postulate such a condition in his model, and if postulated, it could not be achieved in an explosively generated crack.

Lesser and Stone (49) presented a modification of the model of Thomas which uses 1000^{o}F steam presumably because a condensing fluid moves through the formation in the direction of lower temperature rather than lower pressure. The steam is introduced along a horizontal line in the formation but how this is accomplished is not explained. For very rapid steam injection, heat flow aproaches linearity but for slow rates cylindrical radial flow is approximated. Since steam will not condense above 705^{o}F a retorting temperature of 900^{o}F can be obtained only by using the small amount of superheat in the steam. Also, as Figure 2-9 shows the net energy recoverable from Antrim shale vanishes for surface temperatures below 920^{o}F.

The models of Tyner and Hammert (106) and of Crowl and Piccirelli (18) are more sophisticated models that allow for a variety of effects, such as the kinetics of kerogen pyrolysis, of inorganic carbonate decomposition, and of gaseous combustion of hydrogen, CO, and methane. Also included is the pressure gradient resulting from diffusion of kerogen pyrolysis products through the rock. The most unrealistic assumption involved in their model is that the region between injection well and production well behaves like a packed bed. Rubblized beds of shale for which this type of model was originally designed are normally considered to require 20 percent void volume as produced in the modified in situ process by some form of conventional mining.

With Antrim shale about 20 percent void volume is produced by kerogen disappearance during retorting. However, as explained in Chapter Four, under C-3.4, these voids are very small in diameter, they do not contribute appreciably to permeability, and they are not compressible in a way that could be used for rubblization. The use of these later models assumes, therefore, that such bed behavior may be obtained by explosive fracturing of the formation to produce a network of cracks with close spacing and of widths distributed to permit combustion of gases and distribution of temperature as desired. The likelihood of such a lucky explosion seems very remote, especially under overburden pressure where the cracks must not only be opened but maintained open by smaller rocks of the right size falling into the cracks.

Furthermore, the volume of such a fortuitously created effectual packed bed of Antrim shale would have to be 500,000 cubic feet or more

in order to justify just the drilling cost for the production and injection wells. Also, based on the minimum crack spacing given by Tyner (106), the new surface area created would have to be more than a million square feet. By contrast, under DOE contract 2346 for which the models of Crowl and Piccirelli were developed, the best communication actually obtained between wells was a crack 60x40 feet having a width calculated in Appendix E to be about 0.005 cm.

The central cavity model, on the other hand, is achievable by predictable techniques. The hole can be drilled and the proper distribution and controls set up. Dow Chemical Company in their field tests under DOE contract 2346 did drill and test a similar well (41), but did not keep the entire surface of the cavity hot as the present model.

The central cavity model gives much more hot surface area than an injection-well production-well set up in which the burning front moves in a straight line between the wells. This is particularly true for Antrim shale where the formation is 200 feet deep and the distance between communicating wells in the field tests was typically 40 feet and sometimes as low as 15 feet. The central cavity model assumes cylindrical radial heat flow, while a progressive retorting front movement between wells will typically involve a considerable amount of spherical radial heat flow. Thus, while the central cavity model is not economically advantageous, it is more advantageous than other reasonably achievable models.

4. Analysis of assumptions

It is now necessary to examine the simplifying assumptions used in the central cavity model and show that they give a more favorable economic picture than would an actual central cavity operation.

(a) Instantaneous ignition is assumed with operation continuing until energy input is equal to output. Easy ignition is a very optimistic assumption. Dow, for example, had great difficulties achieving ignition in their field test (112). Dow used 6,250 pounds of coal and 3,165 pounds of charcoal (41) to accomplish ignition at the bottom of their well. Also, the model ignores the energy required for air compression. Thus, energy input will equal energy output sooner than calculated.

(b) The assumption of a wall temperature of 1750^{o}F gives more retorting per Btu input than much lower temperatures (See Figure 2-9). Appreciably higher temperatures in Antrim shale are not practical because of the tendency toward glazing. Experiments conducted as a part of this thesis show that at temperatures around 1800^{o}F glazing of the shale can occur, sealing off the evolution of product gases and vapors. (See Chapter Four, C-5).

(c) Heat transfer to the formation is by conduction only. Other mechanisms for supplying heat to the formation are considered in this thesis. One of them is penetration of hot gases through horizontal cracks formed during retorting, but as shown in Chapter Four, C-4 of this thesis, such cracks do not occur under overburden pressure. Another mechanism, involving diffusion of oxygen into cracks followed by combustion of residual carbon, as described in Chapter Four, G-3, also does not occur in the presence of overburden pressure. The absence of oxygen diffusion as a contributing mechanism is further supported by the diffusion calculations given in Appendix G.

(d) An effective heat capacity for Antrim shale is plotted as a function of temperature in Figure 2-8. Values were calculated taking

into account heat capacities of the inorganic and organic components of the shale given in Figure 2-7, and the loss of organics during retorting as given in Figure 2-6. These calculations are explained more fully in Part D. It may be seen that the average value over the range of 572 to 1750^{o}F is 0.315 and the value used of 0.3 Btu/lb^{o}F is optimistically low. It may also be seen that the effective heat capacity is remarkably constant considering that it includes the heat of retorting.

The rock density is taken as 145 lbs original shale weight per cubic foot which is the value measured by Musser (68). It corresponds closely to the measurements of Table 4-1.

The value of the thermal conductivity cancels out in the calculation of energy input per pound of shale retorted, but it does affect the rate both of energy input and output. With the central cavity model, time does not affect the calculated economics since the net energy output reaches zero the first day.

Some authors (99, 49) point out a variation of thermal conductivity with direction of retorting and with the extent of retorting. If the spent shale has a lower thermal conductivity as these articles indicate, it would worsen heat utilization. Heat transfer from the heated surface to the retorting temperature would be slower than heat transfer from the retorting temperature into the cold formation. The assumption of constant thermal conductivity is then optimistic since it gives better heat efficiency than these authors expect.

(e) Instantaneous and complete retorting is assumed in the model to occur when the temperature reaches 900^{o}F. Actual retorting begins around 572^{o}F (300^{o}C), and is complete around 1112^{o}F (600^{o}C). The weight average temperature for retorting may be calculated from the

correlating equation of Figure 2-6 to be 932°F (500°C) (also Appendix I). Since the assumption of a lower temperature means more energy output, the 900°F assumption is slightly on the optimistic side.

(f) The model assumes the high heating value for the gases and vapors released per pound of shale to be 1000 Btu. The correlating equation of Figure 2-6 based on the data of Table 4-10 shows a maximum weight loss of 9.8% which may be seen from Figure 4-13 to correspond to a loss of 957 Btu/lb in the heat of combustion of the shale. If there are no endothermic chemical reactions occurring during retorting, 957 Btu/lb of shale would also represent the heating value of the gases produced, and the 1000 Btu figure would then be seen to be optimistically high.

Of course, the heat of the retorting reaction is endothermic and approximately 144 Btu per lb of kerogen or 15 Btu per pound of Antrim shale. Also, the heat of decomposing calcite is 500 Btu per pound of calcite or based on a 2 percent $CaCO_3$ composition 10 Btu per pound of shale (9, 39). It will be seen that these endothermic reactions represent a very small proportion of the total heat of combustion.

Figure 4-13 shows a considerable discrepancy between the reduction in the heat of combustion of shale per pound of organic evolved at the beginning of retorting versus that at the end of retorting. However, as explained in Chapter Four, D-2.4, the discrepancy is better explained by weight loss due to H_2O evolution, than by endothermic reactions. Therefore, the figure of 1000 Btu/lb shale is somewhat on the high side.

Data from the sequential and non-sequential runs of Tables 4-9 and 4-7 would indicate higher heats of combustion than 1000 Btu/lb.

However these runs were made under no mechanical pressure and do not simulate underground conditions where overburden pressure is always present.

(g) The assumption of a value of $3 per 1,000,000 Btu for the gases leaving the top of the central cavity is based on the currently quoted value of natural gas delivered to power plants (107). Such natural gas typically has a heating value of 1000 Btu per standard cubic foot of gas. With the central cavity model, the gases leaving have high heating values of 60 Btu per standard cubic foot at the start of the operation. (Calculations in Appendix H). At the end of the operation, the energy content is 0 Btu per standard cubic foot. The value of these very low quality gases are, therefore, much lower than the $3 figure assumed.

In summary, it may be seen that the central cavity model is more optimistic than the actual in situ starting conditions expected, and yet its net energy production fails to justify its installation by at least three orders of magnitude.

PART B. THE CENTRAL CAVITY MODEL

The mathematics of unsteady state heat transfer into a region bounded internally by a constant temperature cylinder have been treated by Carslaw and Jaeger (17). The temperature at any point and time may be calculated from the equation.

$$\theta = \frac{T-T_I}{T_S-T_I} = 1 - \frac{2}{\pi}\int_0^\infty e^{-\tau u^2} \quad \frac{Jo(u)Yo(ru/a)-Yo(u)Jo(ru/a)}{Jo^2(u)+Yo^2(u)} \quad \frac{du}{u} \qquad \text{Eq 2B-1}$$

Here $\tau = kt/\rho ca^2$

Jo is the zero order Bessel function of the first kind

Yo is the zero order Weber's Bessel function of the second kind and u is a dummy variable used to evaluate the definite integral.

Equation 2B-1 satisfies the boundary conditions:

$\theta = 0$ at $t = 0$

$\theta = 1$ at $r = a$

$\theta = 0$ at $r = \infty$

and the differential equation

$$\left(\frac{1}{r}\right)\frac{\partial}{\partial r}\left(r\frac{\partial T}{\partial r}\right) = \rho c/k\ )\ \frac{\partial T}{\partial t}$$

The heat flux at the surface is obtained by differentiating T in Eq2B-1 with respect to r at constant t, evaluating at r=a, and multiplying by minus the thermal conductivity.

$$f = -k \left(\frac{\partial T}{\partial r}\right)\Big|_{r=a}$$

$$= -k\,(T_S - T_I)\,\frac{2}{\pi}\int_0^{\infty} e^{-\tau u^2}\,\frac{Jo(u)Y_1(ru/a) - Yo(u)J_1(ru/a)}{Jo^2(u) + Yo^2(u)}\,\frac{du}{a}$$

$$-f\,a/k(T_S - T_I) = \frac{4}{\pi^2}\int_0^{\infty} e^{-\tau u^2}\,\frac{1}{Jo^2(u) + Yo^2(u)}\,\frac{du}{u}$$

Eq 2B-2

Equations 2B-1 and 2B-2 involve very tedious numerical solutions to find flux and temperature as functions of time and radial distance. However, Carslaw and Jaeger (17) have given the solutions in graphical form as shown in Figures 2-2 and 2-3, and Jaeger (113) has given the solution of 2B-1 in tabular form as shown in Table 2-1. Use of the latter table to calculate the rate at which the 900^{o}F retorting temperature front moves into the shale formation presents problems of interpolation and curve fitting in order to obtain the consistent heat input per pound of shale retorted figures of Table 2-2.

Table 2-2 and 2-3 tabulate data calculated for heat penetration into shale for the temperatures and rock properties specified in the central cavity model. The first column of Table 2-2 is dimensionless time with the geometric progression of values chosen for convenient reading of values for the third column from Figure 2-3.

The second column of Table 2-2 was obtained by interpolating values for r/a from Table 2-1 to give $(T-T_I)/(T_S-T_I)$ = .4941 and correlating the results with an equation. Use of values obtained by direct linear interpolation of Table 2-1 proved to be unsatisfactory since they gave erratic numerical results for $(\partial r/\partial t)_T$. Instead,

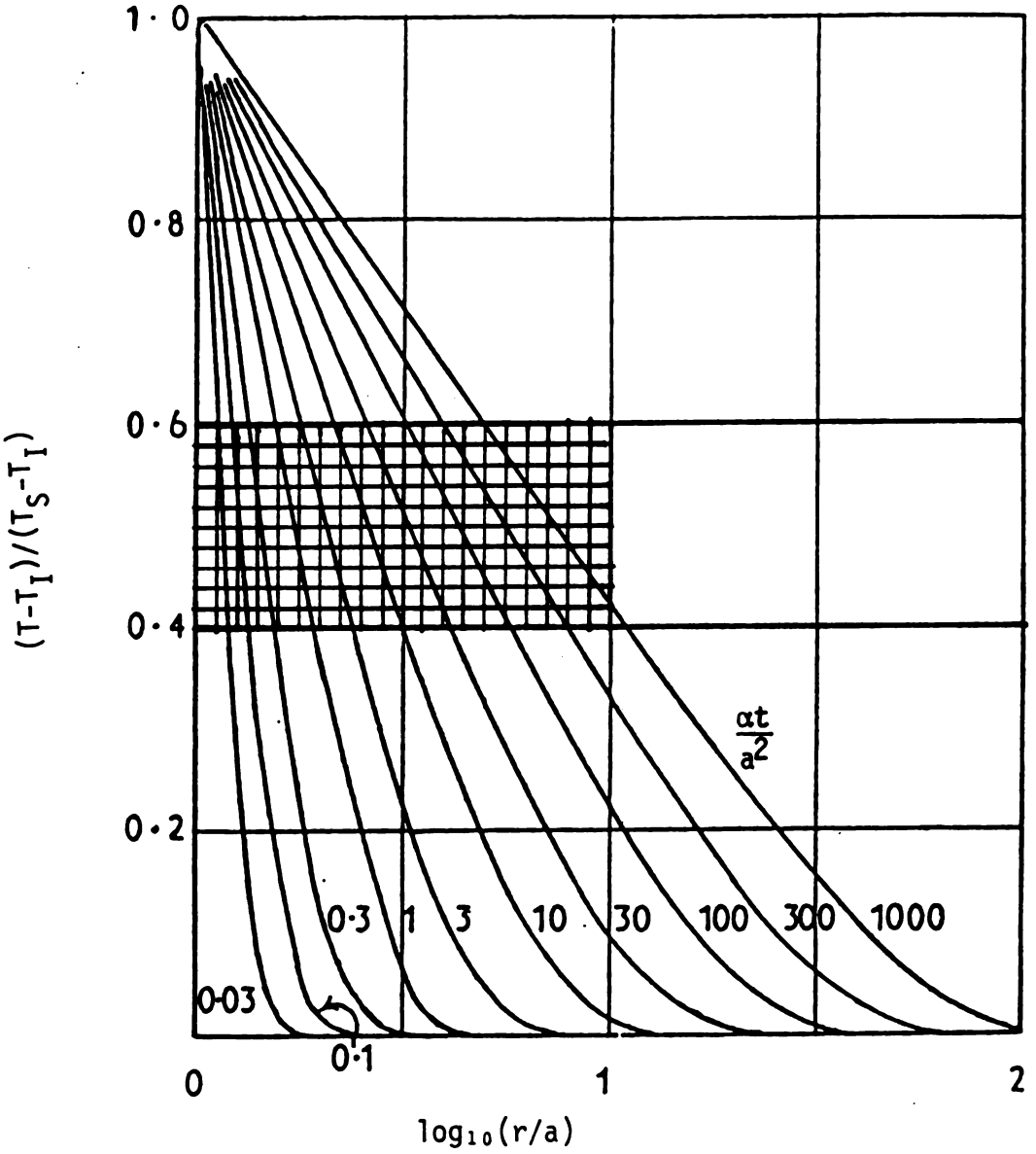

Figure 2-2. Temperature profiles for unsteady state heat conduction in the region bounded internally by the cylinder r=a, with initial temperature T_I and constant surface termperature T_S. [H. S. Carslaw and J. C. Jaeger, Conduction of Heat in Solids. Oxford University Press (1959), page 337.]

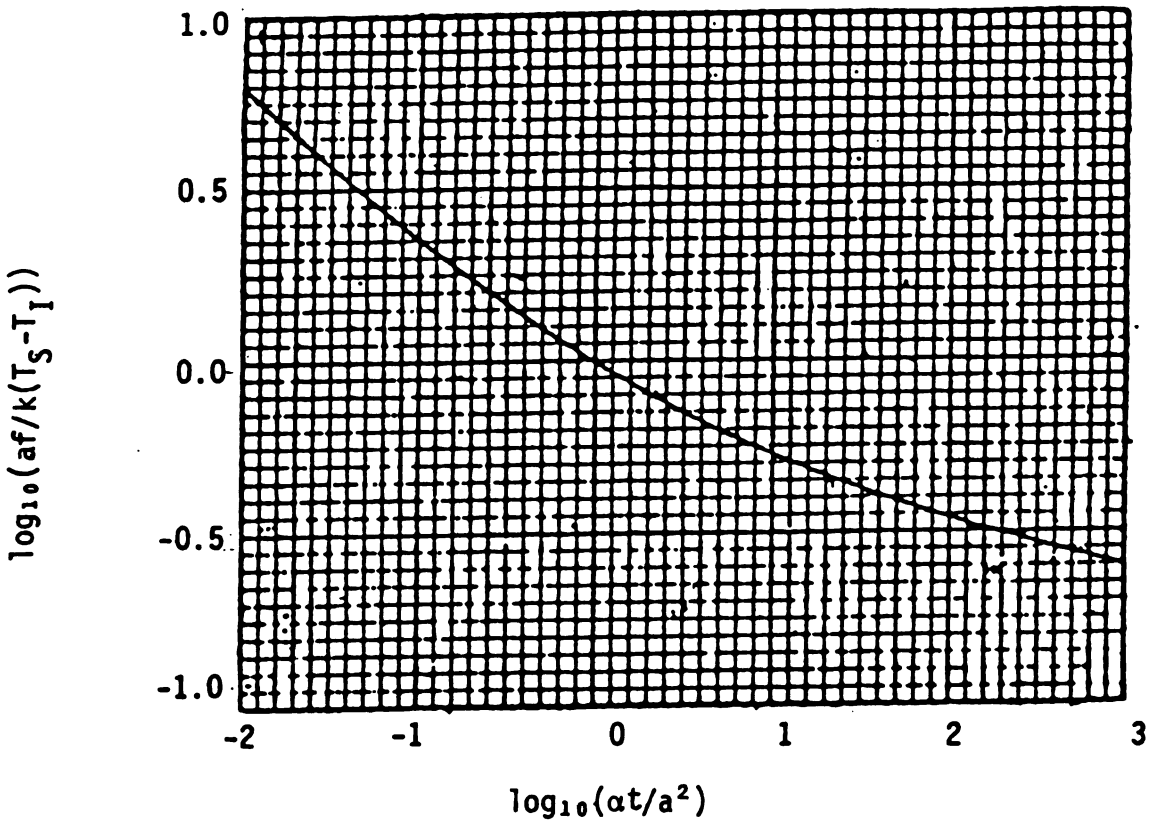

Figure 2-3. The heat flux at the surface of the region bounded internally by a circular cylinder of radius a, with initial temperature of T_I and constant surface temperature of T_S. [H. S. Carslaw and J. C. Jaeger, Conduction of Heat in Solids. Oxford University Press (1959), page 338.]

Table 2-1

Values of $(T_S-T)/(T_S-T_I)$ as a function of $\tau = \alpha t/a^2$ and r/a. Source Jaeger (113)

τ	r/a										
	1.0	1.1	1.2	1.3	1.4	1.5	1.6	1.7	1.8	1.9	2.0
0.001	1.000	0.024	0.000								
0.002	1.000	0.109	0.001	0.000							
0.003	1.000	0.188	0.009	0.000							
0.004	1.000	0.251	0.023	0.001	0.000						
0.005	1.000	0.303	0.042	0.002	0.000						
0.006	1.000	0.345	0.062	0.005	0.000						
0.007	1.000	0.380	0.083	0.010	0.001	0.000					
0.008	1.000	0.410	0.104	0.016	0.001	0.000					
0.009	1.000	0.435	0.124	0.022	0.002	0.000					
0.01	1.000	0.458	0.144	0.030	0.004	0.000	0.000				
0.02	1.000	0.589	0.290	0.117	0.039	0.010	0.002	0.000	0.000		
0.03	1.000	0.652	0.379	0.194	0.087	0.034	0.011	0.003	0.001	0.000	
0.04	1.000	0.691	0.439	0.254	0.133	0.063	0.027	0.010	0.004	0.001	0.000
0.05	1.000	0.718	0.483	0.302	0.175	0.093	0.046	0.021	0.009	0.003	0.001
0.06	1.000	0.739	0.517	0.341	0.211	0.122	0.066	0.033	0.016	0.007	0.003
0.07	1.000	0.754	0.544	0.373	0.242	0.149	0.087	0.047	0.024	0.012	0.005
0.08	1.000	0.767	0.566	0.400	0.270	0.174	0.106	0.062	0.034	0.018	0.009
0.09	1.000	0.778	0.585	0.423	0.294	0.196	0.125	0.077	0.045	0.025	0.013
0.1	1.000	0.787	0.601	0.443	0.316	0.217	0.143	0.091	0.055	0.032	0.018
0.2	1.000	0.837	0.691	0.562	0.450	0.355	0.275	0.209	0.156	0.114	0.082
0.3	1.000	0.860	0.733	0.620	0.519	0.430	0.352	0.286	0.229	0.181	0.142
0.4	1.000	0.873	0.758	0.655	0.562	0.479	0.405	0.339	0.282	0.233	0.191
0.5	1.000	0.883	0.776	0.680	0.592	0.514	0.443	0.380	0.323	0.274	0.230
0.6	1.000	0.890	0.789	0.698	0.615	0.540	0.472	0.411	0.356	0.307	0.263
0.7	1.000	0.895	0.800	0.713	0.634	0.562	0.496	0.436	0.382	0.334	0.290
0.8	1.000	0.899	0.808	0.725	0.649	0.579	0.515	0.457	0.405	0.357	0.313
0.9	1.000	0.903	0.815	0.735	0.661	0.594	0.532	0.475	0.424	0.377	0.334
1	1.000	0.906	0.821	0.743	0.672	0.606	0.546	0.491	0.440	0.394	0.351
2	1.000	0.924	0.854	0.790	0.732	0.677	0.627	0.580	0.536	0.496	0.458
3	1.000	0.932	0.870	0.812	0.760	0.711	0.665	0.623	0.583	0.546	0.511
4	1.000	0.937	0.879	0.826	0.777	0.731	0.689	0.649	0.612	0.577	0.544
5	1.000	0.940	0.886	0.835	0.789	0.746	0.706	0.668	0.633	0.599	0.568
6	1.000	0.943	0.890	0.842	0.798	0.757	0.718	0.682	0.648	0.616	0.586
7	1.000	0.945	0.894	0.848	0.805	0.765	0.728	0.693	0.661	0.630	0.601
8	1.000	0.946	0.898	0.853	0.811	0.773	0.737	0.703	0.671	0.641	0.613
9	1.000	0.948	0.900	0.857	0.816	0.779	0.743	0.711	0.680	0.650	0.623
10	1.000	0.949	0.903	0.860	0.820	0.784	0.749	0.717	0.687	0.658	0.631
20	1.000	0.956	0.916	0.879	0.845	0.813	0.783	0.756	0.729	0.704	0.681
30	1.000	0.959	0.922	0.888	0.856	0.827	0.800	0.774	0.750	0.726	0.705
40	1.000	0.962	0.926	0.894	0.864	0.836	0.810	0.786	0.762	0.741	0.720
50	1.000	0.963	0.929	0.898	0.869	0.843	0.818	0.794	0.772	0.751	0.731
60	1.000	0.964	0.931	0.901	0.874	0.848	0.823	0.800	0.779	0.759	0.739
70	1.000	0.965	0.933	0.904	0.877	0.851	0.828	0.806	0.785	0.765	0.746
80	1.000	0.966	0.935	0.906	0.879	0.855	0.832	0.810	0.789	0.770	0.752
90	1.000	0.966	0.936	0.908	0.882	0.857	0.835	0.813	0.793	0.774	0.756
100	1.000	0.967	0.937	0.909	0.884	0.860	0.838	0.817	0.797	0.778	0.760
200	1.000	0.970	0.943	0.918	0.895	0.874	0.854	0.835	0.817	0.800	0.784
300	1.000	0.972	0.946	0.923	0.901	0.881	0.862	0.844	0.827	0.811	0.796
400	1.000	0.973	0.948	0.926	0.905	0.886	0.867	0.850	0.834	0.819	0.804
500	1.000	0.974	0.950	0.928	0.908	0.889	0.871	0.855	0.839	0.824	0.810
600	1.000	0.974	0.951	0.930	0.910	0.891	0.874	0.858	0.842	0.828	0.814
700	1.000	0.975	0.952	0.931	0.912	0.893	0.877	0.861	0.846	0.831	0.818
800	1.000	0.975	0.953	0.932	0.913	0.895	0.879	0.863	0.848	0.834	0.821
900	1.000	0.976	0.954	0.933	0.914	0.897	0.880	0.865	0.850	0.837	0.824
1000	1.000	0.976	0.954	0.934	0.915	0.898	0.882	0.867	0.852	0.839	0.826

Table 2-1. (continued)

τ	r/a								
	2	3	4	5	6	7	8	9	10
0.1	0.018	0.000							
0.2	0.082	0.001	0.000						
0.3	0.142	0.006	0.000						
0.4	0.191	0.015	0.000						
0.5	0.230	0.027	0.001	0.000					
0.6	0.263	0.040	0.003	0.000					
0.7	0.290	0.054	0.006	0.000					
0.8	0.313	0.068	0.009	0.001	0.000				
0.9	0.334	0.082	0.013	0.001	0.000				
1	0.351	0.095	0.018	0.002	0.000	0.000			
2	0.458	0.194	0.071	0.022	0.005	0.001	0.000		
3	0.511	0.256	0.119	0.049	0.018	0.006	0.002	0.000	
4	0.544	0.300	0.157	0.076	0.034	0.014	0.005	0.002	0.000
5	0.568	0.332	0.188	0.101	0.051	0.024	0.010	0.004	0.002
6	0.586	0.357	0.214	0.123	0.067	0.035	0.017	0.008	0.003
7	0.601	0.378	0.235	0.142	0.082	0.046	0.024	0.012	0.006
8	0.613	0.395	0.254	0.159	0.097	0.056	0.032	0.017	0.009
9	0.623	0.409	0.270	0.175	0.110	0.067	0.039	0.022	0.012
10	0.631	0.422	0.284	0.188	0.122	0.077	0.047	0.028	0.016
20	0.681	0.497	0.370	0.277	0.207	0.153	0.112	0.081	0.057
30	0.705	0.534	0.415	0.325	0.256	0.201	0.157	0.122	0.094
40	0.720	0.558	0.444	0.358	0.290	0.235	0.190	0.153	0.123
50	0.731	0.574	0.464	0.381	0.314	0.260	0.215	0.177	0.146
60	0.739	0.588	0.481	0.399	0.334	0.281	0.236	0.199	0.167
70	0.746	0.598	0.494	0.414	0.350	0.297	0.253	0.216	0.184
80	0.752	0.607	0.505	0.427	0.364	0.312	0.268	0.230	0.198
90	0.756	0.614	0.514	0.437	0.374	0.323	0.280	0.242	0.210
100	0.760	0.621	0.522	0.446	0.385	0.334	0.291	0.254	0.222
200	0.784	0.658	0.569	0.500	0.444	0.397	0.357	0.322	0.291
300	0.796	0.677	0.593	0.528	0.475	0.430	0.392	0.358	0.328
400	0.804	0.690	0.609	0.546	0.495	0.451	0.414	0.382	0.353
500	0.810	0.699	0.620	0.559	0.510	0.468	0.432	0.400	0.372
600	0.814	0.706	0.629	0.569	0.520	0.479	0.444	0.413	0.385
700	0.818	0.712	0.636	0.578	0.530	0.490	0.455	0.424	0.397
800	0.821	0.716	0.642	0.585	0.538	0.498	0.464	0.434	0.407
900	0.824	0.720	0.647	0.591	0.544	0.505	0.471	0.442	0.415
1000	0.826	0.724	0.652	0.596	0.550	0.511	0.478	0.449	0.422

τ	r/a									
	10	20	30	40	50	60	70	80	90	100
10	0.016	0.000								
20	0.057	0.001	0.000							
30	0.094	0.004	0.000							
40	0.123	0.009	0.000							
50	0.146	0.016	0.001	0.000						
60	0.167	0.023	0.002	0.000						
70	0.184	0.031	0.003	0.000						
80	0.198	0.038	0.005	0.000						
90	0.210	0.046	0.007	0.001	0.000					
100	0.222	0.053	0.010	0.001	0.000	0.000				
200	0.291	0.110	0.038	0.011	0.001	0.001	0.000			
300	0.328	0.146	0.064	0.026	0.009	0.003	0.001	0.000		
400	0.353	0.173	0.086	0.040	0.018	0.007	0.003	0.001	0.000	
500	0.372	0.194	0.104	0.054	0.026	0.012	0.005	0.002	0.001	0.000
600	0.385	0.210	0.119	0.066	0.035	0.018	0.008	0.004	0.002	0.001
700	0.397	0.223	0.132	0.077	0.044	0.024	0.012	0.006	0.003	0.001
800	0.407	0.235	0.143	0.087	0.052	0.030	0.016	0.009	0.004	0.002
900	0.415	0.245	0.153	0.096	0.059	0.035	0.020	0.011	0.006	0.003
1000	0.422	0.254	0.162	0.104	0.066	0.041	0.024	0.014	0.008	0.004

Table 2-2

Radial heat penetration into shale from
a 1.0 ft diameter cylindrical cavity

$T_S = 1750$, $T_I = 70$, $T_R = 900$, $c = 0.3$, $k = 1$, $\rho = 145$

$\frac{\alpha t}{a^2}$	$\frac{r-a}{2a}$	$\frac{af}{k(T_S-T_I)}$	Btu input per lb shale retorted
0	0	∞	588
.01	.045	6.04	646
.02	.063	4.44	671
.04	.087	3.28	705
.08	.119	2.46	748
.1	.132	2.26	767
.2	.178	1.73	835
.4	.239	1.35	928
.8	.317	1.08	1050
1	.347	1.01	1100
2	.452	0.82	1280
4	.584	0.69	1520
8	.745	0.58	1830
10	.80	0.55	1940
20	1.02	0.47	2400
40	1.26	0.41	2960
80	1.56	0.36	3700
100	1.67	0.345	4000
200	2.05	0.301	5050
400	2.50	0.274	6480
800	3.05	0.254	8300
1000	3.75	0.250	9000

Table 2-3

Operation of the central cavity model

Time hours	Energy Output		Energy Input		Net Output	
	Btu/hr	Total Btu	Btu/hr	Total Btu	Btu/hr	Total Btu
	10^6x	10^6x	10^6x	10^6x	10^6x	10^6x
0	∞	0	∞	0	∞	0
.1	19.8	4.28	12.8	2.64	7.0	1.64
.2	14.0	6.10	9.4	3.84	4.6	2.26
.4	9.8	8.62	6.9	5.6	2.9	3.02
.9	7.0	12.1	5.2	8.1	1.8	4.0
1.1	6.1	13.6	4.7	9.2	1.4	4.4
2.2	4.4	19.1	3.7	13.6	0.7	5.6
4.4	3.1	27.	2.9	20.6	0.2	6.4
8.7	2.2	38.	2.3	31.5	-.1	6.5
10.9	1.9	43.	2.1	37.1	-.2	5.9

3-point hyperbolic interpolation was used and the values obtained in this manner agreed to ±1% with the correlating equation:

$$(r-a)/2a = (.4836\ S + .25)^{.5} - 0.5 - .01S + .00012\ S^2. \qquad \text{Eq2B-3}$$

where $S = (\alpha t/a^2)^{.5}$.

The last column of Table 2-2 was obtained using the time derivative of the correlating equation for the second column together with the figures in the second and third columns. The values given are:

$$\pi f/\rho(\partial \pi r^2/\partial t)_{T=900}$$

The first column of Table 2-2 is dimensionless time and may be converted to time in hours by multiplying by 10.875. The second is the retorting zone penetration divided by the cavity diameter and is therefore numerically equal to the penetration in feet. The third column is dimensionless flux and may be converted to Btu/hr ft^2 of surface by multiplying by 3360. The last column has special significance since there will be no net energy production if the heating value of the shale per pound is less than the heat input per pound. Thus for Antrim shale values in this column greater than 1000 result in net energy losses.

Table 2-3 extends the data of Table 2-2 to the projected hour-by-hour operation of the central cavity model. The first column gives the hour elapsed after ignition calculated as indicated above. The third column was obtained by calculating the retorted volume from the second column of Table 2-2 and multiplying by 145 lb/ft^3 density and 1000 Btu/lb. The second column was obtained in the same way but using the correlating equation 2B-3 and differentiating the result with respect to time.

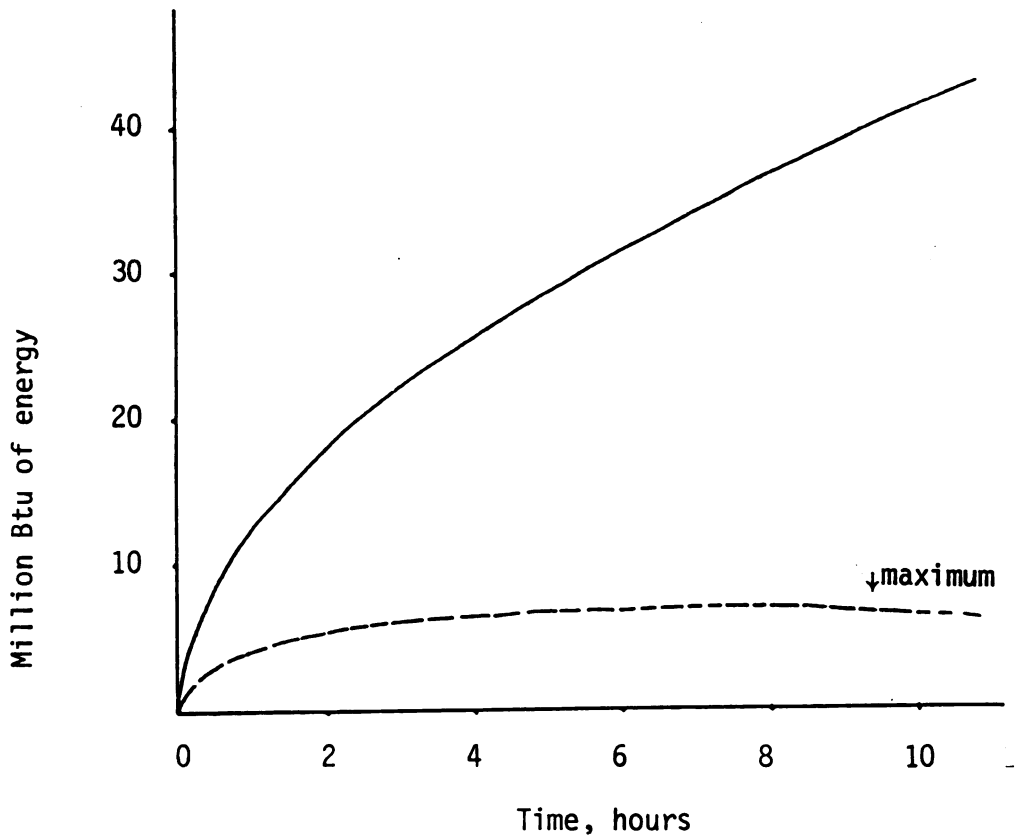

Figure 2-4. Energy production from central cavity model well 1.0 ft dia x 200 ft at 1750°F.

——— cumulative gross energy output

– – – – cumulative net energy output

The fourth column was calculated from the third column of Table 2-2 multiplying by 3360, 200, and π . The fifth column was calculated from the third column by summing its increments multiplied by the arithmetic average of adjacent values from the last column of Table 2-2 and dividing by 1000. The sixth and seventh columns are respectively the fourth minus the second and the fifth minus the third. Figure 2-4 is a plot of the third and the last columns of Table 2-3. It shows how the gross energy output from the central cavity model increases with time, but the gross energy input represented by the difference in the two curves increases faster. Therefore, the cumulative net energy reaches a maximum of something less than 10,000,000 Btu.

PART C. HEAT INPUT PER POUND OF SHALE AS A FUNCTION OF FLOW DIRECTION

Radial heat flow from a central cylinder occurs not only in the central cavity model but in any in situ situation where the hottest part of the formation lies along a line. Two other basic directions of heat flow are analyzed here and compared with radial cylindrical flow.

Radial spherical flow is the type of heat flow to be expected when the hot region is a spot rather than a line, and linear heat flow maybe expected from a uniformly heated plane. Linear heat flow was assumed in a number of unrealistic models discussed in Part A. Spherical radial heat flow probably occurs frequently as in forward combustion along a line connecting injection and production wells.

The mathematical analysis for linear and spherical radial flow is much simpler than for cylindrical radial flow. It is easier to manipulate the equations and to understand the implication of the results. For linear flow the problem becomes the simple semi-infinite slab problem.

The temperature distribution in such a case is given by:

$$1-\theta = (T-T_S)/(T_I-T_S) = \mathrm{erf}(x/\sqrt{4\alpha t}) = \mathrm{erfp} \qquad \text{Eq2C-1}$$

where θ is $(T-T_I)/(T_S-T_I)$ and $p = x/\sqrt{4\alpha t}$

The flux at the surface in such a case in Btu/hr:

$$f = -k(dT/dp)(\partial p/\partial x)\Big|_{x=0} = k\,(T_S-T_I)/\sqrt{\pi\alpha t}$$

and the pounds retorted per hour

$$\rho(\partial x_R/\partial t)_{T=T_R} = p_R\sqrt{\alpha/t}\ \rho$$

since the constant $p_R = \text{erf}^{-1}\ (1-\theta_R) = x_R/\sqrt{4\alpha t}$

The Btu input per pound of shale retorted, B, then is given by:

$$B = c\ (T_S-T_I)/\sqrt{\pi}\ p_R \qquad \text{Eq 2C-2}$$

and if $c = 0.3$, $T_S-T_I = 1680$, $T_R = 900$, and $p_R = \text{erf}^{-1}\ (850/1680) = .4836$ then 588 Btu must be input per pound of shale retorted. For linear heat flow this value is a constant and not a function of x or t. For radial cylindrical or spherical heat flow this value applies as t or x approach zero and there is no variation in cross section. The 588 at the top of the last column of Table 2-2 is based on this reasoning. It should also be noted that the heat input per pound of shale is not dependent on thermal conductivity or on density. The same will be shown for radial spherical and may be presumed for radial cylindrical flow although it is not easy to demonstrate it in the last case because charts and empirical equations were used.

Table 2-4 presents for linear heat penetration the same data that Table 2-2 presents for cylindrical radial flow. The headings are made to correspond as nearly as possible. For example, x is substituted for $(r-a)/2a$, $4\alpha t$ for $\alpha t/a^2$, and $f/2k$ for af/k.

Table 2-4

Linear heat penetration into shale from a flat heated surface

$T_S = 1750$, $T_I = 70$, $T_R = 900$, $c = .3$, $k = 1$, $\rho = 145$

$4\alpha t$	x_R	$\frac{f}{2k\ (T_S-T_I)}$	Btu input per lb shale retorted
0	0		588
.01	.048	5.64	588
.02	.068	3.99	588
.04	.097	2.82	588
.08	.137	1.99	588
.1	.153	1.78	588
.2	.216	1.26	588
.4	.306	.89	588
.8	.433	.63	588
1	.48	.56	588
2	.68	.40	588
4	.97	.28	588
8	1.37	.20	588
10	1.53	.178	588
20	2.16	.126	588
40	3.06	.089	588
80	4.33	.063	588
100	4.8	.056	588
200	6.8	.040	588
400	9.7	.028	588
800	13.7	.020	588
1000	15.3	.018	588

The mathematics of radial heat flow from an internal high temperature sphere is only a little more difficult than flow into a semi-infinite slab. The temperature distribution for such spherical radial flow is given by:

$$\theta = (T-T_I)/(T_S-T_I) = (a/r)(1-\text{erf}[(r-a)/\sqrt{4\alpha t}]) = (1-\text{erf } p)/s \qquad \text{Eq2C-3}$$

where $p = (r-a)/\sqrt{4\alpha t}$ and $s = r/a$

The flux at the surface in such a case in Btu/hr

$$f = -k\,(\partial T/\partial r)_t\Big|_{r=a} = k(T_S-T_I)(1/a+2/\sqrt{\pi 4\alpha t}) \qquad \text{Eq2C-4}$$

and the pounds retorted per hour per ft^2 cavity

$$\rho(\partial r^3/\partial t)_{T=T_R} / 3a^2 = \rho s^2 r'$$

where $r' = (\partial r/\partial t)_{T=T_R}$ and can be evaluated by differentiating equation 2C-3, making use of the retorting front relations:

$$1-\text{erf } p_R = s_R\theta \quad \text{and} \quad p_R = a(s_R-1)/\sqrt{4\alpha t}$$

Then

$$0 = -\theta r'/as_R - 2e^{-p_R^2}\, p'/\sqrt{\pi}\, s_R$$

$$0 = \sqrt{\pi}\,\theta\, e^{p_R^2}\, r' + 2ap'$$

and

$$p' = r'/\sqrt{4\alpha t} - a\,(s_R-1)/2+\sqrt{4\alpha t}$$

$$= p_R\, r'/(s_R-1)a - 2\alpha\, p_R^3/(s_R-1)^2\, a^2$$

Combining we get

$$0 = [\sqrt{\pi}\,\theta\, e^{p_R^2}\,(s_R-1)\,a + 2ap_R]\,r' - 4a\alpha p_R^3/(s_R-1)a$$

$$r' = \frac{4\alpha p_R^3}{(s_R-1)a\,[\sqrt{\pi}(s_R-1)\theta\, e^{p_R^2} + 2p_R]}$$

Substituting back, we then find B, the Btu input per pound of shale retorted in the spherical radial direction.

$$B = f/\rho s^2\, r'$$

$$= c\,(T_S-T_I)\,(s_R-1 + 2p_R/\sqrt{\pi})[\sqrt{\pi}(s_R-1)\, e^{p_R^2}\theta/2 + p_R]$$

$$/2s_R^2\, p_R^3 \qquad \text{Eq 2C-5}$$

Equation 2C-5 is identical with Equation 2C-2 at the start of the operation when $s_R = 1$, and for $c = 0.3$, $T_S = 1750$, $T_I = 70$, and $T_R = 900$ again gives 588 as the Btu input per pound of Antrim shale retorted. This figure is again independent of the thermal conductivity or the density of the shale bed.

It is also interesting that as $s_R\,\theta$ approaches unity the value of p_R and the value of $\exp(p_R^2)/p_R^3$ become infinite. Thus, with a one foot diameter spherical cavity at 1750°F and a bed initially at 70°F a retorting temperature of 900°F will never penetrate more than (1750-900)/2(900-70), or 0.51 feet into the formation.

For radial cylindrical heat flow the retorting front continues indefinitely to penetrate the formation but requires progressively more heat input per pound of shale retorted. In the case of linear heat flow, the retorting front continues to penetrate and the heat input per pound retorted is a constant. These effects are well illustrated in Figure 2-5, which shows heat input per pound of shale retorted versus retorting temperature penetration into the formation in feet.

It may be seen from the chart that as the front moves into the shale the direction of heat transfer is a very important factor in determining the heat requirement. Also shown on the same chart are lines representing the energy output, also in Btu/lb of shale retorted for Antrim (1,000), Western (2,000), and Jordanian (3,000) shales. Where intersections of input and output lines occur, there is, of course, no net energy production and further heating in situ becomes useless. For Antrim shale with spherical radial heat flow, this occurs at less than an inch penetration. For cylindrical radial it occurs after four inches penetration, and for linear flow it never occurs. The spherical flow data for plotting the line in Figure 2-5 are given in the second and fourth columns of Table 2-5. The table is similar to Tables 2-2 and 2-4 except for heat flow direction. The values in the second and fourth columns were calculated from the first column using Equations 2C-3 and 2C-5. This was done on a TI-59 programmable calculator using a convergence procedure to get r to fit Eq2C-3. Also involved was a series approximation of the error function. The third column of Table 2-5 was obtained from Equation 2C-4.

Table 2-5

Radial heat penetration into shale from
a 1.0 ft diameter spherical cavity

$T_S = 1750$ $T_I = 70$, $T_R = 900$, $c = 0.3$, $k = 1$, $\rho = 145$

$\frac{\alpha t}{a^2}$	$\frac{r-a}{2a}$	$\frac{af}{k(T_S-T_I)}$	Btu input per lb shale retorted
0	0		588
.01	.044	6.64	718
.02	.059	4.99	777
.04	.080	3.82	866
.08	.105	2.99	1004
.1	.115	2.78	1063
.2	.148	2.26	1320
.4	.186	1.89	1750
.8	.228	1.63	2500
1	.242	1.56	2860
2	.285	1.40	4600
4	.327	1.28	8100
8	.365	1.20	15500
10	.377	1.18	19500
20	.408	1.13	42×10^3
40	.434	1.09	95
80	.454	1.063	230
100	.460	1.056	307
200	.474	1.040	780
400	.484	1.028	2050
800	.492	1.020	5×10^6
1000	.494	1.018	8×10^6
∞	.512	1.000	∞

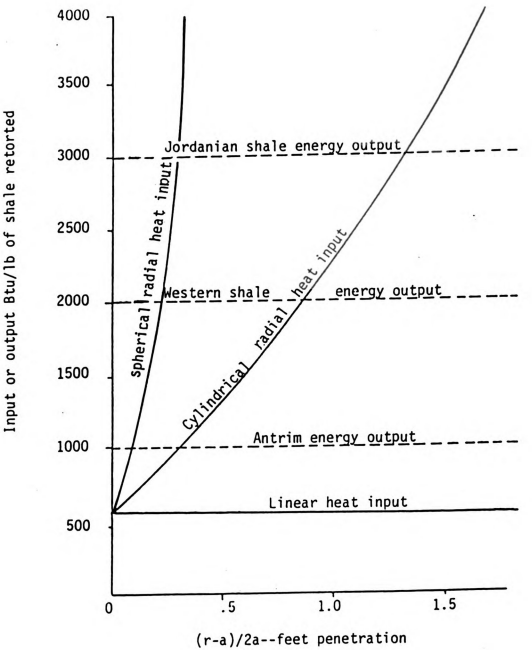

Figure 2-5. Effect of heat flow direction on Btu/lb shale energy input and output (c=0.3, T_S=1750, T_I=70, T_R=900).

PART D. SHALE RETORTED AND HEAT CAPACITIES AS FUNCTIONS OF TEMPERATURE

Three important assumptions of the central cavity model are the retorting temperature T_R taken as 900°F, the energy output of Antrim shale taken as 1000 Btu/lb, and the heat capacity of Antrim shale taken as 0.3. The energy output and retorting temperature will be considered first.

Figure 2-6 presents data taken from Tables 4-6, 4-7 and 4-10 of the experimental work of this thesis giving accumulated weight loss as a function of temperature. The data from Tables 4-6 and 4-7 are based on sequential and non-sequential runs made without mechanical pressure on the rock. These data agree very well with each other considering the very different techniques used and the large number of samples used in the non-sequential runs. However, the data of Table 4-10 taken from runs under external mechanical pressure give considerably lower weight loss at each temperature.

As explained in the experimental section of this thesis, part of the mechanism of organic vapor evolution from the shale involves the opening of horizontal cracks in the shale, and such cracks do not form under the mechanical pressure due to the overburden in true in situ conditions. Therefore, it seems reasonable to use the data taken under mechanical pressure as a basis for energy output and retorting temperature. The points representing these conditions in Figure 2-6 fit

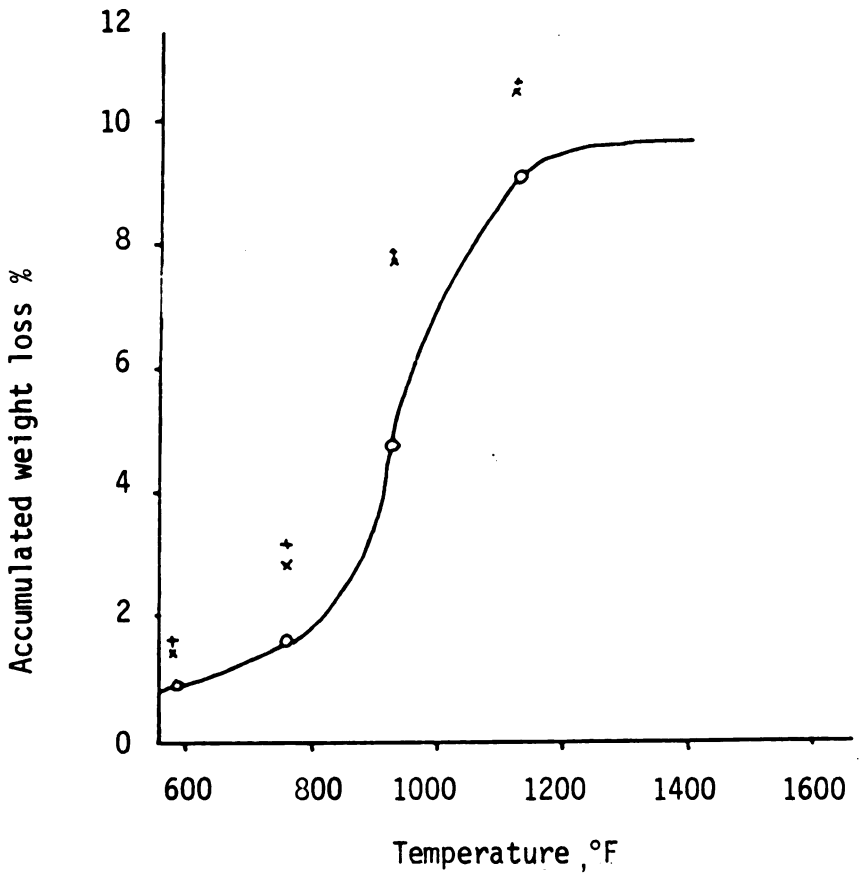

Figure 2-6. Retorting weight loss as a function of temperature and overburden pressure.

x sequential points from Table 4-6

\+ non-sequential points from Table 4-7

o with mechanical pressure from Table 4-10

—— correlating equation

$$\text{loss} = 0.021/(1+u) + 0.077/(1+v)$$

$$u = (600/t)^4 \quad v = (957/t)^{18}$$

a correlating equation for the cumulative fraction weight loss from the shale of

$$F = 0.021/(1+u) + 0.077/(1+v) \qquad \text{Eq2D-1}$$

where $u = (600/T)^4$ and $v = (957/T)^{18}$

with T the temperature in ^{o}F

The total fraction weight loss from this equation is 0.021 + 0.077 = 0.098. The corresponding loss in the heat of combustion of the shale is 957 Btu/lb, according to Figure 4-13 and Equation 4D-1. This may also be considered a good approximation for the gain in heat of combustion of the gas after taking into account the small exothermic and endothermic effects discussed in connection with Experiments D-2. The figure of 1000 Btu/lb used in the model is then conservatively and optimistically on the high side.

The fraction weight loss for T = 936 is 0.049 or half the total. If this temperature is assumed as the retorting front we might expect the combustibles evolved at lower temperature to equal the combustibles not yet evolved at higher temperature. The lower figure of 900 used in the model is then conservative since it shows a little more shale retorted than expected.

The most important physical property in determining the heat input for shale retorting is the heat capacity. Also, the mathematical analysis assumes that the heat capacity is constant and we need to examine how close this assumption is to the truth. Important considerations in this respect are the variation in heat capacity of the components with temperature, the loss of some of these components during the retorting process, and the heat of reaction which contributes to the Btu of heat needed for each degree rise in temperature.

Figure 2-7 shows data on the heat capacity of some shale component as a function of temperature. Aluminum and silicon oxides are the most important inorganic components of the shale, they have similar heat capacity curves, and a correlation equation for the inorganic portion of the solid fits their values closely. It should be noted that heat capacities of solids at room temperatures are often much lower than the fully developed Dulong-Petit values at higher temperatures, and the common practice of taking low temperature handbook values can lead to considerable error.

To represent the organic part of the shale data on pure carbon are shown as a function of temperature together with one naphthalene point at 600^{o}F. While kerogen and naphthalene are quite different in structure, they both have about the same carbon to hydrogen ratios and that is mainly what determines the heat capacity. Of course, naphthalene heat capacity rises with temperature as does carbon heat capacity, but during the retorting process the vapors evolved are richer in hydrogen than the solid residue and the heat capacity of the latter moves toward the value of pure carbon. The straight line approximation for the organic part follows this pattern and, while not accurate in itself, it represents only a small fraction of the total heat capacity. An even smaller fraction is the combined water in the inorganic and organic portion of the shale. This would also add to the heat capacity and more at low temperature than at high.

Figure 2-8 gives calculated values for the effective heat capacity of the shale, based on the correlating equations of Figure 2-7 for the organic and inorganic parts as well as the heat of the retorting reaction multiplied by the temperature derivative of the correlating

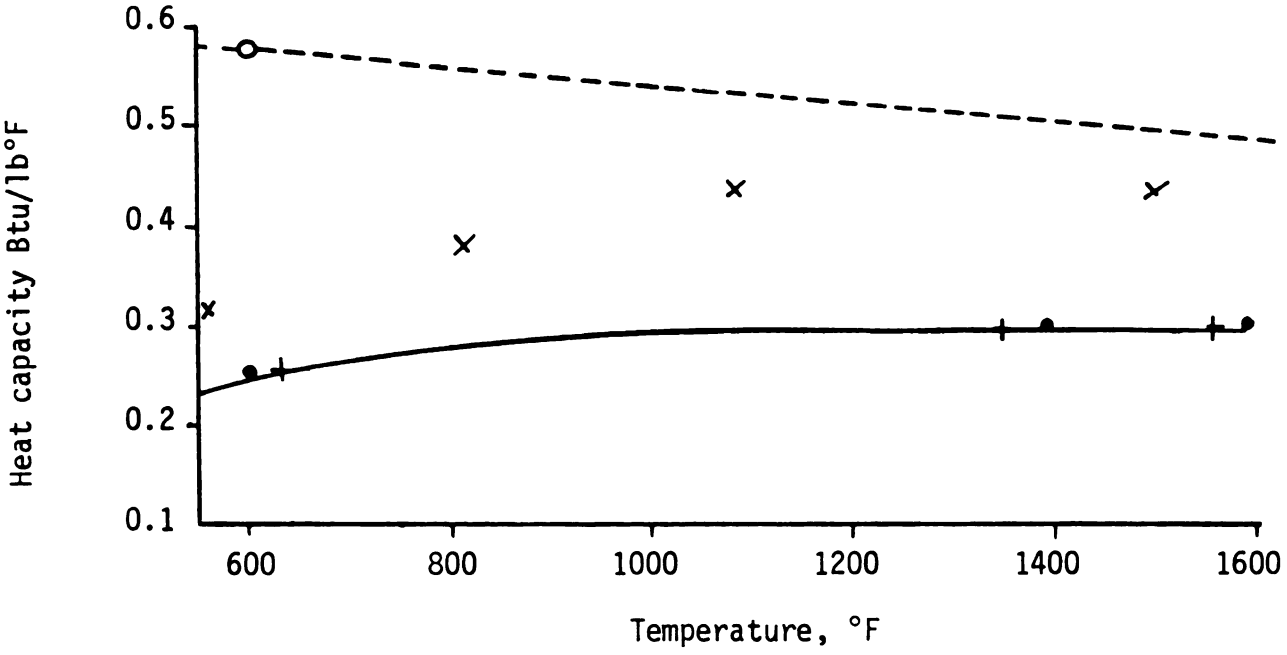

Figure 2-7. Heat capacity of shale components.

× Carbon
○ Naphthalene (70)
+ $Al_2 O_3$
● $Si O_2$
—— Average inorganic
$C_i = 0.335 - 80/(t+460)$
---- Average organic
$C_o = 0.58 - .0001\ (t-600)$

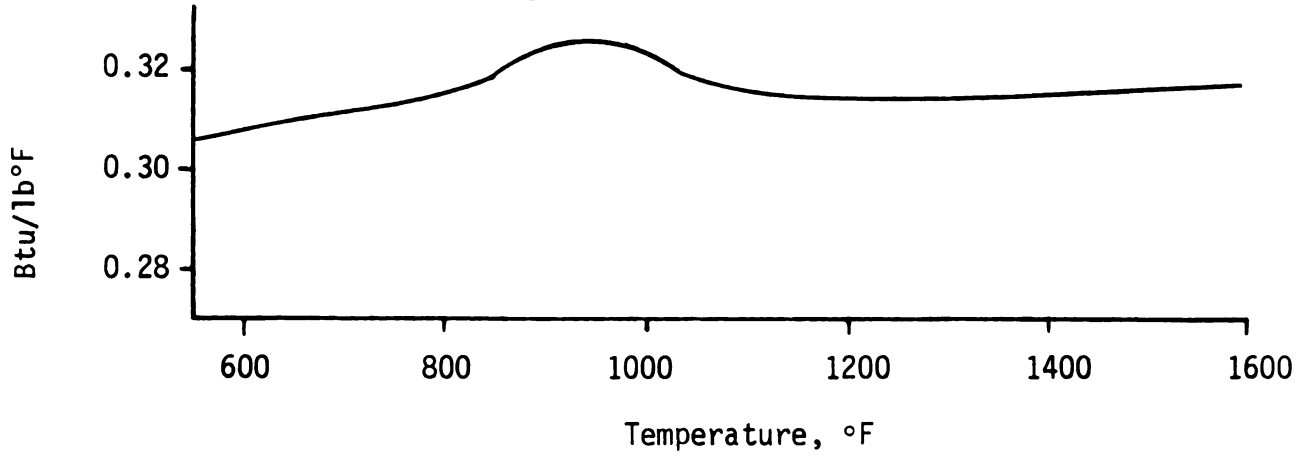

Figure 2-8. Effective heat capacity of Antrim shale including heat of retorting.

$$C = 0.86\ C_i + 0.14\ C_o\ (1\text{-loss}) + 12.1u/(1+u)^2\ t + 44.35v/(1+v)^2\ t$$

equation of Figure 2-6. It will be seen that the heat of reaction and the lowered heat capacities at temperatures under 1000^{o}F are compensating effects resulting in a fairly constant effective heat capacity between the surface temperature and the retorting range.

In situ conditions for Antrim shale then are close to those of the Jaeger problem for a heat capacity taken as constant at 0.315 Btu/lb^{o}F. The mass referred to in this calculated effective heat capacity is that of the original shale. The actual heat capacity of the spent shale at these temperatures is about 10% higher. The use of 0.3 in the model is low and shows a smaller heat input than would actually be experienced.

PART E. RETORTING RATE AND NET HEAT RECOVERED AS A FUNCTION OF SURFACE TEMPERATURE

Some of the experiments of this thesis showed that at around temperatures 1800°F incipient fusion of some shale components occur resulting in glazing of the surface. The model surface temperature of 1750°F is uncomfortably close to this figure. It has been assumed that a higher surface temperature would result in faster and more effective retorting, but it is necessary to show by calculation that such would be the case.

Since the linear flow path is the simplest mathematically and corresponds to radial flow at the start of retorting, it will be used. Table 2-6 has been calculated from Equation 2C-1 and the pounds retorted relation. The retorting rate ratio is the ratio of pounds of shale retorted per hour at T_S divided by the same value for 1750°F. The retorting efficiency ratio is 588 divided by the Btu input per pound of shale retorted with the corresponding T_S value. At 1100°F, for example, 1000 Btu input would be required right from the start which for Antrim shale would represent zero net output.

Figure 2-9 is a plot of these same data. It will be seen from the plot that both rate and efficiency are improving with temperature at 1750°F although the efficiency is not improving very fast. Somewhat lower temperatures would be all right, but not as low as the 1000°F proposed by Lesser.

Table 2-6

Effect of applied temperature on retorting rate and retorting efficiency

$^{o}_{F}T_{S}$	Retorting rate ratio	Retorting efficiency ratio
1750	1.000	1.000
1700	.970	.995
1600	.911	.978
1500	.851	.950
1400	.792	.905
1300	.732	.838
1200	.673	.737
1100	.613	.586
1000	.554	.357
900	.494	0

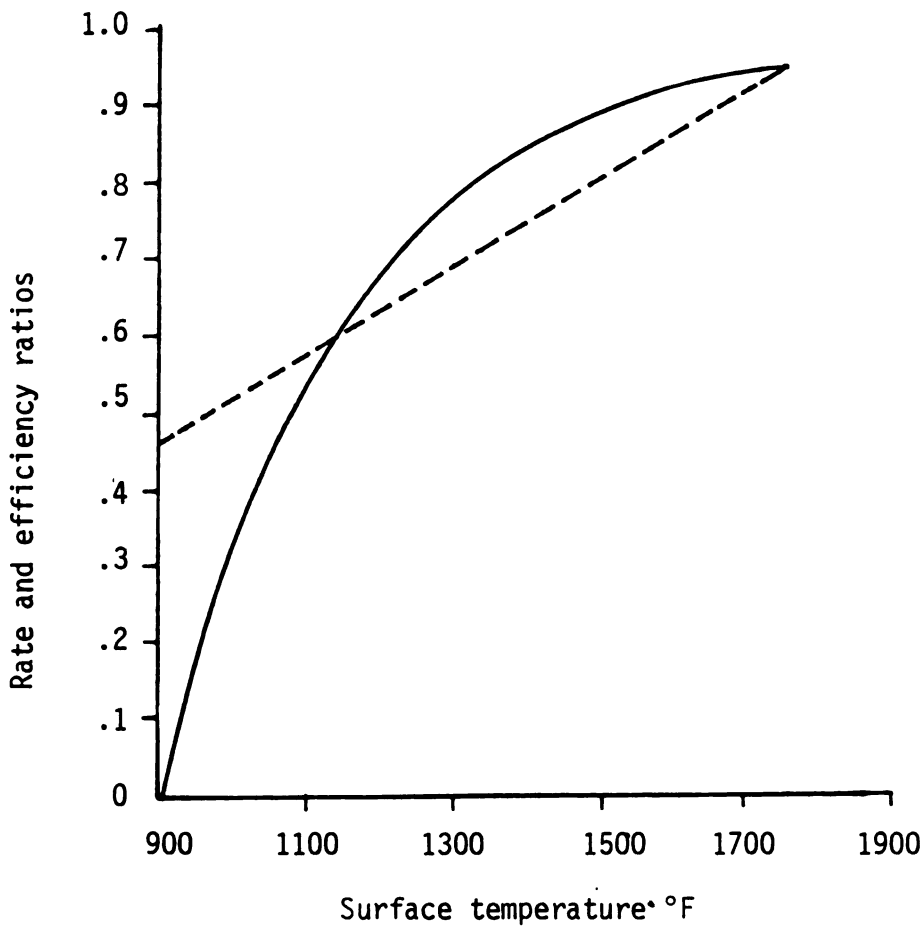

Figure 2-9. Effect of temperature on retorting rate and retorting efficiency.

– – – – Retorting rate ratio ($rate_T/rate_{1750}$)

——— Retorting efficiency ratio (B_{1750}/B_T)

CHAPTER THREE

LITERATURE REVIEW

A comprehensive bibliography on oil shale is maintained by the DOE Technical Information Center at Oak Ridge (115). More than 10,000 references are cited and these are arranged by subject category with some of the more pertinent categories being as follows:

(1) Mining and fracturing

(2) Aboveground retorting

(3) In situ retorting, true and modified

(4) Properties and composition

(5) Economics

Other categories such as geology, general, health and safety, waste research, regulations and environmental aspects are also included in the bibliography.

Two major sources of data on Western shales are the annual oil shale symposium proceedings sponsored since 1964 by the Colorado School of Mines and the Laramie Energy Center, and the reports of investigations published by the U.S. Bureau of Mines. Both of these two sources were used extensively in this thesis. Some of the important literature in each of the above five categories is described in the following:

(1) Mining and fracturing

Room-and-pillar oil shale mining for the Colony aboveground retorting process was well described by Marshall (55). An outline of the work done by the Bureau of Mines in oil shale mining for aboveground retorting until 1976 was summarized by Utter (116).

The publications in areas related to fracturing shale as a way of enhancing the in situ process, true or modified, are numerous. Many fracturing techniques have been suggested. Some work used hydraulic fracturing, or the use of high pressure air or water (3, 31, 101). Other work used chemical explosives (65, 66). Electric methods (29, 63, 84) and nuclear methods (47, 49) have also been suggested. The combining of different types of techniques has also been investigated (14, 61, 72, 102, 103).

(2) Aboveground retorting

Aboveground oil shale retorts were classified by Hull and others (40) into four general categories depending on the method for transferring heat to the shale. The last column of the Table below was brought up to date by the writer. These categories are:

Class	Method of Heat Application	Examples
I	Heat is transferred to the shale through a wall.	Pumpherstone (40)
II internal-combustion retort	Heat is generated within the retort by combustion of product gases and residual carbon remaining in the shale.	1) Bur. of Mines Combustion retort (33, 34 56, 82)
		2) Union "A" retort (91)
		3) Paraho vertical retort (71, 72)

III hot gas recycle retort	Heat-carrier gas is heated in the retort zone and is then passed through a moving bed of oil shale.	1) Union "B" retort (50) 2) Paraho Unit with air injection (43)
IV	Heat transfer by contact between fresh shale and hot recycled spent shale.	Lurgi-Ruhrgas (85)

As discussed by Hull and others (40), each class of retorts has special advantages and disadvantages, as follows:

Class	Disadvantages	Advantages
I	1) inefficient heat transfer	1) gas produced not contaminated with air or fuel
	2) low production rate	
II	1) low oil recovery	1) mechanically simple
	2) fine shale needs retreatment	2) thermally efficient
	3) product gas has low heating value	
III	1) mechanically complex	1) high oil yield
	2) thermally inefficient	2) product gas has high heating value
	3) low product rate	
IV	1) mechanically complex	1) high oil recovery
	2) thermally inefficient	2) product gas has high heating value

(3) In situ retorting, true and modified

A review article by Carpenter and Sohns summarizes the work done by the Bureau of Mines and the Laramie Energy Center through 1974 (16). This work included operation of 10 and 150 ton batch retorts simulating in situ process, the operation of a small high-pressure batch retort, the operation of a simulated-overburden pressure retort and finally the development of mathematical retorting model. Other review articles are those by Ridley (76, 77) on the Occidental process of modified in situ processing of oil shale through 1978 and by Campbell (13) on the same process through 1981. An interesting overview article was published by Schramm (86).

Other publications which investigate one or several aspects of the in situ process are also available in the literature. Some of the areas which have been investigated include field testing and pilot plant operations (8, 15, 22, 31, 74, 75), kinetics of kerogen decomposition (2, 9, 11, 12, 27, 39, 58, 59, 97), experimental work supporting or simulating the in situ process (7, 12, 21, 24, 36, 53, 67, 89, 90, 95, 100, 104, 111) and finally mathematical modeling of the in situ process (3, 6, 10, 11, 12, 28, 49, 54, 57, 81, 87, 92, 99, 106, 109). Work on the use of disposed spent shale can also be found in the literature (30, 62, 105).

(4) Properties and composition

A number of publications have appeared in areas related to the properties and composition of oil shale can be found in the literature (35, 37, 78, 79, 80, 89, 104). These data are largely on Western shale and include elemental analysis of the organic and mineral parts of the

shale, variations and comparative analysis of these properties. Properties such as density, permeability and porosity can also be found.

(5) Economics

Articles on the economics of proposed shale oil processes have appeared in the literature from time to time. An excellent article by Kaiser and Maass (117) discusses the many factors which must be taken into account to justify a large aboveground installation such as the Exxon-Tosco Colony Project. Among these are heat requirements, solid handling, engineering manhours, procurement problems, construction costs, safety and environmental problems. Sladek (88) presents a technology assessment for developments of this size and larger which included additional factors such as government policies, proposed legislation, land management, water availability, socioeconomic effects, regulatory disincentives, and the unreliability of cost estimates. In connection with the last of these, it is interesting that the 1.7 billion dollar cost he cites for a 50,000 barrel/day facility was increased less than two years later to 6 billion dollars (See Appendix D).

Less extensive economic studies on proposed modified in situ installations operating on Western shale may also be found in the literature (32, 51, 96).

There had been little experimental or theoretical work done on Antrim shale when Dow started the project with DOE. However, as a part of Dow's four year program to test the feasibility of using the true in situ process with Antrim shale, both experimental and theoretical work has been done. This work, together with the results of mining,

fracturing and field testing done by Dow are reported in quarterly progress reports published by the Department of Energy. Some of these reports are cited in the Bibliography (41, 98, 112). A number of papers on Antrim shale were also presented at the AIChE Annual Meeting in Detroit in August 1981 (1, 45, 54, 108).

Work on properties and composition of Antrim shale were done by Leedy and others, they reported that Antrim kerogen is a crosslinked polymeric structure consisting of roughly equal amounts of aromatic and aliphatic carbons (40). Ruotsala and others reported that in typical Antrim shale, the inorganic part is composed of 50-60% quartz, 20-35% illite, 5-10% kaolinite, 0-0.5% chlorite and 0.5% pyrite (83). Physical properties like density, porosity, permeability and thermal expansion were reported for Antrim shale by Hockings (38). A modified Fischer assay oil yield average of 4.67 gal/ton was reported by Leffert and others. They also reported the potential of Antrim shale to be 2.8 trillion barrels of oil (45).

Work on kinetics of kerogen decomposition and mathematical modeling were done by Crowl and Piccirelli (18, 20). They used the model of Tyner and Hammert (106) which was derived for Colorado shales, to true in situ energy production from Antrim shale. This model was discussed in Part A of Chapter Two.

CHAPTER FOUR

EXPERIMENTAL WORK

PART A. INTRODUCTION

Studies of the potential of true in situ processing have generally involved three different types of attack: field tests, mathematical modeling, and laboratory experimentation. Of these, field tests are by far the most expensive and are difficult to interpret since one cannot see what is going on underground. Modeling is interesting, but the reasonability of the results are highly dependent on the assumptions made. While the three types of attack are all important in bringing in situ processing close to the commercial stage, simulating underground condition experiments coupled with simplified mathematical modeling are relatively inexpensive and, if done first, yield reliable information which is needed to evaluate the advisability and feasibility of field tests.

This research was begun during the period in which Dow field tests were in progress. At that time, some laboratory work by others on Antrim shale was in progress, but it was largely directed toward finding the average chemical analysis of the organic and inorganic parts of the shale (38, 44), surveying the richness of Antrim shale from various sources by the Fischer assay method (45), and studying the kinetics of retorting using powder samples (17). Very little work had been done on chunk samples of Antrim shale simulating underground conditions. This

type of work was available in the literature on Western shale, and it could have been assumed that Antrim shale is similar to Western shale, but there is so much variation between the two sources that this would clearly have been a poor assumption. Even on Western shale, no work was found on the combustion of shale under overburden pressure, the behavior of shale at elevated temperatures, or the use of heat of combustion to evaluate the total energy recoverable, and not just the oil potential as measured by Fischer assay.

Laboratory scale experiments under a variety of operating conditions were devised and performed to investigate the possibilities and limitations of in situ production from Antrim shale. Several series of experiments were carried out, and are outline below as they appear in the thesis:

Part B. Sources and preparation of shale samples.

Part C. Experiments related to the accessibility of shale surface.

- C-1 Measurement of density and void space created in shale retorting.
- C-2 Expansion of shale as a result of retorting at atmospheric pressure.
- C-3 Compaction of shale as a result of retorting under mechanical pressure.
- C-4 Formation of cracks in the shale during retorting.
- C-5 Sealing of shale access surface at elevated temperatures.

Part D. Experiments related to the energy content of Antrim shale.

D-1 Measurement of heat of combustion.

D-2 Evaluation of Antrim shales on the basis of weight loss and heat of combustion.

Part E. Experiments related to the effects of temperature and nitrogen gas pressure during shale retorting.

E-1 Sequential runs.

E-2 Nonsequential runs.

Part F. Experiments related to the effect of overburden pressure during shale retorting.

F-1 Sequential runs.

F-2 Nonsequential runs.

Part G. Experiments related to the penetration of oxygen into spent shale and combustion of residual carbon.

G-1 Oxygen gas pressure and temperature effects, sequential runs.

G-2 Oxygen gas pressure and temperature effects, nonsequential runs.

G-3 Overburden pressure effect during spent shale combustion, sequential runs.

G-4 Overburden pressure effect during spent shale combustion, nonsequential runs.

PART B. SOURCES AND PREPARATION OF SHALE SAMPLES

The Antrim shale samples, intended for investigation, came from the Dow Chemical Company, Antrim Well #103, Sanilac County, Michigan. These Antrim samples are cylindrical cores 3.5 inches in diameter and came from a depth of 1191-1202 feet.

Colorado shale samples were obtained from Richard A. Martel of the Laramie Energy Center. Jordanian shale samples were obtained by the writer from outcrops at the El Lajune area.

Antrim shale samples, of 0.7 inch diameter and 1.5 inch high, were obtained by cutting the original 3.5 inch core sample, using a small core drill. Also, 0.7 inch diameter and 1.5 inch high cylindrical Colorado and Jordanian shale samples were obtained by cutting the original chunk samples (approximately 4x4x1.5 inches) using the small core drill.

A 200 ml alloy steel jar mill with alloy steel balls was used to pulverize the sample whenever the experiment required the use of powdered samples. In the combustion experiments, a pellet press was used to obtain pellet samples. The pellet press consisted of a 0.7 inch diameter steel rod fitted into a 0.7 inch diameter by 1.5 inch deep hole in a 4 inch diameter and 2 inch high steel cylinder.

Due to the significant variations of shale properties, an inspection, elimination, and selection sampling strategy was employed. An original large sample was visually inspected and selected, if it appeared to be reasonably representative and uniform. The 0.7 inch

small samples, resulting from the core drilling of the large one, were also visually inspected and were eliminated if:

(a) It showed richness in pyrite.

(b) It was not compact (many samples were broken during the drilling process).

(c) The light color of the sample indicated deficiency in organic content.

(d) The soft, oily texture of the sample indicated excessive richness in organic content.

After the elimination process was complete, representative 0.7 inch samples were randomly chosen among those obtained from a single 3.5 inch one and were used for a given set of experiments. In addition, duplicate samples were used in either simultaneous or consecutive runs, to assure that the samples were not unique in their behavior. Because of the limited number of 0.7 inch samples obtainable from a single 3.5 inch one, and the large variabiity of the latter, no attempt was made to treat the data statistically. The results should therefore be regarded as representing typical behavior of good Antrim shale samples, rather than average behavior of all material obtained in core drilling.

Except for the experiments on the behavior of shale at elevated temperatures, only reproducible and consistent experiments were reported.

PART C. EXPERIMENTS RELATED TO THE ACCESSIBILITY OF SHALE SURFACE

These experiments were conducted in order to obtain information useful in determining what paths could be made available for the flow of hot gases or oxygen into the formation, and for the flow of organic gases and vapors and products of combustion out of the formation. Five series of experiments were conducted as follows:

C-1 Measurement of density and void space created in shale retorting.

C-2 Expansion of shale as a result of retorting at atmospheric pressure.

C-3 Compaction of shale as a result of retorting under mechanical pressure.

C-4 Formation of cracks in the shale during retorting.

C-5 Sealing of shale access surface at elevated temperatures.

Experiments C-1. Measurement of density and void space created in shale retorting.

C-1.1 Purpose. The purpose of these experiments is to determine the fraction of void space created in the shale as a result of kerogen decomposition and evolution of the product gases and vapors from the rock.

C-1.2 Apparatus and Materials:

- 4x5x10 inch, 1832^{o}F (1000^{o}C) electric muffle furnace with L&N potentiometer control.
- Electric drying oven.

- Electric hot plate.
- 200 ml alloy steel jar mill with alloy steel balls.
- Torbal torsion analytical balance.
- 25 ml glass pycnometer with thermometer.
- Laboratory aspirator pump.
- Distilled water.
- Micrometer.
- 200 ml vacuum flask.
- 0.7 inch diameter and 1.5 inch high cylindrical Antrim shale samples cut with a small core drill from a single core sample 3.5 inches in diameter.
- 0.7 inch diameter and 1.5 inch high cylindrical Colorado and Jordanian shale samples cut from single chunk samples about 4x4x1.5 inches.

C-1.3 Procedure.

(a) A cylindrical sample was weighed on the analytical balance and measurements of diameter and height were taken with the micrometer. Geometric density was obtained by dividing the weight by the calculated volume of the cylinder.

(b) A second cylindrical sample was weighed. It was then placed in the electric furnace after preheating to 1112^{o}F (600^{o}C). It was removed from the furnace after two hours, cooled, weighed, and the percentage weight loss determined.

(c) The raw sample and the spent sample were each ground in the jar mill separately to approximately -325 mesh.

(d) A large portion of each ground sample was then transferred to the bottom of the vacuum flask covered with about

100 ml of distilled water. The flask was then placed on a hot plate and connected to the aspirator pump. After boiling under vacuum for one hour to remove all air in the pores, the slurry was cooled. The set up is shown in Figure 4-1.

(e) A portion of the slurry was then transferred to a 25 ml tared pycnometer and supernatent liquid poured into the top. After closing the pycnometer and wiping the tip, it was weighed on the analytical balance and the temperature noted.

(f) The pycnometer was then placed in the drying oven at 220°F (105°C) with the stoppers removed and left for 12 hours. At the end of this time, all visible moisture had evaporated leaving only the solid portion in the bottom of the pycnometer. (There was no visual evidence of deposition of additional solids from solution.)

(g) The pycnometer was then cooled and weighed, and the weight of solids and of water evaporated determined by comparison with the weight of the full pycnometer and the empty one. Also the volume of water evaporated was calculated from water density and the volume of solids remaining by difference.

(h) Using calculations of the type shown in Appendix A, densities of raw shale, of retorted shale, and of material lost in retorting were calculated along with the void space created by the retorting operation.

C-1.4 Results and Interpretation: Results of these experiments are shown in Table 4-1. The first column of the table gives the type of shale for which the determinations were made, namely Antrim, Colorado, or Jordanian, with the samples obtained and selected as described in

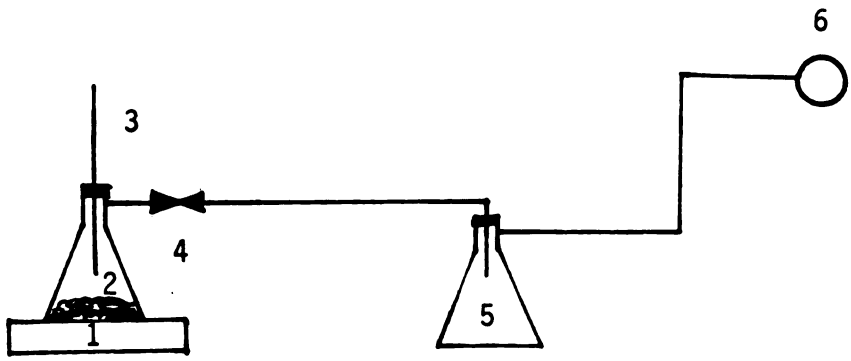

Figure 4-1. Sketch of apparatus for boiling shale slurry under vacuum (step (d) of procedure C-1.3).

1 Hot Plate

2 Shale Slurry

3 Thermometer

4 Screw Clamp

5 Condensate Collecter

6 Aspirator Pump

Table 4-1

Voids formed in retorting

Kind of shale	Solid material density, lb/ft^3			Weight loss %	Void fraction %
	Raw shale	Retorted shale	Material lost		
Antrim	140.6	160.8	61.8	9.16	20
Colorado	138.4	168.2	62.7	12.82	28
Jordanian	127.7	171.1	62.4	19.5	40

Part B. The second column gives the density of the solid material in raw shale, determined using ground material in the preceding procedures. The figure for Antrim shale (140.6) is in good agreement with the density of the chunk sample (139.9) obtained by weighing and micrometer measurement. The small difference indicates that pores in the original shale samples are largely filled with kerogen.

The third column gives the density of the solid material in the spent shale determined by the same procedure as above. The fourth column gives the apparent density of the material lost during retorting, calculated as shown in Appendix A, dividing weight loss by volume loss. The fifth column gives the percent weight loss and the sixth column the percent volume loss during retorting.

Calculation of the void volume assumes that the inorganic material in the original shale sample is the same as the inorganic material in the spent sample as well as the inorganic material left in the flasks after water evaporation. It also assumes that no significant amount of gas-filled closed pore volume is opened during retorting. The good agreement between the micrometer and pycnometer density measurements also indicates that no more than 0.005 of the original volume consists of closed gas-filled pores opened during grinding.

The density calculated for the material lost is in good agreement with values for the density of kerogen (68), and also of water, the most likely source of material loss during retorting. If the original shale had porosities in the range of 5 to 10% like some reported in the literature (38) the material lost would calculate to densities in the 80-120 lb/ft^3 range: a very unlikely situation. Also most inorganic decompositions would create much higher calculated densities than

actually found. Thus, the reasonableness of the values obtained support the reasonableness of the assumptions used in calculating them.

It should be noted that the percentage void volume created during retorting is different from a porosity obtained for example, by mercury penetration of the spent sample. As following experiments show, retorting at atmospheric pressure creates volume expansion and cracks easily filled in porosity measurement. Since we are interested in voids in the formation remaining after retorting in situ, the percentage void volume created is the more meaningful figure.

The results of density measurements of raw shale samples also show that the oil shale is more dense with less organic content and less dense with more organic content. This might indicate a theoretical relationship between the density of oil shale and its organic content. Smith reported just such a theoretical relationship for Colorado shales (89). This is supported by the fact that oil shale consists of a mineral fraction with a density near that of sedimentary rock (160-180 lb/ft^3) and an organic fraction with density about that of water.

The void fraction of the richest shale (Jordanian) is the highest, because retorting creates more pore structure in the richer shales.

Experiments C-2. Expansion of shale as a result of retorting at atmospheric pressure.

C-2.1 Purpose. The purpose of these experiments is to determine the percentage of shale expansion due to crack formation as result of retorting.

C-2.2 Apparatus and Materials:

- 4x5x10 inch, 1832^{o}F (1000^{o}C), electric muffle with furnace L&N potentiometer control
- Torbal torsion analytical balance
- Micrometer
- 0.7 inch diameter and 1.5 inch high cylindrical Antrim shale samples cut from a single core sample 3.5 inch diameter.
- 0.7 inch diameter and 1.5 inch high cylindrical Colorado and Jordanian shale samples cut from a single chunk sample about 4x4x1.5 inch.

C-2.3 Procedures:

(a) A set of core samples of Antrim, Colorado, and Jordanian oil shale were retorted in the electric furnace at temperatures of 932^{o}F (500^{o}C) and 1112^{o}F (600^{o}C) for two hours.

(b) The lengths of the samples were measured using a micrometer before heating, and the same samples were measured after heating and subsequent cooling.

C-2.4 Results and Interpretation: The results (Table 4-2) show that the length increase was the highest for the richest oil shale. An explanation for this might be the visually observed mechanism of the release of organic matter from the rock. When oil shale is heated at atmospheric pressure, the organic vapor migrates out of the rock through the openings of many minute cracks. The opening of these cracks is caused by the build-up of internal gas pressure from kerogen decomposition. It is expected that the length increase of the shale is due to those cracks. The richer the shale is, the more cracks will be opened.

Table 4-2

Expansion of oil shale chunk samples
resulting from retorting at atmospheric pressure

Kind of shale	At 932°F (500°C)		At 1112°F (600°C)	
	Length expansion %	Weight loss %	Length expansion %	Weight loss %
Michigan	2.8	8.91	2.82	9.37
Colorado	4.2	12.82	4.26	13.13
Jordanian	6.5	19.31	6.58	19.84

A similar explanation may account for the slight increase in expansion at higher temperatures. Since the organic part of oil shale consists of different organic compounds, some of which decompose around 932°F (500°C) and others around 1112°F (600°C), gas evolution and some crack formation may be expected over the entire range. At the higher temperatures, much of the gas evolved migrates mainly through the already developed cracks and so few new cracks appear.

This increase of length gives an additional porosity increase during the heating of rich oil shale at atmospheric pressure. This lengthening is expected to occur during field tests at outcroppings, but not underground, due to the effect of mechanical overburden pressure.

Experiments C-3. Compaction of shale as a result of retorting under mechanical pressure.

C-3.1 Purpose. The purpose of these experiments is to obtain information about the usefulness of void fraction created due to kerogen decomposition, by measuring the compaction of the shale.

C-3.2 Apparatus and Material:

- Electric 2 inch tube furnace
- Micrometer
- Torbal torsion analytical balance
- 0.7 inch diameter and 1.5 inch high cylindrical shale samples cut from a single core sample 3.5 inch diameter.
- 0.7 inch diameter and 1.5 inch high cylindrical Colorado and Jordanian shale samples cut from a single chunk sample about 4x4x1.5 inch.

C-3.3 Procedure.

(a) Core samples of Antrim, Colorado and Jordanian oil shales were retorted in the tube furnace under a weight, which simulated a pressure of 900 psig, at temperatures of 932^{o}F (500^{o}C) and 1112^{o}F (600^{o}C) for two hours. (See Figure 4-2).

(b) The lengths of the samples were measured using a micrometer before heating, and the same samples were measured after heating and subsequent cooling.

C-3.4 Results and Interpretation: The results of the compaction (Table 4-3) experiments show that very few of the pore structures created by the removal of organic material were closed physically by the mechanical pressure.

The results also show that the richest shale gave the greatest contraction and that the increased contraction was more than proportional to the increased weight loss. Spent Jordanian shale with the greatest loss was obviously softer and more friable than spent Antrim shale and with more pressure could be compacted to a much smaller volume. Antrim shale, on the other hand, was mechanically very strong after retorting, and as Table 4-3 indicates, could not be compacted to provide void volumes more than 1-2%. This is only a small fraction of the 20% voids shown in Table 4-1. The fine pore structure of spent Antrim shale was also reported by Hockings (38).

Also spent lean shale produces less porosity and is less likely to provide air or oxygen passages through the rock than rich shale. It may therefore be expected when treated with these gases to retain a higher proportion of carbon residues formed during retorting.

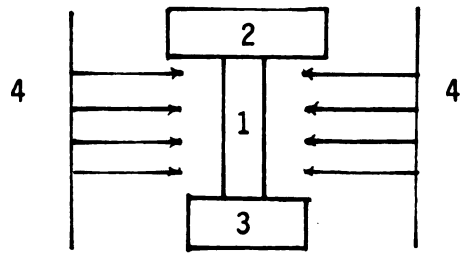

Figure 4-2. Sketch of the experimental set up for retorting under mechanical pressure (experiments C-2).

1 Core Shale Sample

2 Physical Weight

3 Stand

4 Tube Furnace Wall

→ Direction of Heat Flow

Table 4-3

Compaction of oil shale chunk sample
resulting from retorting under mechanical pressure

Kind of shale	At 932°F (500°C)		At 1112°F (600°C)	
	Length contraction %	Weight loss %	Length contraction %	Weight loss %
Michigan	1.53	8.52	1.67	8.73
Colorado	2.48	12.47	2.75	12.67
Jordanian	4.34	18.69	4.63	18.94

With a retorting temperature of 1112°F (600°C), the length contraction percent was slightly higher than at 932°F (500°C) because of the creation of more pore structures at the higher temperature.

Experiments C-4. Formation of cracks in the shale during retorting.

C-4.1 Purpose. The purpose of these experiments is to observe physical changes in the shale during retorting and their effect on the way in which organic material is released from the rock. Observations with and without mechanical pressure are to be made.

C-4.2 Apparatus and Materials:

- 4x5x10 inch, 1832°F (1000°C) electric muffle furnace with L&N potentiometer control.
- Torbal torsion analytical balance.
- 0.7 inch diameter and 1.5 inch high cylindrical Antrim shale samples cut with a small core drill from a single core sample 3.5 inch in diameter.
- Stainless steel pressure clamp (See Figure 4-3). It was designed with three bolts for the best equalization of pressure. The bolt shafts are made of soft steel and have necks turned to a diameter such that the yield point load will be in the range of the desired overburden pressure (about 1500 feet). The pure aluminum inserts above and below the sample expand more than the steel during heating and this keeps the pressure on the sample during operation. In addition aluminum under the operation temperature is soft enough to absorb minor surface irregularities and help distribute the load evenly.

C-4.3 Procedure.

(1) Without mechanical pressure

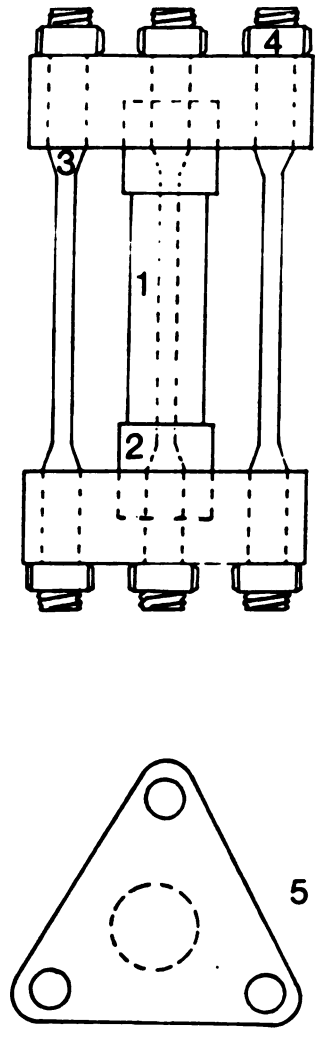

Figure 4-3. Schematic of pressure clamp

1 Cylindrical Shale Sample (one piece)
2 Pure Aluminum Inserts (two pieces)
3 Steel Shaft (three pieces)
4 Nuts (six pieces)
5 Clamp Ends (two pieces)

(a) An Antrim core shale sample was wrapped with aluminum foil (to reduce combustion effect) except at the top and was weighed and put in the furnace.

(b) The furnace was switched on and was allowed to heat up to $932^{o}F$ ($500^{o}C$) and was maintained at that temperature for one hour.

(c) The furnace was switched off, and the sample was removed, cooled, and weighed after unwrapping the aluminum foil.

(d) The same retorted sample without the aluminum foil was put back in the furnace and steps (b) and (c) were repeated.

The same procedure was followed for 0.7 and 3.5 inch diameter samples.

(2) With pressure clamp

(a) A 0.7 inch diameter weighed Antrim core sample was wrapped with aluminum foil and put in the pressure clamp.

(b) The pressure clamp with the sample was put in the furnace.

(c) The furnace was switched on and was allowed to heat up to $932^{o}F$ ($500^{o}C$) and then maintained at the temperature for one hour.

(d) The furnace was switched off, the pressure clamp and the aluminum foil were removed and the sample was weighed.

Using the same retorted sample, the same procedure was repeated except that the sample was retorted in air (with no aluminum foil).

C-4.4 Results and Interpretation: Figure 4-4 shows a side view of a 3.5 inch diameter Antrim shale sample after retorting without mechanical pressure and with aluminum wrapping. Figure 4-5(a) shows the top view of the sample before retorting. Figure 4-5(b) shows a cross-section of the same sample after retorting. The same sample was further retorted without the aluminum foil. Figure 4-6 shows the appearance of the sample after it was cut vertically. Figure 4-7 shows a side view of a sample retorted under mechanical pressure with aluminum foil wrapping. Figure 4-8 shows a cross-section of the same sample after it was further retorted without aluminum foil wrapping and with mechanical pressure.

As shown in Figure 4-4, many horizontal cracks were created and it was observed that the organic material was released along these cracks. Thus the mechanism for the release of organic matter from the shale is the opening of many minute horizontal cracks along the bedding plane of the shale. The opening of these cracks is caused by the building up of internal pressure of gas from kerogen decomposition. The release of organic material occurred horizontally and through the cracks which developed on heating. The following observations are in support of this mechanism.

(a) It took less time to evolve the organic material from a 3.5 inch diameter than from a 0.7 inch diameter.

(b) When the sample was split along one of the many cracks, it appeared that the crack did not go all the way through the sample surface and therefore, the split was part light and part dark. This observation is shown in Figure 4-5.

When the sample was retorted in air and cut vertically, multiple layers of dark and light were seen. This is illustrated in Figure 4-6.

Figure 4-4. Horizontal cracks created when Antrim shale sample was retorted with aluminum foil wrapping and without mechanical pressure.

(a)

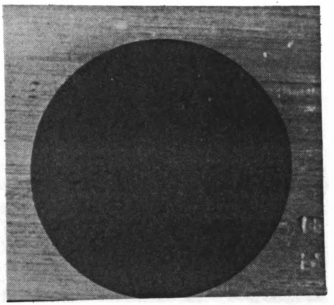

(b)

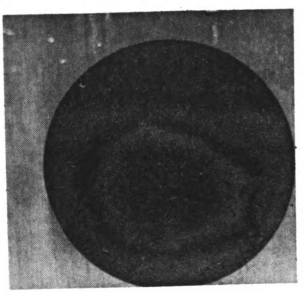

Figure 4-5. (a) The same sample of Figure 4-4 before retorting.
(b) The same sample of Figure 4-4 after it was split along one of the many cracks created as a result of retorting.

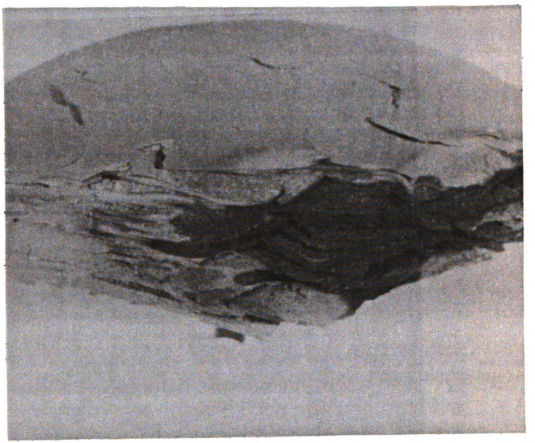

Figure 4-6. The appearance of the same sample of Figure 4-4 after it was further retorted without aluminum foil wrapping and without mechanical pressure.

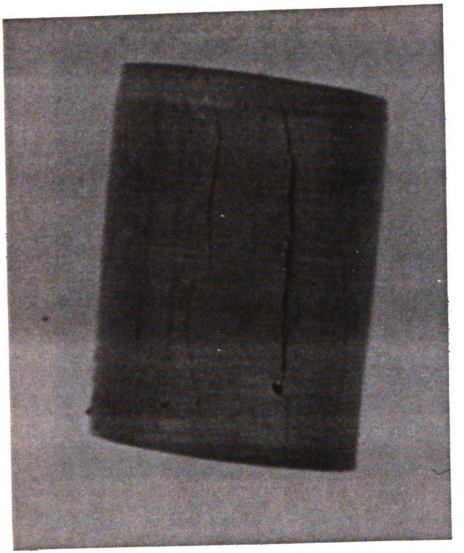

Figure 4-7. Shallow vertical crack created when Antrim shale sample was retorted with aluminum foil wrapping and with mechanical pressure equivalent to 1500 feet.

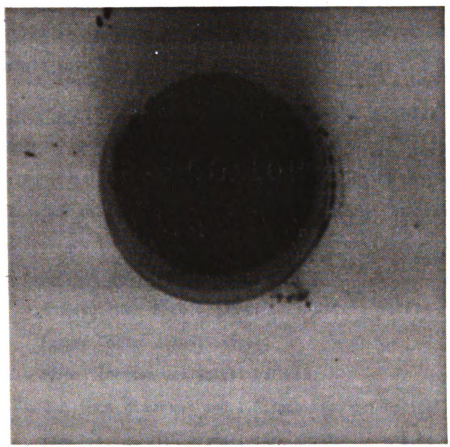

Figure 4-8. The same sample of Figure 4-7, sawed horizontally after it was further retorted without aluminum foil and with mechanical pressure equivalent to 1500 feet.

It appears that air penetrated through the horizontal cracks which were created during retorting and the air only reacted with the residual carbon at the surface of the crack.

When mechanical pressure was used the opening of horizontal cracks was prevented. However, one shallow vertical crack did open (See Figure 4-8) possibly caused by the building up of internal gas pressure. After the sample was further heated in air, it appeared that the air penetation occured only in a thin zone near the external surface of the core sample as shown in Figure 4-8.

Experiments C-5. Sealing of shale access surface at elevated temperatures.

C-5.1 Purpose. The purpose of these experiments is to investigate the behavior of shale at elevated temperatures, because elevated temperatures are likely to occur in the underground combustion of shale.

C5.2 Apparatus and Materials:

- 6x8x10 inch 3000^{o}F (1649^{o}C) electric muffle furnace with Barber Colman potentiometer.
- Torbal torsion analytical balance.
- 0.7 inch diameter and 1.5 inch high cylindrical Antrim shale samples cut with a small core drill from a single core sample 3.5 inch in diameter.
- 2.5x1.5x0.25 inch Antrim shale sample cut with a 10 inch diamond saw from 3.5 inch cylindrical sample.

C-5.3 Procedures.

Experiment 1

(a) An Antrim shale sample of 2.5x1.5x2.5 inch was weighed and put in the furnace.

(b) The furnace was switched on and allowed to heat up to 1800°F (982°C), then maintained at that temperature for 24 hours.

(c) The furnace was allowed to cool down to room temperature and the sample was removed and weighed.

Experiment 2

(a) The same size sample of that used in experiment 1 was put in the furnace, which was already preheated to 1800°F (982°C).

(b) The furnace was maintained at that temperature for 24 hours.

(c) The sample was then removed, cooled, and weighed.

Experiment 3

(a) An Antrim shale sample 0.7 inch in diameter was weighed and put in the furnace.

(b) A teaspoon of salt (NaCl) was thrown around the sample with some portion landing on the sample.

(c) The furnace was switched on, allowed to heat up to 2000°F (1093°C), and maintained at that temperature for 24 hours.

(d) The furnace was allowed to cool down to room temperature. The sample was then removed and weighed.

Experiment 4

The same procedure of experiment 3 was repeated except no salt was added.

Experiment 5

(a) A weighed Antrim core sample was put in the furnace, which as already preheated to 2300°F (1260°C).

(b) The furnace was maintained at that temperature for 24 hours.

(c) The sample was then removed, cooled and weighed.

C-5.4 Results and Interpretation

Experiment 1.

The weight loss percent was 11.27. A picture of the sample used in this experiment is shown in Figure 4-9. It was found that glazing occurred on the external surface of the sample, thus causing sealing of the access surface and preventing cracks from occurring. In underground in situ conditions, combustion temperatures around 1800°F (982°C) are likely. Smith reported a combustion temperature range of 1800 - 2200°F for in place combustion of Colorado oil shale (90). Duvall in a laboratory study of true in situ combustion of Colorado oil shale, observed a maximum combustion temperature of 2200°F (1204°C) in the fracture space (24). In its field test on Antrim shale, Dow reported that the temperature in the cavity got so high that the thermocouple burned out (98) and that Hastelloy parts melted (melting point 2300°F (1260°C)). Therefore, the same phenomena of glazing could easily occur. This glazing would eliminate permeability and prevent migration of air in and/or product out of the shale.

Experiment 2

The weight loss due to heating this sample was 3.1 percent. Slight glazing of the access surface occurred. However, since heating

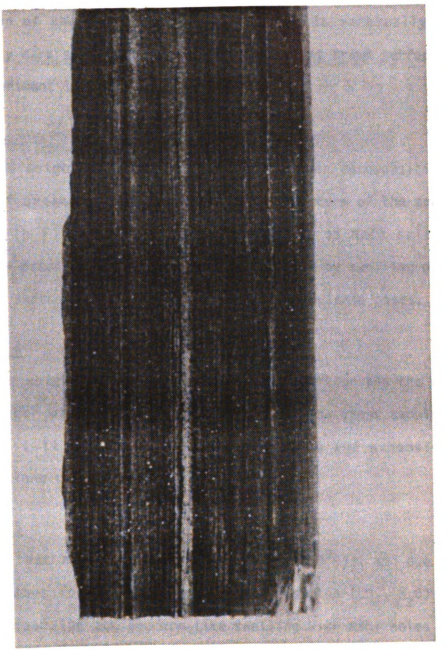

Figure 4-9. Antrim shale slab heated at 1800°F for 24 hours causing glazing of the external surface.

occurred suddenly, sealing of the access surface prevented the product vapor from migrating out of the rock and, therefore, the weight loss was only 3.1%, as compared to 11.27% when the heating process was slow. Inspection of the spent sample, by cutting it vertically, showed a completely dark surface as compared to the light brown surface observed as in experiment 1.

Experiment 3

The weight loss percent due to kerogen decomposition and the release of organic vapor was about 11%. A picture of the spent sample is shown in Figure 4-10. In the presence of NaCl salt, glazing apparently occurred much more rapidly, followed by swelling of the core sample and shattering of the glazed surface to release gases.

Experiment 4

The weight loss due to kerogen decomposition and the release of organic vapor was about 11% and a picture of the spent sample is shown in Figure 4-11. Slight glazing took place and expansion caused splitting along the natural cracks.

Experiment 5

At that high a temperature (2300^{o}F 1260^{o}C)), and due to sudden heating, gases formed by inorganic decomposition (CO_2, H_2O) caused an internal expansion and popcorn-like swelling with many holes formed at the outer surface. The expansion caused a volume increase of about four times the original size.

C-5.5 Summary

Due to the great variation in the composition of the mineral fraction of Antrim shale, many of the above mentioned experiments could not be consistently repeated.

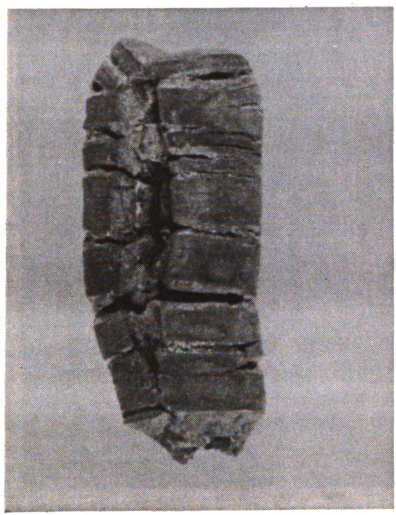

Figure 4-10. Antrim shale cylindrical sample heated at 2000°F for 24 hours in the presence of sodium chloride, causing glazing, swelling and shattering of the sample.

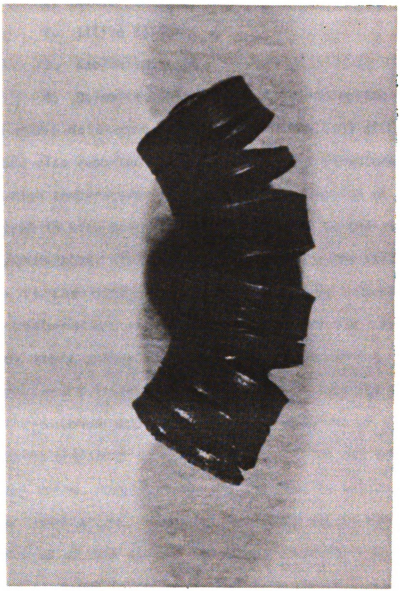

Figure 4-11. Antrim shale cylindrical sample heated at 2000°F for 24 hours, causing slight glazing and uneven expansion with opening of natural fractures along the bedding planes.

Ruotsala (83) showed that the mineral fraction of Antrim shale, which makes up about 90% of the weight of the shale, typically varies in composition as follows:

1. Quartz 50-60%
2. Illite 20-35%
3. Kaolinite 5-10%
4. Dolomite, chlorite, calcite and pyrite 0-5%

The above data were taken from one well at different depths. Mackenzie (52) also reported that the thermal and structural behavior of minerals at high temperatures is a very strong function of composition.

In true in situ processes heat is brought to the kerogen by heat transfer (conduction) through the formation. The driving force for conduction is the difference in temperatures between the normal formation temperature and the temperature in the cavity (surface temperature) where combustion of the gases is occurring. Thus, a high surface temperature increases heat penetration into the shale, (Figure 2-9) but if the temperature is too high, sealing of the surface can occur preventing transport of evolved gases both in and out of the rock.

It was noted, however, that all the samples tested did not glaze at the same temperature. This is apparently due to variations in the mineral make-up of the shale. It would therefore be advisable to perform glazing experiments on samples from any well which is proposed for field testing in order to determine what cavity temperature is allowable. Once that temperature is determined, models like the central cavity model (Chapter Two) can be applied.

PART D. EXPERIMENTS RELATED TO THE ENERGY CONTENT OF ANTRIM SHALE

These experiments were conducted in order to obtain information about the amount of energy produced as a result of penetration of heat into shale followed by kerogen decomposition during retorting under conditions simulating in situ process. Two series of experiments were conducted as follows:

D-1 Measurement of heat of combustion of Antrim shale.

D-2 Evaluation of Antrim shale on the basis of weight loss and heat of combustion.

Experiments D-1. Measurement of heat of combustion of Antrim shale.

D-1.1 Purpose. The purpose of these experiments is to determine the energy content of Antrim shale powdered, pellet and chunk samples. The amount of ignition agent needed for the complete combustion is also to be determined.

D-1.2 Apparatus and Material.

- Emerson fuel calorimeter (Parr bomb), which consists of two hemispherical cups joined by a heavy stainless steel closing nut. (See Figure 4-12).
- 2 inch diameter metallic pan.
- Torbal torsion balance.
- Fuse wire.
- Spanner wrench.
- Oxygen cylinder.

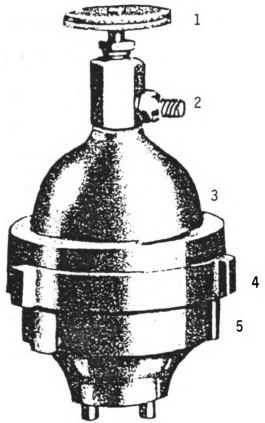

Figure 4-12. Emerson fuel calorimeter (Parr bomb)

1 Valve

2 Oxygen at 300 psig, Inlet Line

3 Upper Hemispherical Stainless Steel Cup

4 Stainless Steel Closing Nut

5 Lower Hemispherical Stainless Steel Cup

- 1900 grams of water
- Bucket
- Electric stirrer
- Thermocouple.
- 200 ml alloy steel jar mill with alloy steel balls.
- Pellet press. The pellet press consists of a 0.7 inch diameter steel rod fitted into a 0.7 inch diameter and 1.5 inch deep hole in a 4 inch diameter and 2 inch high steel cylinder.
- Naphthalene as an ignition agent with heat of combustion of 17,000 Btu/lb.
- 0.7 inch diameter and 1.5 inch high cylindrical Antrim shale samples cut with a small core drill from a single core sample 3.5 inches in diameter.

D-1.3 Procedure.

(a) The sample (pulverized, pellet or chunk) was weighed an placed in the metallic pan.

(b) Naphthalene was also weighed and placed in the same metallic pan. The naphthalene to shale ratio was 1:1.

(c) The pan was placed in the Parr bomb.

(d) A piece of fuse wire was connected from the terminal of the fuel pan support to the binding post on the opposite side of the bomb. The wire was of sufficient length to dip down and make contact with the sample and with the naphthalene.

(e) The upper half of the bomb was placed in position, and the closing nut screwed, then tightened by using a spanner wrench.

(f) The bomb was gradually filled with oxygen up to 300 psig pressure.

(g) The bomb was then immersed in water to detect any possible leakage.

(h) 1900 grams of water was placed in the calorimeter bucket.

(i) The bomb was then placed in the bucket and the stirrer and the thermocouple were lowered into position.

(j) The terminal of the ignition wire leads were connected to the bomb.

(k) The stirrer was switched on and allowed to run for five minutes to equalize the temperature throughout the calorimeter.

(l) The ignition system was switched on to allow the combustion to start.

(m) Temperature readings were taken for the next five minutes.

(n) From the measured temperature rise of the water the heat of combustion of the shale-naphthalene mixture was calculated. Using this value and the standard heat of combustion of naphthalene, the heat of combustion of the shale was calculated. Then the same procedure was repeated for naphthalene to shale ratio of 1:2, 1:3, 1:4, 1:5 and with no naphthalene for each type of sample (pulverized, chunk and pellet). For more detailed procedure, see the operation manual (25).

D-1.4 Results and Interpretation. The results are shown in Table 4-4. For the chunk, pellet and pulverized samples used, it was shown that best combustion occurs at a naphthalene to shale ratio of 1:1. Above that limit, adding naphthalene does not improve the combustion. Only the pulverized sample can be burned partially without the addition of naphthalene. Inspection of the spent pulverized samples after combustion experiments without naphthalene showed that the combustion did not occur completely and some unburned carbon was found with the ash. Additional heat of combustion experiments were performed on some of the spent samples. For example, for a pulverized sample the first run without naphthalene gave a heat combustion of 918 Btu/lb. The second run on the spent sample gave 204 Btu/lb. with naphthalene to shale ratio of 1:1. Thus, the total of these two experiments is just slightly higher than the single experiment with naphthalene to shale ratio of 1:1. The third run showed no improvement. The heat of combustion of chunk samples were about half of that of powdered samples. Inspection of the spent chunk samples showed that the combustion only took place near the external surface (the interior of the sample was completely dark).

The heat of combustion used to evaluate the energy contents of shale in this thesis was based principally on runs with a naphthalene to pulverized shale ratio of 1:1.Less combustion occurred at lower ratios, but above this ratio the combustion did not improve.

Table 4-4

Heat of combustion of pulverized, pellet and chunk Antrim shale samples measured at different naphthalene to shale ratio

Naphthalene to shale ratio	Heat of combustion Btu/pound of shale		
	Pulverized sample	Pellet sample	Chunk sample
1:1	1117	973	537
1:2	1063	824	466
1:3	1038	733	431
1:4	1002	706	417
1:5	984	682	403
No Naph.	913	0	0

Experiments D-2 Evaluation of Antrim shale on the basis of weight loss and heat of combustion.

D-2.1 Purpose. The purpose of these experiments is to establish a correlation between the loss of energy and the loss of weight as a result of kerogen decomposition during retorting.

D-2.2 Apparatus and Materials: In addition to the apparatus and materials used in experiments D-1, the following are used in this series of experiments.

- 4x5x10 inch, 1832^{o}F (1000^{o}C) electric muffle furnace with L&N potentiometer control.

D-2.3 Procedure.

(a) Three Antrim core samples were separately dried, weighed and heated for one hour at 752^{o}F (400^{o}C), 932^{o}F (500^{o}C) and 1112^{o}F (600^{o}C) temperatures.

(b) The weight loss percentage due to retorting was determined

(c) The three spent samples were separately pulverized using the jar mill.

(d) The heat of combustion of these spent samples were separately determined using the procedure of the previous section. Naphthalene to shale ratio of 1:1 was used.

(e) The heat of combustion of a raw Antrim shale sample was also determined as in (d).

D-2.3 Results and Interpretation. The results are shown in Table 4-5 and Figure 4-13. The first column shows the temperature of retorting. In the second column is the percentage of weight loss due to retorting,

Table 4-5

Reduction in heat of combustion of Antrim shale as a function of retorting weight loss

Temp.	Retorting weight loss fraction	Heat of combustion of retorted shale Btu/lb of sample	Reduction in heat of combustion Btu/lb of raw sample		Heat of combustion Btu/lb of material evolved
			exper.	correl.	
752°F (400°C)	0.051	521	596	595	11686
932°F (500°C)	0.078	293	824	828	10564
1112°F (600°C)	0.101	144	973	972	9633

Heat of combustion of raw sample = 1117 Btu/lb shale

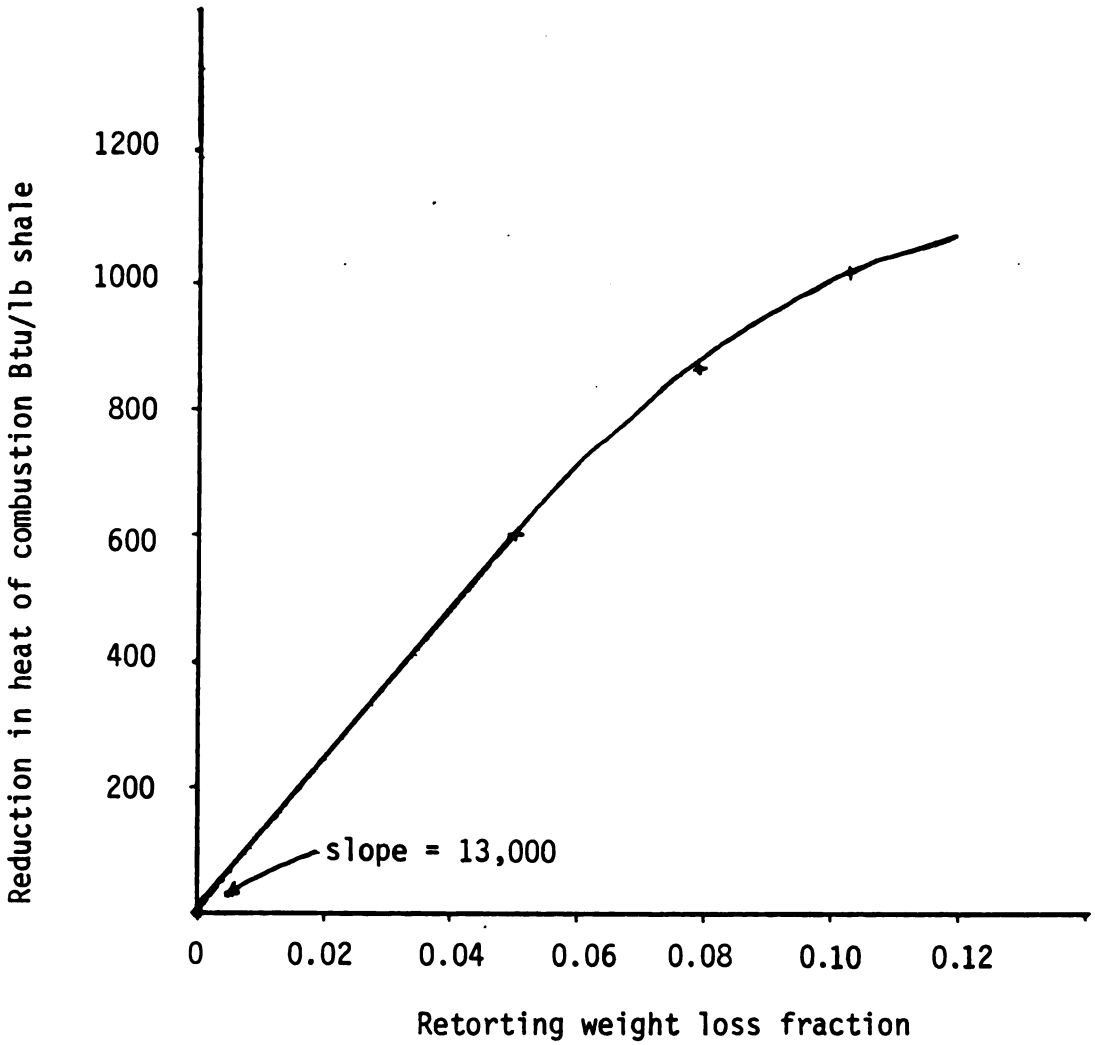

Figure 4-13. Reduction in heat of combustion of Antrim shale as a function of retorting weight loss.

\+ Experimental points from Table 4-5

——— Correlating equation

$$y = 13{,}000\,x - 74{,}500\,(x)^{2.35}$$

measured as the difference between the weights of the sample before and after retorting. The third column is the heat of combustion of the retorted sample. The fourth column obtained by the difference between the experimental heat of combustion of raw shale and that of the spent sample corrected back to the original weight. Also shown is the same value based on the correlation of Figure 4-13. The last column, the heat of combustion of the organic matter is obtained by dividing the experimental reduction of heat of combustion by the weight loss fraction.

The results shown in Figure 4-13 and Table 4-5 show a considerable difference between the reduction in the heat of combustion of Antrim shale per pound of material evolved at the beginning of retorting versus at the end of retorting. As the retorting progress, the heating value per pound of material evolved presented by the slope of the curve is decreasing.

A correlation

$$= 13{,}000x - 74{,}500(x)^{2.35} \qquad \text{Eq 4D-1}$$

was derived to correlate the heat of combustion of material evolved to the percentage weight loss. Using the correlation the slope of the curve at 0.0 and 0.1 weight fraction are calculated to be 13,000 and 5780 Btu/lb of material evolved. The value of 13,000 at zero weight loss agrees with heat of combustion of kerogen calculated on the basis of elemental analysis of kerogen published in the literature (83). The calculation is shown in Appendix B.

The reduction of the heating value of product as retorting progresses might be explained from the fact that at low temperature, the part of the kerogen decomposed is largely hydrocarbon in nature, and as

the temperature increases, it is asphaltic type residue that decompose to give some water and other oxygenated compounds. This would be consistant with the data of Table 4-1 which shows a liquid density of the material evolved of about 62 lb/ft^3. Another explanation would be that the decrease of the heating value is due to the endothermic reaction of kerogen. However, the endothermic reaction of kerogen is only 144Btu/lb of kerogen (9,20,87); therefore, the heat of reaction of kerogen will not be a significant heat sink in the decrease of the heating value of the products.

Another possible endothermic reaction would be decomposition of carbonates. However, the principal carbonate present, calcite, has a heat of reaction of 500 Btu/lb (9) or less than 10 Btu/lb of shale (Antrim shale has 0-2% calcite (38,83)). Therefore, this amount does not represent an appreciable effect on the decrease of the heating value of the product.

It is also possible that part of the H_2O evolved as the temperature rises comes from loss of hydration of the illite rather than from decomposition of the asphaltic residues of kerogen. It is reported that some decomposition of this sort occurs in natural illites in the range 600 to 1100^oF (52,104). The effect would be essentially the same whether the H_2O evolved came from the kerogen or the illite.

The method of heat of combustion for assaying Antrim shale is better for the purposes of this thesis than the most commonly used method of Fischer assay (95). The Fischer assay method is valuable for estimation the amount of oil recoverable from the shale. However, since in situ energy production from Antrim shale is expected to be largely in

the form of hot and combustible gases, heat of combustion give the required information more directly.

Correlation equation 4D-1 is useful in converting weight loss fraction to the energy released during retorting, and this correlation permits measurements of weight loss only in most of the experiments of this thesis.

PART E. EXPERIMENTS RELATED TO THE EFFECTS OF TEMPERATURE AND NITROGEN GAS PRESSURE DURING SHALE RETORTING

These experiments were conducted in order to obtain information about the effects of nitrogen gas pressure during retorting of shale. Two series of experiments were conducted as follows:

E-1 Temperature and nitrogen gas pressure effects during shale retorting, sequential runs.

E-2 Temperature and nitrogen gas pressure effects during shale retorting, nonsequential runs.

Experiments E-1. Temperature and nitrogen gas pressure effects during shale retorting, sequential runs.

E-1.1 Purpose. The purpose of these experiments is to determine the amount of combustible material released as a result of retorting under a variety of temperatures and nitrogen gas pressures: 572°F (300°C), 752°F (400°C), 932°F (500°C), and 1112°F (600°C), and 600 psig, 300 psig, and 15 psig. These runs were sequential in the sense that the same shale sample was subjected to a series of increasingly severe treatments. This eliminated the effect of variations in shale properties. It also gives a direct measure of the effects of increased temperature and lowered gas pressure.

E-1.2 Apparatus and Materials:

- Reactor, a special type stainless steel reactor was constructed with a special closure which makes it capable of withstanding pressures up to 2000 psig at temperatures up to

1472°F (800°C). A photograph of the reactor with the closure is shown in Figure 4-14 and a dimensional drawing in Figure 4-15.

- 4x5x10 inch, 1832°F (1000°C) electric muffle furnace with L&N potentiometer control.
- Torbal torsion analytical balance.
- 0.7 inch diameter and 1.5 inch high cylindrical Antrim shale samples cut with a small core drill from a single core sample 3.5 inch in diameter.
- Nitrogen gas cylinder.
- Wet test meter.

E-1.3 Procedure:

(a) An Antrim core sample was weighed and put in the reactor.

(b) The reactor was placed in the furnace.

(c) The inlet pipe of the reactor was connected to the nitrogen gas cylinder regulated at 600 psig. The needle valve on the outlet pipe of the reactor was slightly opened to prevent back pressure on the nitrogen cylinder. The outlet pipe was connected to the wet test meter.

(d) The furnace was switched on and was allowed to heat up to 572°F (300°C) and was maintained at that temperature for half an hour. The wet test meter indicated a flow of 1.4 liter/min and no pressure rise on the nitrogen cylinder was noticed.

(e) The outlet valve was shut and the nitrogen cylinder was disconnected.

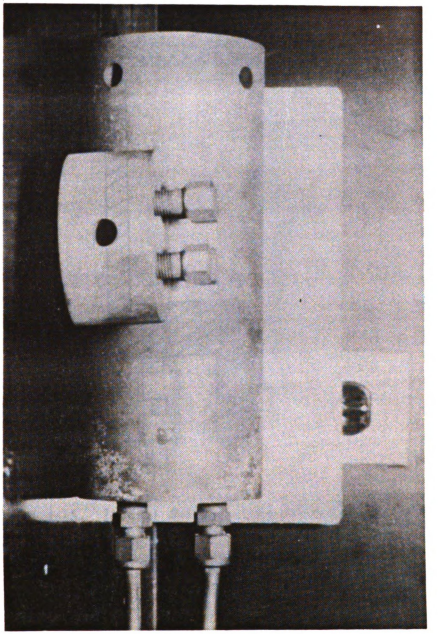

Figure 4-14. Stainless steel type 316 flow reactor with high pressure closure, used for retorting and combustion of shale.

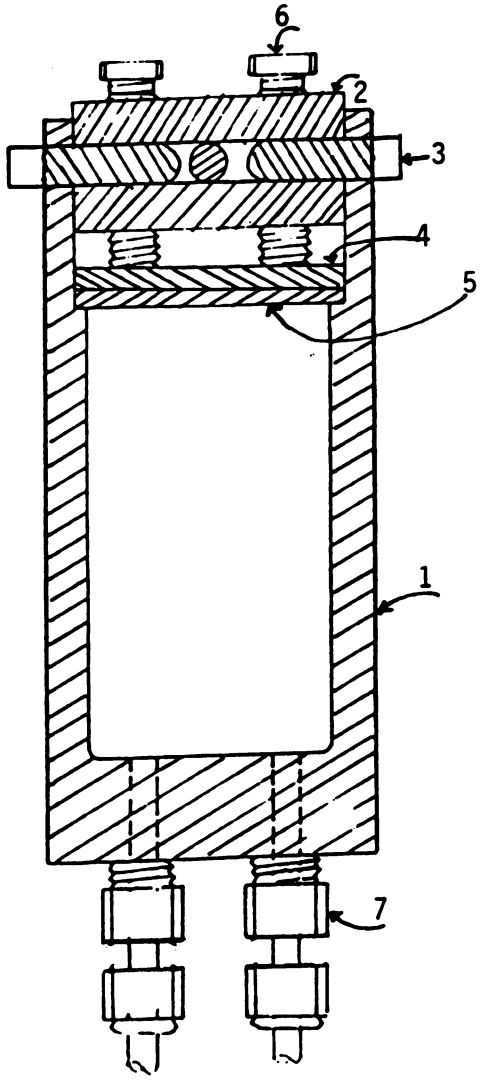

Figure 4-15. Special design, type 316 stainless steel reactor (200 psig pressure tested).

1 Reactor Shell 3" OD x 2.25" ID x 7.25" long.

2 Reactor Head 2.25" diameter x 1.25" thick.

3 Retaining Rods 0.375" diameter, one long and two short.

4 Closure Plate 2.5" diameter x 0.25" thick.

5 Aluminum Gasket 2.5" diameter x 0.125" thick.

6 Bolts, 4 required, 0.375" diameter.

7 Swagelok Fittings to Tubing, 2 required.

(f) The reactor was removed from the furnace and cooled to room temperature.

(g) The sample was removed from the reactor and weighed.

(h) Steps (b)-(g) were repeated using the same sample, giving an additional half hour of heating.

(i) The same procedure (b)-(h) still using the same sample, was repeated for two periods of half hours each at pressures of 300 psig and 15 psig keeping the temperature at 572^{o}F (300^{o}C).

(j) Still using the same sample, the entire procedure (b)-(i) was repeated for temperatures of 752^{o}F (400^{o}C), 932^{o}F (500^{o}C), and 1112^{o}F (600^{o}C).

(k) The sample was labeled and saved to be used again in oxygen penetration Experiments G-1.

E-1.4 Results and Interpretation: The results of this experiment are shown in Table 4-6 and Figures 4-16 and 4-17. Figure 4-16 was constructed by taking the total organic material loss of 10.54 as the available amount for retorting at time zero and then subtracting from that the weight loss after each consecutive half hour period. Figure 4-17 was constructed by plotting the weight loss for each half hour period as a function of time.

The results show that the release of organic matter occurred mainly in the first time period at each temperature. The high internal pressure produced by the vapor product caused the development of a network of small cracks, through which the vapor evolved quickly. For the second half hour at the same temperature, very little additional vapor was released. Because kerogen consists of different organic materials, and those materials decompose at different temperatures, one

Table 4-6

Weight loss of one shale sample undergoing a sequence of nitrogen gas pressure, time and temperature changes (sequential runs)

Temp.	Weight loss % 600 psig N_2		Weight loss % 300 psig N_2		Weight loss % 15 psig N_2		Accum. weight loss %
	1/2 hr	1/2 hr	1/2 hr	1/2 hr	1/2 hr	1/2 hr	
572°F (300°C)	0.84	0.27	0.07	0.03	0.08	0.03	1.32
752°F (400°C)	1.02	0.31	0.12	0.04	0.13	0.05	2.99
932°F (500°C)	2.93	1.16	0.21	0.07	0.22	0.08	7.65
1112°F (600°C)	1.78	0.73	0.15	0.03	0.16	0.03	10.54

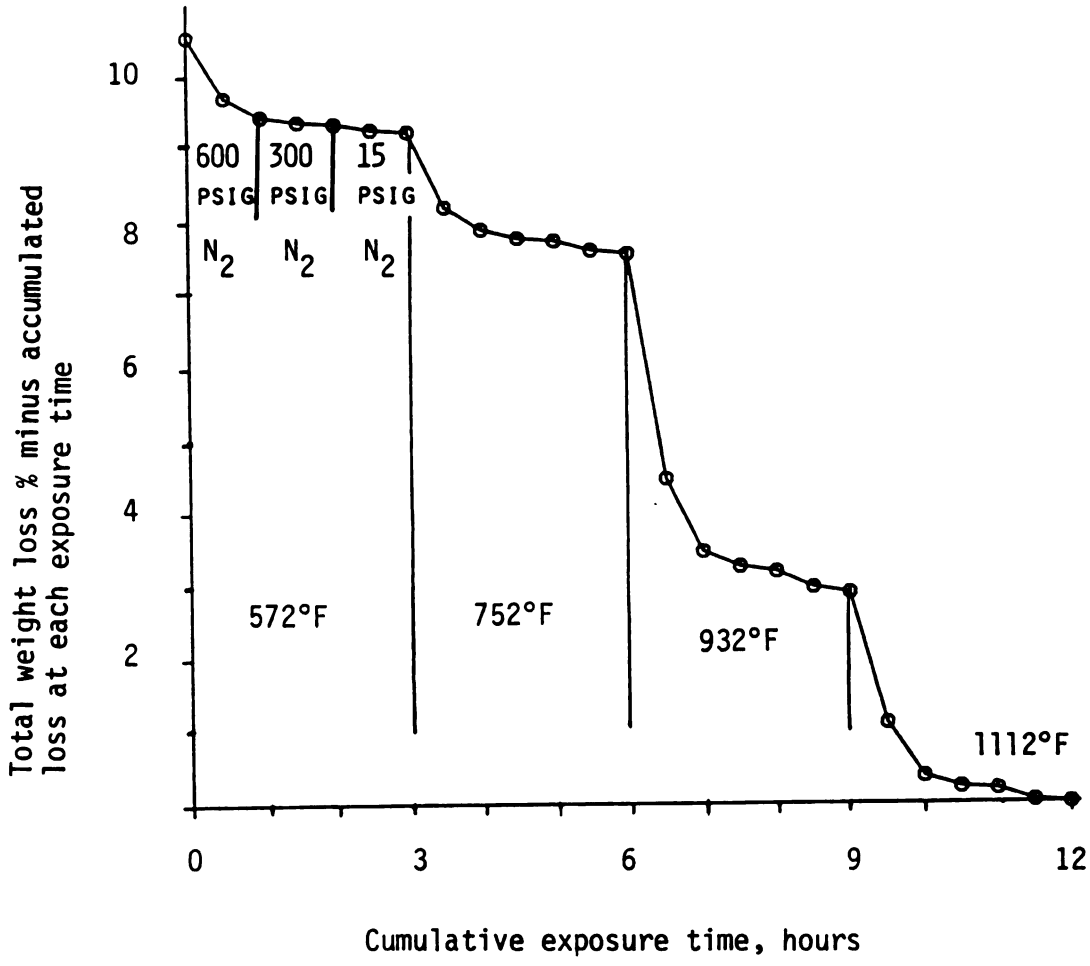

Figure 4-16. Retorting weight loss remaining in Antrim sample throughout a sequence of increasing severe treatments.

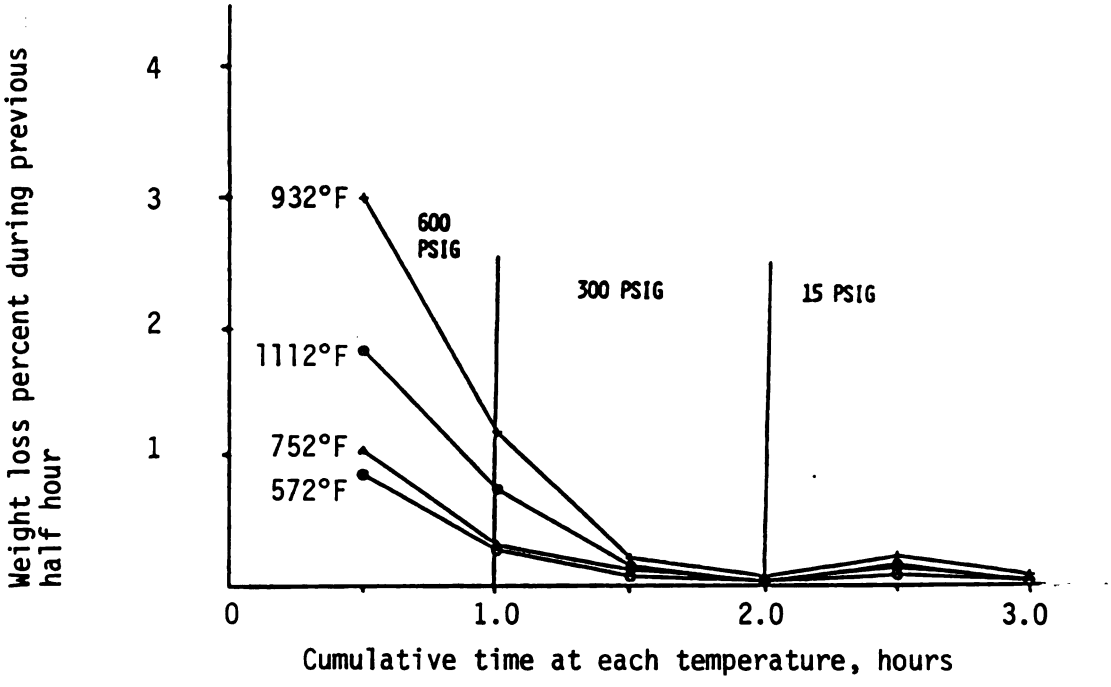

Figure 4-17. Weight loss percent in half hour intervals for Antrim shale sample retorted at different temperatures under a sequence of nitrogen gas pressures: 600, 300 and 15 psig.

must raise the temperature before another significant evolution takes place. For example, at 572°F (300°C) the weight loss percent after the first half hour is 0.84 and the next half hour is only 0.27 (Table 4-6). However, when the temperature was raised to 732°F (400°C), the same sample produced 1.02 weight loss percent in the first half hour. More kerogen decomposition takes place at 932°F (500°C) than at either 752°F (400°C) or 1112°F (600°C) (See Figure 4-17).

The results in Table 4-6 show that high inert gas pressure does retard evolution of combustible material. It can be observed that in every case when the pressure was lowered from 300 psig to 15 psig at constant temperature (See Figure 4-17) there was an increase in organic material released. Similar results were observed by Carpenter and Sohns on Colorado shales (16). They reported that in an inert retorting atmosphere (nitrogen), increasing gas pressure decreases oil yield. However, no explanations of the mechanism were suggested. Campbell and others observed that decreasing the heat rate of the shale increased the coking reaction and therefore decreased the yield (11). Campbell and others also suggested that during retorting, the coking and cracking reactions are competing each other (11). This type of competition between coking and cracking reactions may offer some explanations of their reduced oil yields. However, coking would not account for the release of additional organics when the pressure was released. It appears that some of the organic material remaining in the shale at 300 psig must have vapor pressures or decomposition pressures between 15 psig and 300 psig.

Experiments E-2. Temperature and nitrogen gas pressure effects during shale retorting, nonsequential runs.

E-2.1 Purpose: The purpose of these experiments is to determine the amount of combustible material released as a result of retorting under a variety of temperatures and nitrogen gas pressures: 572°F (300°C), 752°F (400°C), 932°F (500°C), and 1112°F (600°C), and 600 psig, 300 psig, and 15 psig. These runs were nonsequential in the sense that the retorting under nitrogen gas pressure was carried out using a new sample at each temperature, gas pressure and exposure time. The samples were carefully selected as described in Part B in order to reduce the effect of shale variations. Nonsequential runs give the total retortable organics at a given exposure time, temperature and nitrogen gas pressure, while the sequential runs give the additional amount retorted at the new condition.

E-2.2 Apparatus and Materials:

- All the apparatus and materials of Experiments E-1.
- 0.7 inch diameter and 1.5 inch high cylindrical Jordanian shale samples cut with a small core drill from a single chunk sample 4x4x1.5 inches.

E-2.3 Procedure:

(a) Twelve Antrim shale samples were weighed and put in the reactor.

(b) The reactor was placed in the furnace.

(c) The inlet pipe of the reactor was connected to the nitrogen gas cylinder regulated at 600 psig. The needle valve on the outlet pipe of the reactor was slightly opened to prevent

back pressure on the nitrogen cylinder. The outlet pipe was connected to the wet test meter.

(d) The furnace was switched on and was allowed to heat up to 572°F (300°C) and was maintained at that temperature for one hour. The wet test meter indicated a flow of 1.4 liter/min and no pressure rise on the nitrogen cylinder was noticed.

(e) The outlet valve was shut and the nitrogen cylinder was disconnected.

(f) The reactor was removed from the furnace and cooled to room temperature.

(g) One sample was removed from the reactor and was weighed.

(h) Steps (b)-(g) were repeated for a second and a third hour.

(i) Steps (b)-(h) were repeated three times for temperatures of 752°F (400°C), 932°F (500°C), and 1112°F (600°C).

(j) Steps (a)-(i) were repeated twice for nitrogen gas pressures of 300 psig and 15 psig.

(k) Steps (a)-(j) were repeated for Jordanian samples.

(l) The samples were labeled and saved to be used again in oxygen penetration Experiments G-2.

E-2.4 Results and Interpretation: The results of the experiments using Antrim shale are shown in Table 4-7 and Figure 4-18. Figure 4-18 was constructed by taking the final weight loss at each gas pressure to be the available amount for retorting at time zero. For example 9.49% for the 600 psig set was plotted at time zero, and the weight loss after one

Table 4-7

Weight loss percent of Antrim shale retorted under nitrogen pressure (new sample used for each temperature, pressure and exposure time) (nonsequential runs)

Temp.	600 psig nitrogen pressure			300 psig nitrogen pressure			15 psig nitrogen pressure		
	1 hr	2 hr	3 hr	1 hr	2 hr	3 hr	1 hr	2 hr	3 hr
572°F (300°C)	1.17	1.22	1.22	1.24	1.31	1.33	1.39	1.46	1.49
752°F (400°C)	2.53	2.61	2.63	2.67	2.78	2.81	3.08	3.23	3.30
932°F (500°C)	6.69	6.70	6.73	6.89	7.23	7.23	7.65	7.91	7.94
1112°F (600°C)	9.41	9.46	9.49	9.53	9.76	9.86	10.32	10.58	10.61

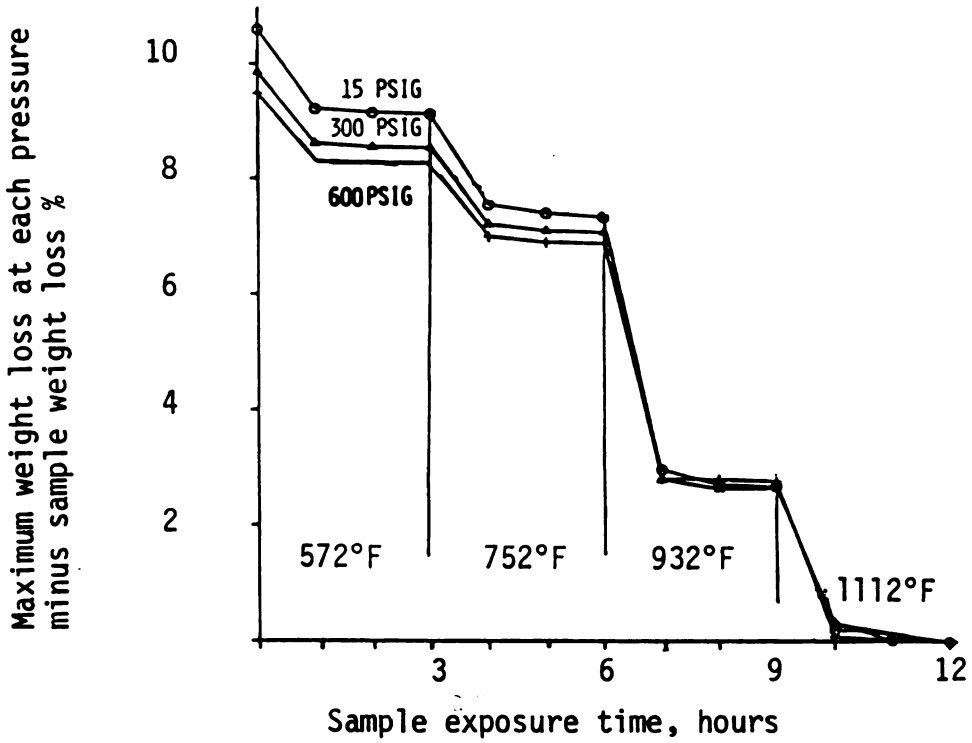

Figure 4-18. Retortable organics remaining in Antrim shale at various nitrogen pressures, temperatures, and exposure times.

hour at 572°F (300°C) of 1.17% was subtracted from the final weight loss and plotted at time one hour. The same plotting procedure was repeated such that for each gas pressure the remaining retortable organic material is zero at the end of 12 hours.

The results of the experiments using Jordanian shale are shown in Table 4-8 and Figure 4-19. Figure 4-19 was constructed in the same way as Figure 4-18.

The results in Table 4-7 and 4-8 show that retorting the shale for two or three hours does not produce much more weight loss than for one hour, since at a given temperature, almost all the organic materials which decompose at that temperature come off quickly. As shown in Figures 4-18 and 4-19, the samples which were retorted at 15 psig nitrogen gas pressure produced a higher weight loss than those retorted at 300 psig and 600 psig.

It might seem that the coking reaction is the cause of the reduced weight loss under high nitrogen gas pressure. It was shown from the sequential runs (Experiments E-1), however, that when the gas pressure was released, additional weight loss was obtained from the same sample. This would not be the case if the coking reactions were the cause of the lower weight loss at high pressure. It appears that the most likely the cause of reduced weight loss under high nitrogen gas pressure is that the organic material remaining in the shale has a low vapor pressure.

The effect of temperature and nitrogen gas pressure during shale retorting are similar for Jordanian shale. The total weight loss for Jordanian, however, was about twice that for Antrim shale.

Table 4-8

Weight loss percent of Jordanian shale retorted under nitrogen pressure (new sample used at each temperature, pressure and exposure time) (nonsequential runs)

Temp.	600 psig nitrogen pressure			300 psig nitrogen pressure			15 psig nitrogen pressure		
	1 hr	2 hr	3 hr	1 hr	2 hr	3 hr	1 hr	2 hr	3 hr
572°F (300°C)	1.34	1.38	1.38	1.41	1.49	1.49	1.58	1.66	1.66
752°F (400°C)	7.87	7.95	7.98	8.11	8.24	8.27	8.94	8.98	8.98
932°F (500°C)	13.04	13.12	13.16	13.27	13.41	13.41	14.11	14.16	14.18
1112°F (600°C)	19.63	19.68	19.69	19.80	19.86	19.86	21.37	21.39	21.4

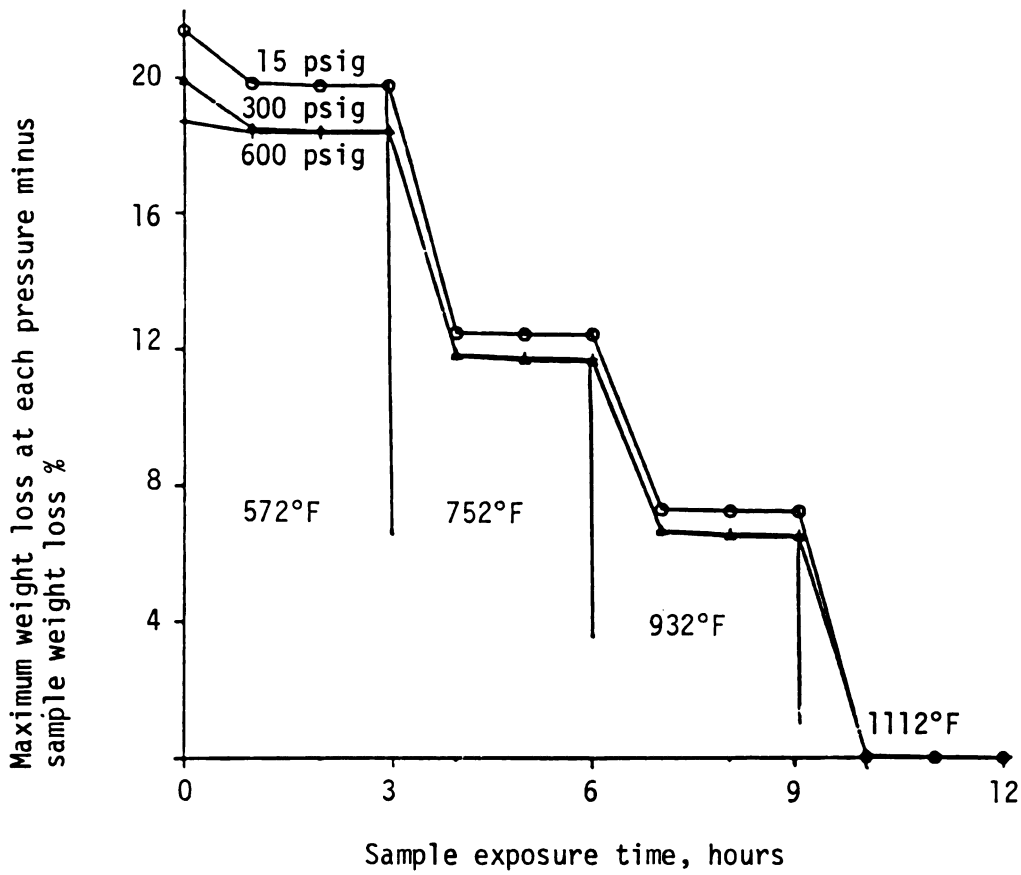

Figure 4-19. Retortable organics remaining in Jordanian shale at various nitrogen pressures, temperatures and exposure times.

PART F. EXPERIMENTS RELATED TO THE EFFECT OF OVERBURDEN PRESSURE DURING SHALE RETORTING

These experiments were conducted in order to obtain information about the effect of overburden pressure during retorting of shale. Two series of experiments were conducted as follows:

F-1 Overburden pressure effect during shale retorting, sequential runs.

F-2 Overburden pressure effect during shale retorting, nonsequential runs.

Experiments F-1. Overburden pressure effect during shale retorting, sequential runs.

F-1.1 Purpose. The purpose of these experiments is to determine the amount of combustible material released as a result of retorting Antrim shale samples under simulated overburden pressure by using the clamp. The effect of retorting under overburden pressure is to be examined under 15 psig nitrogen pressure and a variety of temperatures: 572°F (300°C), 752°F (400°C), 932°F (500°C), and 1112°F (600°C). These runs were sequential in the sense that the same shale sample was subjected to a series of increasingly severe treatments. This eliminated the effect of variations in shale properties. It also gives a direct measure of the effect of overburden pressure by sequentially loading and unloading the clamp at each temperature and exposure time.

F-1.2 Apparatus and Materials:

- All the apparatus and materials of Experiments E-1.

- Stainless steel pressure clamp which was described in Experiment C-4 (See Figure 4-3).

F-1.3 Procedure.

(a) A sample was chosen, weighed and placed in the pressure clamp between the two aluminum fillers.

(b) The pressure clamp was then put in the reactor, and the reactor was placed in the furnace.

(c) The inlet pipe of the reactor was connected to the nitrogen gas cylinder regulated at 15 psig. The needle valve on the outlet pipe of the reactor was slightly opened to prevent back pressure on the nitrogen cylinder. The outlet pipe was connected to the wet test meter.

(d) The furnace was switched on and was allowed to heat up to 572^{o}F (300^{o}C) and was maintained at that temperature for half an hour. The wet test meter indicated a flow of 1.4 liter/min and no pressure rise on the nitrogen cylinder was noticed.

(e) The outlet valve was shut and the nitrogen cylinder was disconnected.

(f) The reactor was removed from the furnace and was cooled to room temperature.

(g) The pressure clamp was removed from the reactor, and the sample was removed from the pressure clamp and was weighed.

(h) Steps (b)-(h) were repeated using the same sample.

(i) Steps (b)-(g) were repeated four times using the same sample without the clamp.

(j) Steps (a)-(i) were repeated three times still using the same sample but at temperatures of 752^{o}F (400^{o}C), 932^{o}F (500^{o}C), and 1112^{o}F (600^{o}C).

(k) The sample was labeled and saved to be used in Experiments G-3.

F-1.4 Results and Interpretation. The results of these experiments are shown in Table 4-9 and Figures 4-20 and 4-21. Figure 4-20 was constructed in the same way as Figure 4-16 by taking the total organic material loss as the available amount for retorting at time zero and then subtracting from the cumulative weight loss after each consecutive half hour period. Figure 4-21 was constructed in the same way as Figure 4-17, by plotting the weight loss for each half hour period as a function of time.

The results in Table 4-9 show that overburden pressure does retard evolution of combustible material. It can be observed that in every case when the pressure clamp was released at constant temperature (See Figure 4-21) there was additional organic material released, and at 572°F (300°C) and 752°F (400°C) more was released than in the previous half hour.

It is interesting to note that the total weight loss over the period of 12 hours (4 hours with the clamp and 8 hours without) was very similar to the total weight loss observed in Experiments E-1 without utilizing the clamp. On the other hand, comparison of the first two columns of Tables 4-6 and 4-9 shows that the weight loss before unloading the clamp was much less than was observed in the case where no mechanical pressure was applied. Therefore, the organic materials retained when the clamp was loaded were released after unloading the clamp. This indicates that the coking reaction would not account for the retaining of some organic material when retorting takes place under mechanical pressure. It appears that some of the organic material

Table 4-9

Weight loss percent of one shale sample undergoing a sequence of time, temperature and mechanical pressure changes (sequential runs)

Temp.	15 psig nitrogen gas pressure						Accum. weight loss
	With clamp 1/2 hr	1/2 hr	Without clamp 1/2 hr	1/2 hr	Without clamp 1/2 hr	1/2 hr	
572°F (300°C)	0.14	0.04	0.27	0.05	0.05	0	0.55
752°F (400°C)	0.58	0.18	0.62	0.14	0.07	0.04	2.18
932°F (500°C)	2.79	1.22	0.38	0.25	0.09	0.05	6.96
1112°F (600°C)	1.91	0.73	0.45	0.13	0.08	0.03	10.29

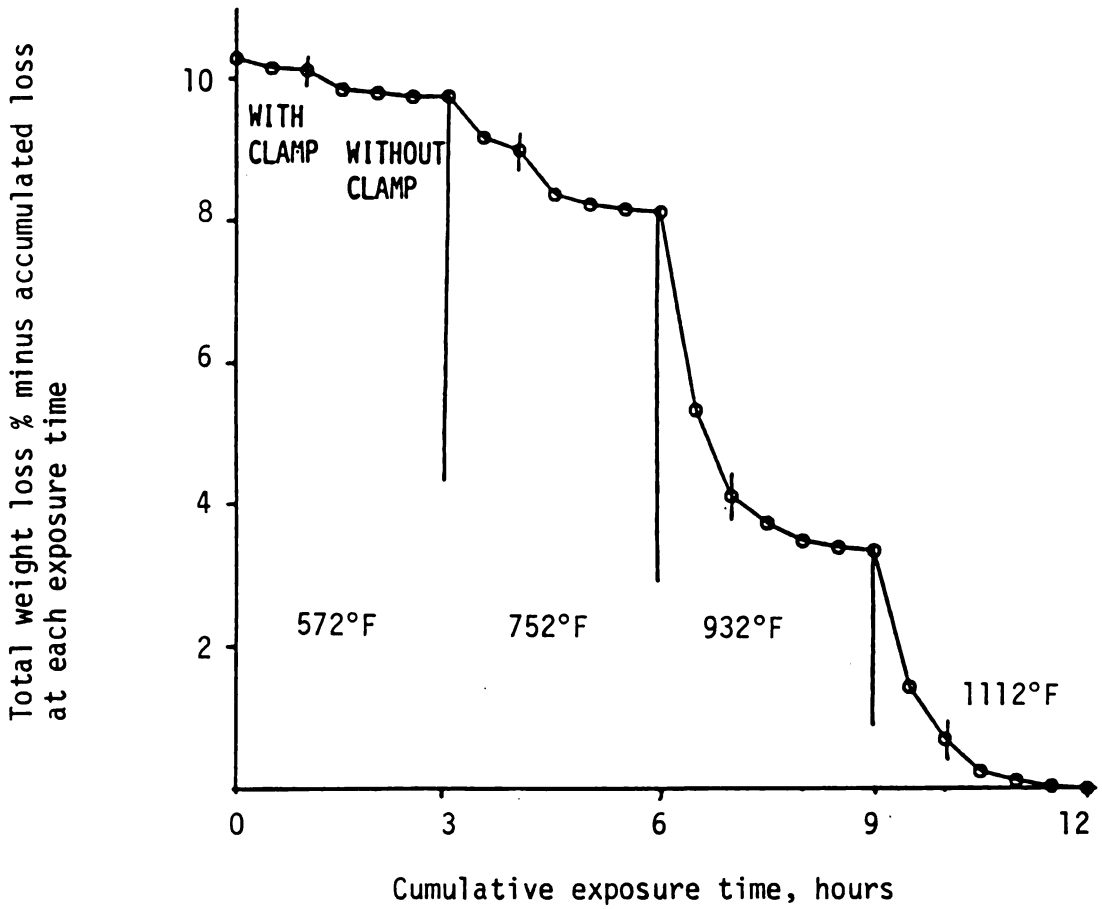

Figure 4-20. Retorting weight loss remaining in Antrim sample throughout a sequence of time, temperature and mechanical pressure changes.

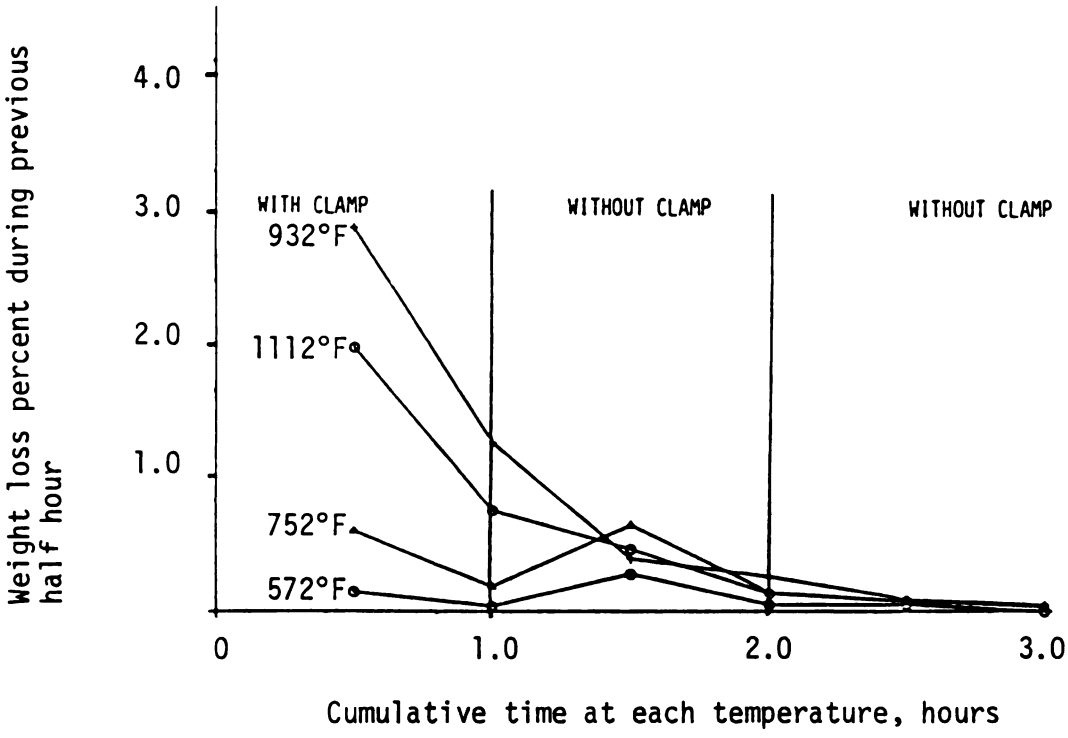

Figure 4-21. Weight loss percent in half hour intervals for Antrim shale sample retorted as in Figure 4-20 in a sequence of temperatures and mechanical pressures.

remaining in the shale under mechanical pressure have low vapor pressures or decomposition pressures (see Appendix I).

Experiments F-2. Overburden pressure effect during shale retorting, nonsequential runs.

F-2.1 Purpose. The purpose of these experiments is to determine the amount of combustible material released as a result of retorting Antrim samples under simulated overburden pressure by loading the clamp. The effect of overburden pressure is to be examined under 15 psig nitrogen pressure and a variety of temperatures: 572°F (300°C), 752°F (400°C), 932°F (500°C), and 1112°F (600°C). These runs were nonsequential in the sense that the retorting under mechanical pressure was carried out by using a new sample at each temperature and exposure time. Nonsequential runs allow the determination of the total retortable organics under mechanical pressure at a given exposure time and temperature.

F-2.2 Apparatus and Materials;

- All the apparatus and materials of Experiments E-1 and F-1.

F-2.3 Procedure.

(a) An Antrim shale sample was weighed and placed in the pressure clamp between the two aluminum fillers.

(b) The pressure clamp was then put in the reactor, and the reactor was placed in the furnace.

(c) The inlet pipe of the reactor was connected to the nitrogen gas cylinder regulated at 15 psig. The needle valve on the outlet pipe of the reactor was slightly opened to prevent back pressure on the nitrogen cylinder. The outlet pipe was connected to the wet test meter.

(d) The furnace was switched on and was allowed to heat up to 572°F (300°C) and was maintained at that temperature for one hour. The wet test meter indicated a flow of 1.4 liter/min and no pressure rise on the nitrogen cylinder was noticed.

(e) The outlet valve was shut off and the nitrogen cylinder was disconnected.

(f) The pressure clamp was removed from the reactor, and the sample was removed from the pressure clamp and was weighed.

(g) Steps (a)-(f) were repeated except that the sample was held in the furnace for three hours instead of one hour.

(i) Steps (a)-(f) were repeated except that the sample was held at 572°F (300°C) for three hours and then the furnace temperature was increased to 752°F (400°C) and maintained at that temperature for one hour.

(j) This sequence was continued through further temperature increases to 932°F (500°C) and 1112°F (600°C) such that the samples underwent:

3 hours at 572°F and 2 hours at 752°F

3 hours at 572°F and 2 hours at 752°F

3 hours at 572°F and 3 hours at 752°F and 1 hour at 932°F and so on up to

3 hours at 572°F and 3 hours at 752°F and 3 hours at 932°F and 3 hours at 1112°F

(k) The samples were labeled and saved to be used again in oxygen penetration Experiments G-4.

F-2.4 Results and Interpretation. The results of these experiments are shown in Table 4-10 and Figure 4-22. Figure 4-22 was constructed by

Table 4-10

Weight loss percent of shale samples with clamp versus temperature and exposure time (nonsequential runs)

Temperature	In nitrogen atmosphere 15 psig		
	1 hour	2 hours	3 hours
572°F (300°C)	0.86	0.86	0.96
752°F (400°C)	1.34	1.41	1.56
932°F (500°C)	4.63	4.68	4.73
1112°F (600°C)	8.93	8.97	9.13

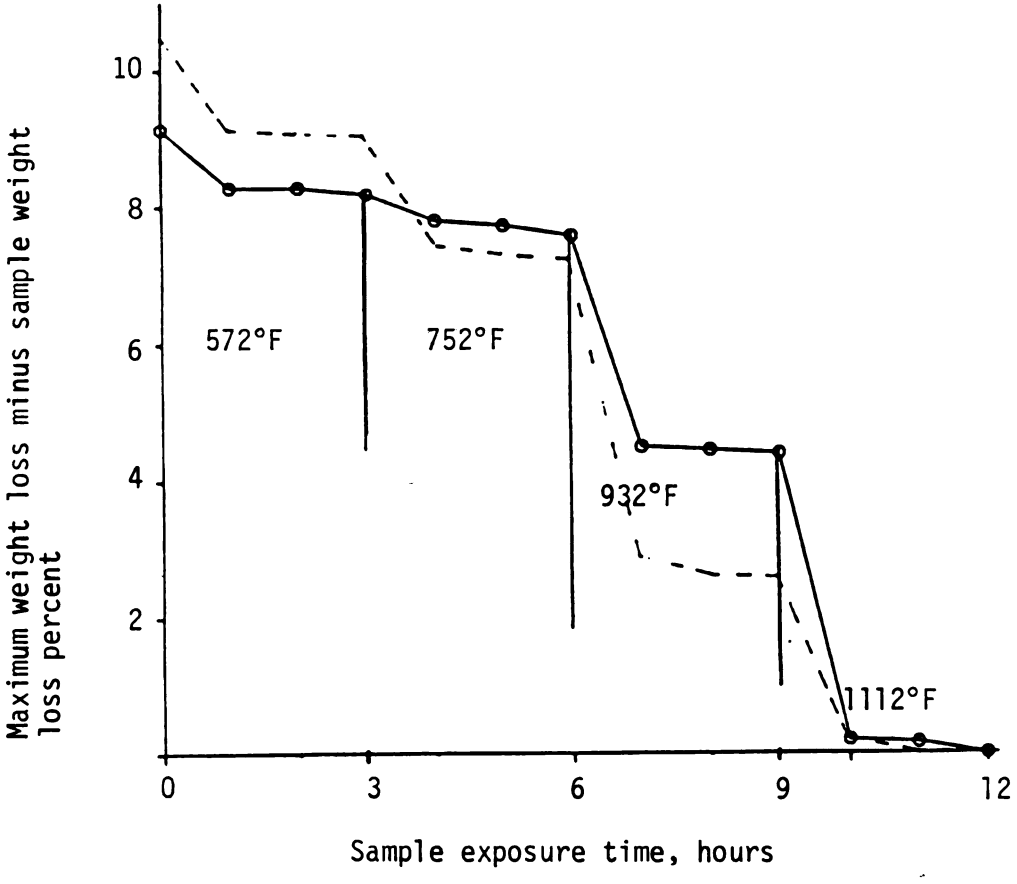

Figure 4-22. Retortable organics remaining in Antrim shale after treatment at 15 psig nitrogen pressure at various temperatures and exposure times.

——— with mechanical pressure

– – – – – without mechanical pressure

taking the total organic material loss of 9.13 as the available amount for retorting at time zero and then subtracting from that the weight loss after each time period. Also shown in Figure 4-22 are some of the results of Experiments E-2 for comparison purposes. A comparison of Table 4-7 and Table 4-10 shows that the amount of organic material release as a result of retorting under mechanical pressure in any exposure time period or at any temperature is considerably less than the amount released in the absence of simulated overburden pressure. This observation is also clearly shown in Figure 4-22. The reduced weight loss as result of retorting under simulated overburden pressure was also observed in the sequential runs (Experiments F-1).

The results of the nonsequential runs alone might indicate that the coking reaction causes the retention of some organic material in the shale. However, it was shown from the sequential runs (Experiments F-1) that additional weight loss was produced from the same sample when the pressure clamp was released. Therefore, the coking reaction would not account for the retention of some organic material in the shale. In summary, some organic material in the shale has low vapor pressure or low decomposition pressure (too low to create cracks in the shale) is likely to be the reason that these organic materials are retained.

As shown in Figure 4-22, there was about 2% of the retortable organic material which was retained in the shale when overburden pressure was simulated. It seems that this amount is not retortable unless the overburden pressure is released. An attempt was made to verify this by retorting Antrim sample under mechanical pressure and at temperatures higher than 1112^{o}F (600^{o}C). This additional retorting at

higher temperatures did not result in the release of any more organic material, which might indicate that at higher temperatures, the organic materials which have low vapor pressure and were retained in the shale might undergo coking.

The question of whether or not the approximate 2% of the recoverable organic material is retained due to overburden pressure and if the rest of the coked residual carbon retained in the shale is recoverable, and are the subjects of the next series of experiments.

PART G. EXPERIMENTS RELATED TO THE PENETRATION OF OXYGEN INTO SPENT SHALE AND COMBUSTION OF RESIDUAL CARBON

These experiments were conducted in order to obtain information about the possibility of burning with oxygen the residual carbon retained in the spent shale after retorting. Such combustion might provide another possible mechanism for getting heat into shale. Four series of experiments were conducted as follows:

G-1 Oxygen gas pressure and temperature effects during spent shale combustion, sequential runs.

G-2 Oxygen gas pressure and temperature effects during spent shale combustion, nonsequential runs.

G-3 Overburden pressure effect during spent shale combustion, sequential runs.

G-4 Overburden pressure effect during spent shale combustion, nonsequential runs.

Experiments G-1. Oxygen gas pressure and temperature effects during spent shale combustion, sequential runs.

G-1.1 Purpose. The purpose of these experiments is to investigate the possibility of forcing or diffusion of oxygen into the shale, followed by combustion of residual carbon deposited within the spent shale, and to determine the amount of combustible material released as a result of combustion under a variety of temperatures and oxygen gas pressures: 572°F (300°C), 752°F (400°C), 943°F (500°C), and 1112°F (600°C), and 600 psig, 300 psig, and 15 psig. These runs were sequential in the sense

that the same shale sample was subjected to a series of increasingly severe treatments. This eliminated the effect of variations in shale properties. It also gives a direct measure of the effects of increased temperature and oxygen gas pressure.

G-1.2 Apparatus and Materials. The same as in Experiments E-1 except using oxygen instead of nitrogen gas, and using the same sample from Experiments E-1.

G-1.3 Procedure. The same sample which underwent retorting in Experiment E-1 is to be used again following the same procedure except using oxygen instead of nitrogen gas and starting with an oxygen gas pressure of 15 psig instead of a nitrogen gas pressure of 600 psig (exploratory experiments showed that oxygen and nitrogen gas pressure have the opposite effect).

G-1.4 Results and Interpretation. The results are shown in Table 4-11 and Figures 4-23 and 4-24. Figure 4-23 was constructed by taking the total organic material loss of 3.54% as the available amount for combustion at time zero and then subtract from that the weight loss after each consecutive half hour period. Figure 4-24 was constructed by plotting the weight loss after each half hour as a function of time.

Most of the combustion took place during the first half hour (See Figure 4-23 and Table 4-11), at each temperature. Apparently, the oxygen migrated through those cracks which developed in the nitrogen run during retorting and reacted with the coked carbon residue on the surface of the rock. It seemed that most of the carbon was consumed in the first period. As the time increased, it was difficult for the oxygen to diffuse inside the rock, except through voids close to the external surface left from the volatilization of organic matter released

Table 4-11

Weight loss percent of one spent sample from Experiments E-1 undergoing a sequence of combustion at different oxygen gas pressure, time, and temperature (sequential run)

Temp.	15 psig of O_2 weight loss %		300 psig of O_2 weight loss %		600 psig of O_2 weight loss %		Accum. weight loss %
	1/2 hr	1/2 hr	1/2 hr	1/2 hr	1/2 hr	1/2 hr	
752°F (400°C)	1.39	0.34	0.32	0.06	0.11	0.04	2.26
932°F (500°C)	0.48	0.15	0.14	0.04	0.06	0.02	3.15
1112°F (600°C)	0.19	0.07	0.06	0.02	0.05	----	3.54

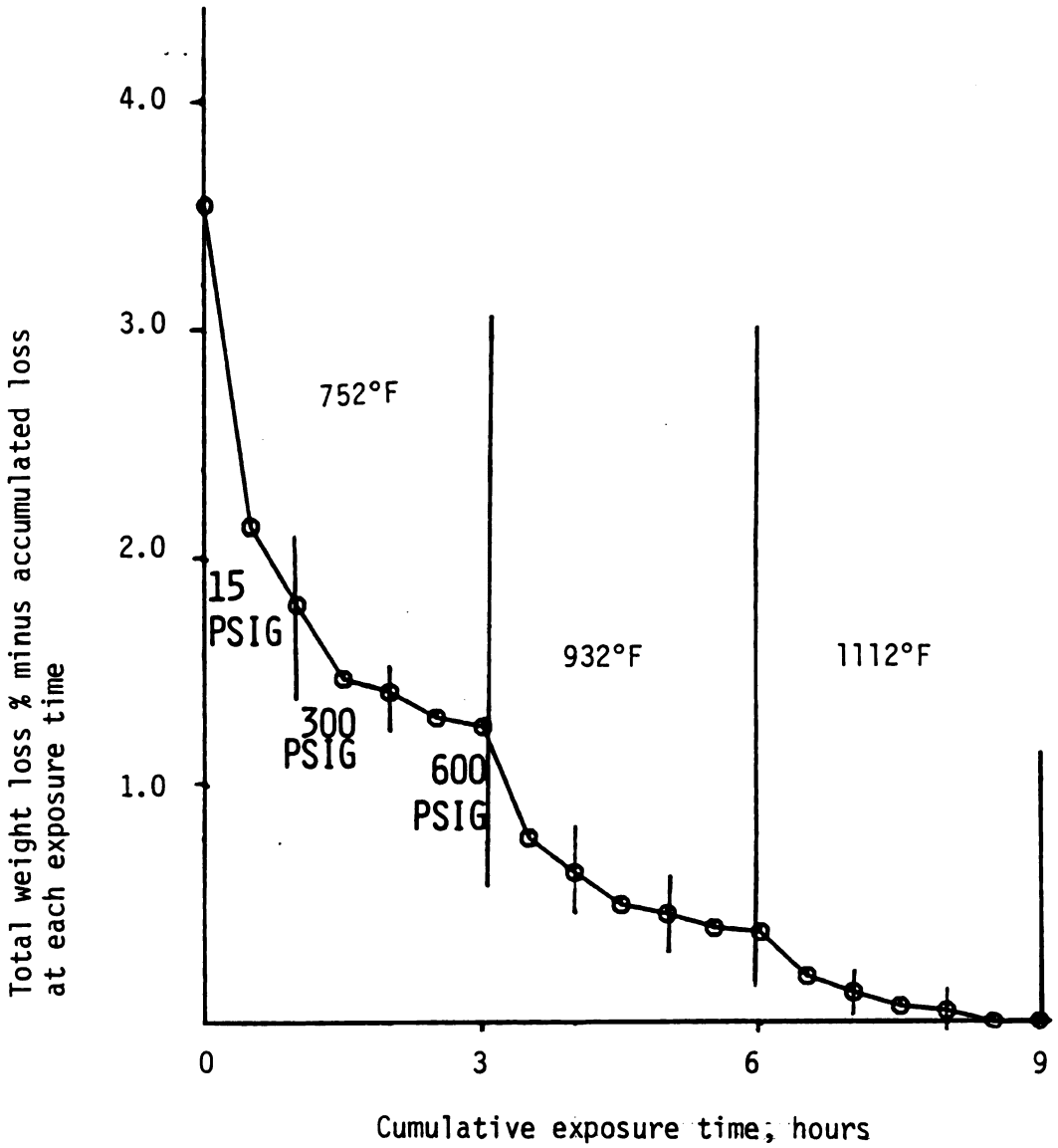

Figure 4-23. Combustion weight loss remaining in Antrim shale sample throughout a sequence of increasing severe treatments.

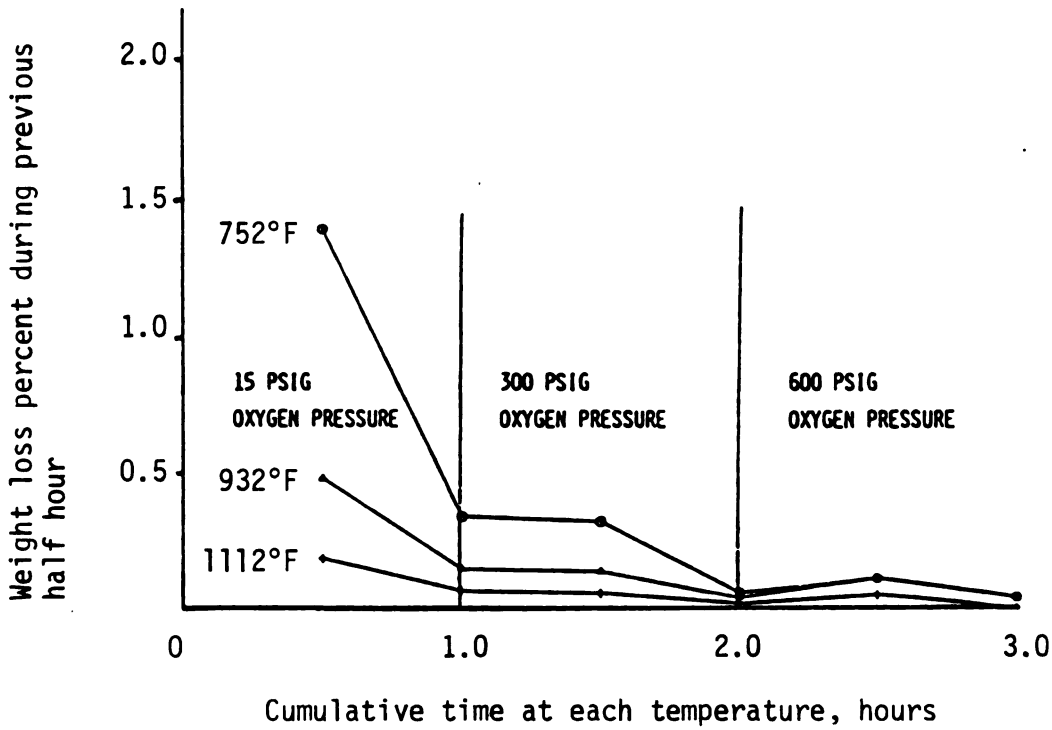

Figure 4-24. Weight loss percent in half hour intervals for Antrim shale sample undergoing combustion at different temperatures under a sequence of oxygen gas pressures: 15, 300 and 600 psig.

during retorting. No combustion took place at a temperature of 572°F (300°C). Most of the combustion took place at 752°F (400°C). (See Table 4-11). The continuous increase of weight loss as the temperature was increased may be explained by assuming that the residual carbon in the spent shale is presumably made up of various compounds with different degrees of reactivity with oxygen. The most reactive compounds react with oxygen at low temperatures, and as the temperature increased the less reactive compounds would begin to react.

The results presented in Figure 4-24 and Table 4-11 show that oxygen gas pressure and nitrogen gas pressure have an opposite effect on combustible material loss. High nitrogen gas pressure suppressed the evolution of combustible material from the rock. High oxygen gas pressure, however, increased the loss of organic material through combustion. As shown in Figure 4-24, an increase of weight loss occurred when the oxygen pressure increased from 300 psig to 600 psig. The gas-solid reaction of oxygen with coked carbon residue is recognized to be complex. Based on visual observations on the physical structure of shale before and after combustion, it is suggested that when the sample undergoes retorting before combustion a network of small cracks develops and when combustion takes place the oxygen diffuses through the rock mainly along those cracks. The disappearance of carbon residue was observd in a thin zone near the external surface. Thus it appears that, in addition to the main diffusion of oxygen through the cracks, there is some penetration of oxygen through the void space left from retorting.

If the sample, after combustion, was broken manually, it split along one of the many visible cracks, and showed no black carbon on the fractured surface. However, if the sample was sawed parallel to the

cracks, but not along them, then a large dark spot was observed in the center. When cut perpendicular to the bedding plane, the sample showed multiple layers of dark and light. (See Figure 4-6).

Experiments G-2. Oxygen gas pressure and temperature effects during spent shale combustion, nonsequential runs.

G-2.1 Purpose. The purpose of these experiments is to determine the possibility of forcing or diffusion of oxygen into the shale, followed by combustion of residual carbon deposited within the spent shale under conditions as in Experiments G-1. Nonsequential runs would give the amount of combustible material at a given exposure time, temperature and oxygen gas pressure.

G-2.2 Apparatus and Materials. The same as in Experiments E-2 except using oxygen instead of nitrogen gas, and using the same spent (retorted) sample from Experiments E-2 and not a raw sample.

G-2.3 Procedure. The same samples which underwent retorting in Experiments E-2 are to be used again following the same procedure except using oxygen instead of nitrogen gas.

G-2.4 Results and Interpretation. The results of Experiments G-2 on Antrim spent shale are presented in Table 4-12 and Figure 4-25. The results of Experiments G-2 on Jordanian spent shale are presented in Table 4-13 and Figures 4-26. Figures 4-25 and Figures 4-26 were constructed by the same way as Figure 4-18 of Experiments E-2.

The results show that the highest weight loss as a result of combustion of residual carbon was achieved at 600 psig oxygen gas pressure. It seems that the conclusion of the sequential runs (Experiments G-1) that high oxygen gas pressure has a positive effect on the combustion of residual carbon is correct.

Table 4-12

Weight loss percent of Antrim spent shale samples from Experiments E-2 undergoing combustion (new one at each temperature, pressure, and exposure time) (nonsequential runs)

Temp.	600 psig oxygen pressure weight loss %			300 psig oxygen pressure weight loss %			15 psig oxygen pressure weight loss %		
	1 hr	2 hr	3 hr	1 hr	2 hr	3 hr	1 hr	2 hr	3 hr
752°F (400°C)	2.09	2.14	2.14	2.0	2.0	2.03	1.59	1.61	1.63
932°F (500°C)	2.73	2.76	2.83	2.47	2.51	2.51	2.21	2.28	2.33
1112°F (600°C)	2.87	2.91	3.13	2.54	2.67	2.71	2.33	2.35	2.35

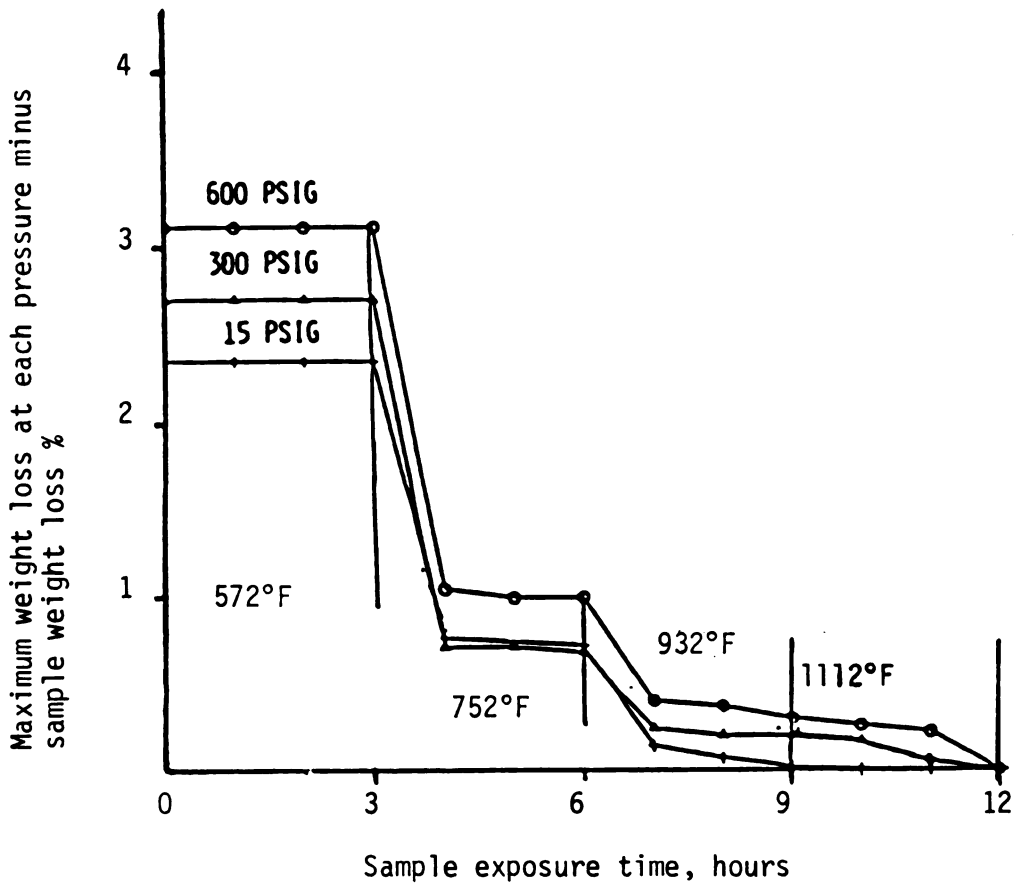

Figure 4-25. Combustible organics remaining in Antrim shale at various oxygen pressures, temperatures, and exposure times.

Table 4-13

Weight loss percent of Jordanian spent shale samples from Experiments E-2 undergoing combustion (new one at each temperature, pressure, and exposure time) (nonsequential runs)

Temp.	600 psig oxygen gas pressure weight loss %			300 psig oxygen gas pressure weight loss %			15 psig oxygen gas pressure weight loss %		
	1 hr	2 hr	3 hr	1 hr	2 hr	3 hr	1 hr	2 hr	3 hr
752°F (400°C)	1.32	1.38	1.38	1.12	1.17	1.19	1.09	1.13	1.14
932°F (500°C)	1.79	1.82	1.83	1.6	1.64	1.66	1.43	1.46	1.47
1112°F (600°C)	2.02	2.06	2.06	1.81	1.87	1.89	1.57	1.62	1.64

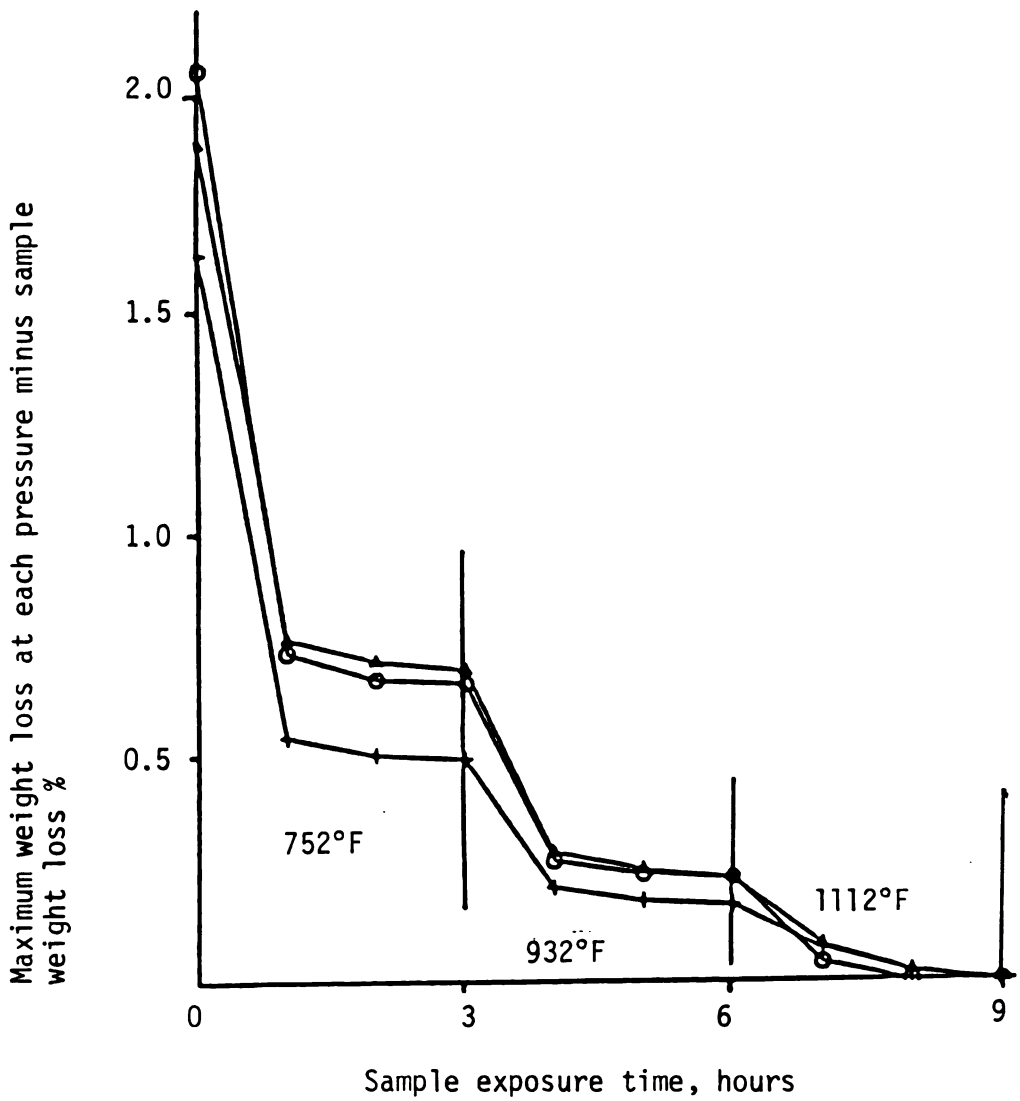

Figure 4-26. Combustible organics remaining in Jordanian shale at various oxygen pressures, temperatures and exposure times.

▲ 600 PSIG

o 300 PSIG

+ 15 PSIG

It is interesting to note that the total weight loss as a result of combustion of Antrim shale is twice that of Jordanian shale (See Table 4-12 and Table 4-13). On the other hand, the results of retorting (See Table 4-7 and Table 4-8) showed almost the opposite effect (Total weight loss for Jordanian shale was twice that from Antrim shale). Apparently rich shale produces less coke than lean shale. This might be explained from the results of Experiments C-1, that Jordanian shale produces twice the pore structure of that of Antrim shale as a result of retorting (Table 4-1). Therefore, the product vapor comes off the rich shale more quickly through the open pores and the cracks than the lean shale. Therefore, the product from lean shale spends more time in the shale which might motivate the coking reaction.

Experiments G-3. Overburden pressure effect during spent shale combustion, sequential runs.

G-3.1 Purpose. The purpose of these experiments is to determine the possibility of forcing or diffusion of oxygen into the shale, followed by combustion of residual carbon deposited within the spent shale with utilizing mechanical pressure, simulated by the use of pressure clamp. The temperatures and time conditions are the same as Experiments G-1.

G-3.2 Apparatus and Materials. The same as in Experiments F-1 except using oxygen instead of nitrogen gas, and using the spent (already retorted) sample from Experiments F-1 and not raw samples.

G-3.3 Procedure. The same sample which underwent retorting in Experiments F-1 are to be used again following the same procedure except using oxygen instead of nitrogen gas.

G-3.4 Results and Interpretation. The results of these experiments are presented in Table 4-14 and Figure 4-27 and 4-28 which were constructed in the same way as Figures 4-20 and 4-21.

Under overburden pressure (Table 4-14) combustion of carbon residue was less than without overburden pressure (Table 4-11), both during the first time period and for the entire period. As shown in Figure 4-28, when the overburden pressure was released (by removing the clamp) an increase in weight loss was resulted, since oxygen was allowed to diffuse along some of the cracks. It seems that loading the clamp closed up some of the cracks, because the total weight loss is about 1% less than that when the clamp was not loaded (Table 4-11). This supports the mechanism, proposed earlier, that the oxygen has to penetrate along the cracks to react with the carbon residue at the fracture surface.

It is important to note that no work was found in the literature on the effect of overburden pressure on the combustion of residual carbon deposited with the spent shale.

Experiments G-4. Overburden pressure effect during spent shale combustion, nonsequential runs.

G-4.1 Purpose. The purpose of these experiments is to determine the possibility of forcing or diffusion of oxygen into the shale, followed by combustion of residual carbon deposited within the spent shale with utilizing mechanical pressure. These experiments give the total weight loss as a result of combustion under overburden pressure.

G-4.2 Apparatus and Materials. The same as in Experiments F-2 except using oxygen instead of nitrogen gas.

Table 4-14

Weight loss percent of one spent sample from Experiments F-1 undergoing a sequence of time, temperature, and mechanical pressure changes (sequential run)

Temp.	With clamp		Without Clamp		Without Clamp		Accum. weight loss %
	1/2 hr	1/2 hr	1/2 hr	1/2 hr	1/2 hr	1/2 hr	
752°F (400°C)	0.39	0.26	0.32	0.11	0.06	0	1.14
932°F (500°C)	0.26	0.14	0.23	0.13	0.04	0.04	1.98
1112°F (600°C)	0.21	0.12	0.17	0.07	0.04	0.02	2.61

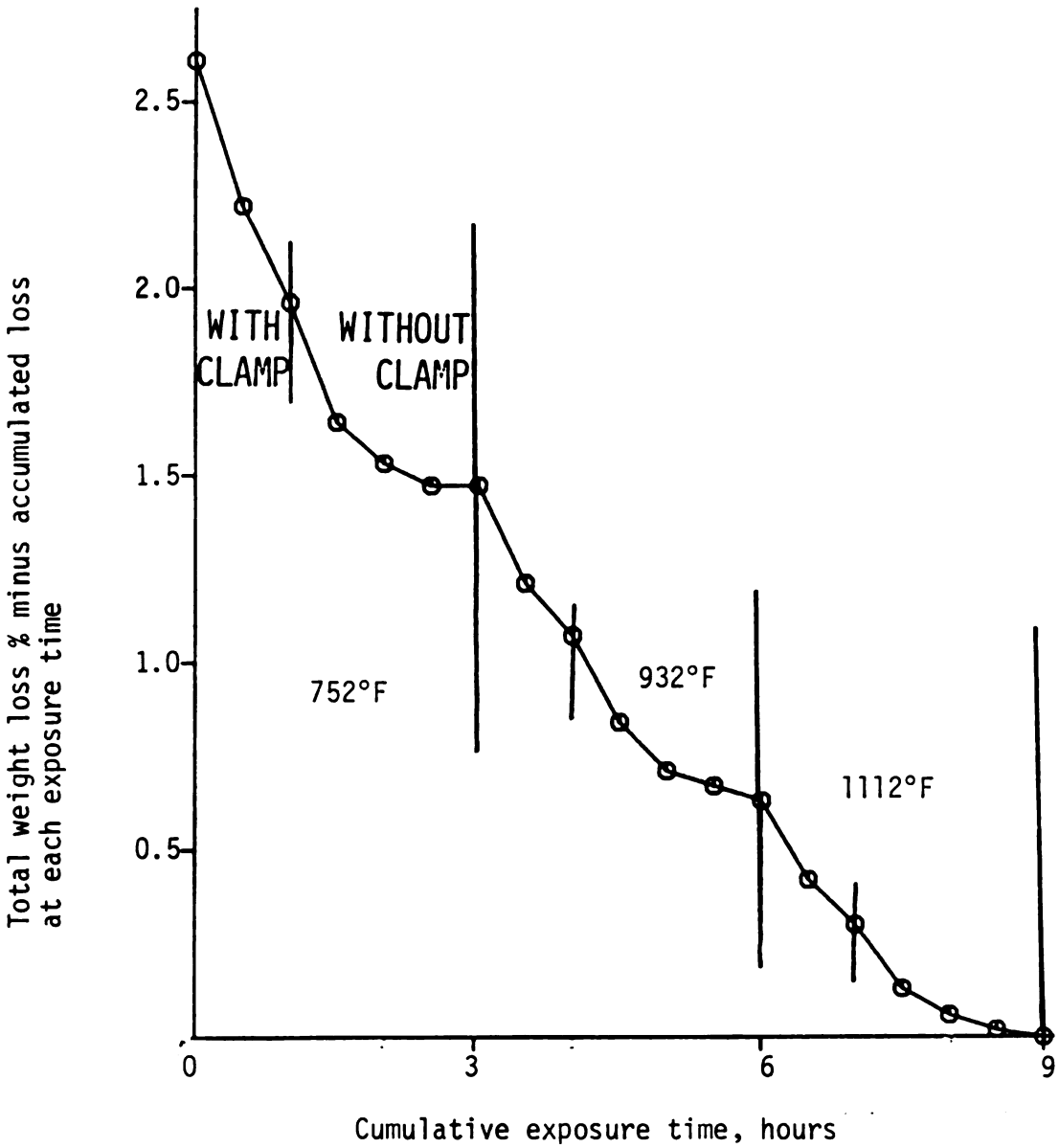

Figure 4-27. Combustion weight loss remaining in Antrim sample throughout a sequence of time and temperature and mechanical pressure changes.

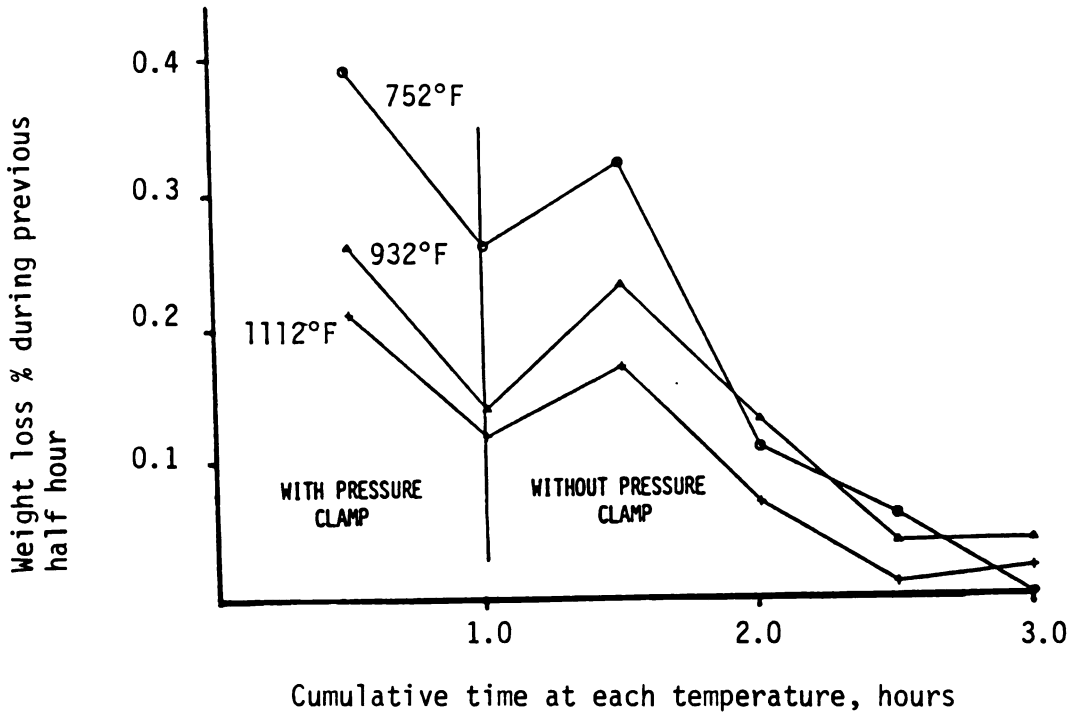

Figure 4-28. Weight loss percent in half hour intervals for Antrim shale sample undergoing combustion as in Figure 4-27 in a sequence of temperatures and mechanical pressures.

G-4.3 Procedure. The same samples which underwent retorting in Experiments F-2 are to be used again following the same procedure except using oxygen instead of nitrogen gas.

G-4.4 Results and Interpretation. The results of these experiments are presented in Table 4-15 and Figure 4-29 which was constructed in the same way as Figure 4-22.

The results of these experiments showed that much less combustion took place under simulated overburden pressure. (See Figure 4-29). It was shown earlier (Table 4-10) that about 2% of organic material was retained in the shale as a result of retorting under simulated overburden pressure. It was also shown that after combustion of Antrim shale without overburden pressure 3.13% was recoverable (Table 4-12). However, the results of these experiments (Table 4-15) showed that only 1.7% was recoverable under overburden pressure.

It appears that underground combustion of carbonaceous residue from retorting deep deposits of shale will be difficult to obtain. This applies particularly to Antrim oil shale, which in addition to having a high overburden pressure, produces a higher proportion of carbon residue.

Table 4-15

Weight loss percent for spent shale samples from Experiments F-2 with pressure clamp versus oxygen exposure time and temperature (nonsequential runs)

Temperature	In oxygen atmosphere 15 psig		
	1 hour	2 hours	3 hours
572°F (300°C)	--	--	--
752°F (400°C)	0.93	0.93	0.97
932°F (500°C)	1.44	1.49	1.54
1112°F (600°C)	1.67	1.71	1.77

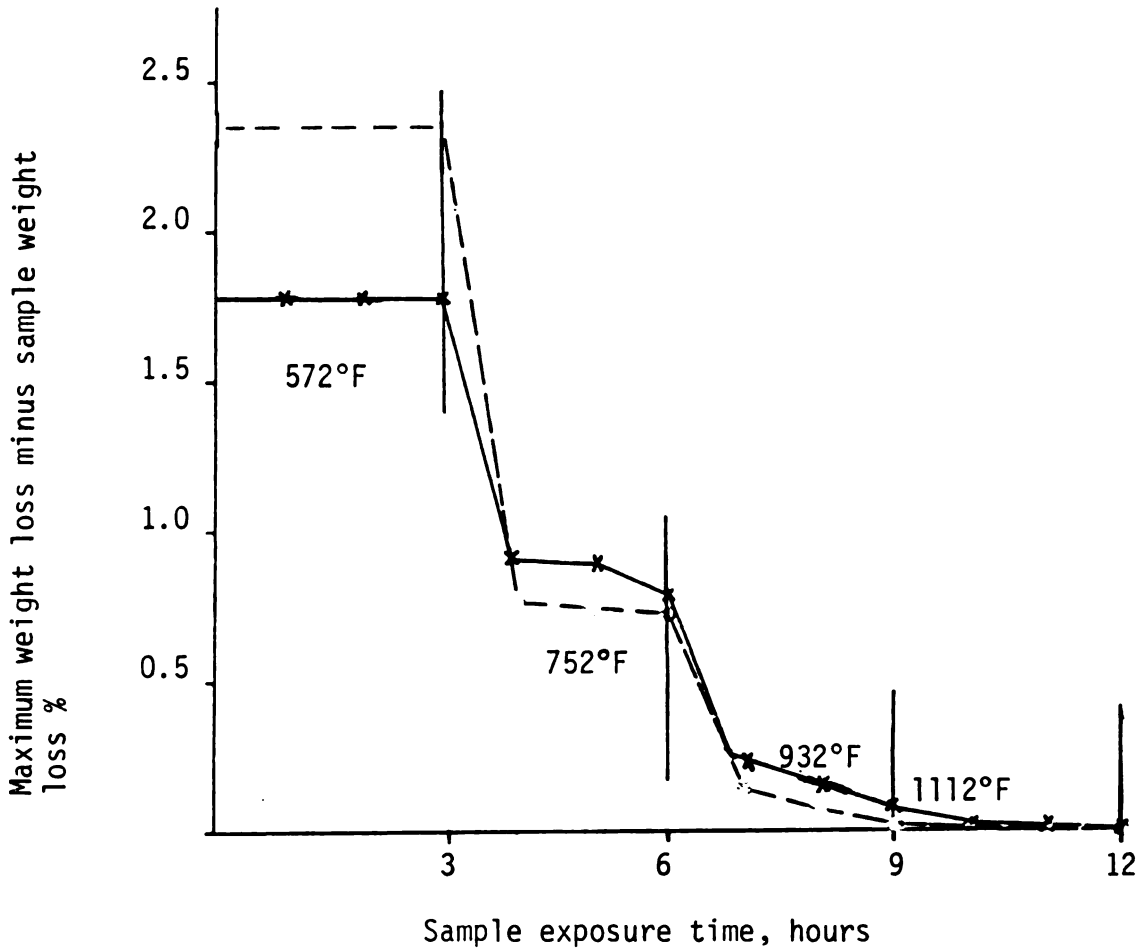

Figure 4-29. Combustible material remaining in Antrim shale after treatment at 15 psig oxygen pressure and at various temperatures and exposure times.

——— with mechanical pressure

– – – – without mechanical pressure

CHAPTER FIVE

DISCUSSION

The purpose of this chapter is to discuss possibilities and problems related to the production of energy from shales with particular reference to in situ processes and to Antrim shale. Separate discussions of the significance of experimental and theoretical approaches and results are included in Chapters Two and Four.

It was shown in Chapter Two that in situ production of energy from Antrim shale was not economical. Important contributing factors include the low energy output per pound retorted, the high energy loss per pound retorted, and the small quantity of shale retorted per well drilled. Improvement in the last two of these might have been realized if it had been possible to penetrate large volumes of the formation with hot gases rather than with heat. However, the natural impermeability of Antrim shale, its compressibility, and tendency of overburden pressure and perhaps heat to close the formation frustrate attempts to create significant artificial permeability by explosive fracturing.

A more suitable shale formation for in situ retorting is the naturally permeable central portion of the Green River formation. This shale is relatively rich (25-40 gal/ton), occurs at about 1200 feet depth and contains deposits of water soluble sodium minerals such as Dawsonite (sodium aluminum carbonate) and Nacholite (sodium bicarbonate) (37). Through the years flow of natural streams through the formations have leached out large portions of these minerals leaving holes into

which surrounding shale has broken up creating its natural permeability to gas flow. Equity Oil Company developed an in situ retorting process in 1962 which was later field tested in this region. In this process, additional water was circulated through the shale beds to leach out more of the soluble minerals. Then hot natural gas was injected into the bed through an injection well (36). When the gas flowed through the leached-out zone it heated it up, and shale oil and gas products flowed to a production well. Even with this relatively rich and permeable shale, the Equity field tests were suspended in 1971, presumably because an economically viable product did not seem likely. With the revival of interest in oil shale around 1977, the U.S. Department of Energy sponsored another project for Equity Oil Company (22). In this process superheated steam was used as heating medium for in situ retorting in the same area. While no report on the technical and economical feasibility of this new process could be found in the literature, similar unfavorable results are expected. This is further evidence of the unsuitability of the leaner and less permeable Antrim.

Another more suitable formation for energy production is Jordanian shale. Jordanian shale occurs close to the surface and has a richness of 35 gal/ton. (See Appendix F). The porosity of Jordanian shale was found to be 40% after retorting. The compressibility of the shale containing this porosity was 4.6% compared to 1.6% for Antrim shale (Table 4-1). Thus the porosity formed as a result of retorting might be of some use in producing space for rubblization. The organic output in retorting Jordanian shale was more than twice as much as for Antrim shale. Also, coking for Jordanian shale was only half as much as for Antrim shale.

The model used in Chapter Two to show Antrim shale uneconomical was based on thermal conduction as the only feasible way to get heat into Antrim shale. The 40% porosity of spent Jordanian shale suggests that flow mechanisms for getting the heat in need to be investigated for Jordanian shale before ruling out its potentiality. Also wherever thermal conductivity must be used, the richness of the shale permits deeper penetration. (See Figure 2-5).

Use of electricity or microwaves for getting heat into deep deposits of shale have been proposed and articles particularly on the latter appear in the literature from time to time. While we have not investigated these experimentally, the articles we have seen do not demonstrate that the cost of retorting shale can be reduced by these technique.

Aboveground retorting of Western oil shale has, of course, generated the greatest interest in recent years and evoked governmental subsidies running into billions of dollars. The richness of the shale, the ease of mining, and the lower heat losses in aboveground retorting should make these processes much more economic than in situ production of Antrim. However, these processes also have not shown themselves capable of meeting the competitive economics of other energy resources. (See Appendix D).

It may be reasoned that shale is basically non-competitive with petroleum or coal as long as these other sources are available to meet our needs. The periodic surges in interest in shale, then, may be attributed to faulty economics, regional politics, and the beneficial effect on the general economy of government subsidies. The faulty economics are generated by analyses which show that shale oil will

become economically feasible when the price of oil reaches a certain number of dollars per barrel. These analyses assume, of course, that prices for equipment, labor, engineering and construction do not change, but because they too are also energy dependent they tend to rise after some lag to an almost proportional level. During the lag however a temporarily favorable economic picture can be generated which coupled with regional interests can produce the necessary government subsidies. Then as costs catch up the basic disadvantages of shale again become apparent.

It seems likely that this cycle will be repeated in the future, and that government and industry will again be called upon to make decisions regarding oil shale investments and subsidies. It is hoped that the present study and other similar small scale studies of shale will be made in the intervening period, so that more enlightened future decisions will result.

As far as the writer is aware, no self-supporting shale oil production facility of any size exists in the United States today. By contrast there are many profitable unsubsidized operations which produce petroleum, natural gas, and coal. One would expect that if shale were even marginally profitable, special situations would occur where very rich and accessible deposits could be processed for profit.

Such a situation may exist in Jordan where very rich shale is part of the overburden covering profitable phosphate deposits. By mining the shale and the phosphate simultaneously it seems possible that the shale oil produced may more than pay for the added cost of mining and treating the shale.

CHAPTER SIX

CONCLUSION AND RECOMMENDATION

Conclusion

On the basis of the experimental and theoretical work done in this study we have concluded the following:

1. True in situ production of energy from Antrim shale using techniques presently available is not sufficient to justify the process.

2. The high temperature driving force necessary for conduction heat transfer is limited by glazing at elevated temperatures.

3. Large surface area accessible to the combustion zone cannot be achieved for Antrim shale because the porosity and compressibility in the spent shale is small and of little use in producing space for fracturing (Table 4-1).

4. The mechanism for the release of organic matter from the rock is the opening of many minute cracks along the bedding planes of the shale. The opening of these cracks would be due to the building up of internal pressure of gas from kerogen cracking.

5. Tests simulating in situ retorting under the expected overburden pressure showed no visible horizontal cracks. Only one small vertical crack on the cylindrical surface which penetrated to perhaps 1/6 the column diameter was observed. Considerably larger amounts of organic material were retained than were retained without overburden pressure (Tables 4-9 and 4-10).

6. High inert gas pressure suppresses the evolution of combustible materials from the rock (Tables 4-6 and 4-7).

7. In the combustion experiment, it appeared that the oxygen migrated mainly through the horizontal cracks

which developed during retorting and reacted with the carbon residue at the fracture surface.

8. Oxygen gas pressure accelerated the diffusion of oxygen through the pore structure created during retorting (Tables 4-11 and 4-12).

9. Overburden pressure was particularly effective in retarding oxygen penetration and subsequent combustion (Tables 4-14 and 4-15).

10. For a rich oil shale, like Jordanian, the higher porosity and compressibility produced in the spent shale, might be of some use in producing space for fracturing.

Recommendation

For any future work on the area of in situ production of energy from other shales, the following points are suggested for future investigations.

1. Experimentally study the ability of increasing the surface area available for heat transfer by measuring the porosity and compressibility of spent shales.

2. Experimentally study the effect of overburden pressure on crack formation.

3. Experimentally study the behavior of shale at elevated temperatures.

4. Study of the economic feasibilility of the process by calculating the energy input and output.

5. Explore new means other than heat conduction to get the energy out of the shale.

APPENDICES

APPENDIX A

APPENDIX A

Sample calculation on densities and void fraction

(1) True density of retorted Antrim shale

Weight of pycnometer with shale and water, grams	= 56.4460
Weight of pycnometer empty, grams	= 22.6571
Weight of shale and water, grams	= 33.7889
Weight of pycnometer with dry shale, grams	= 36.8822
Weight of pycnometer empty, grams	= 22.6571
Weight of dry solid shale, grams	= 14.2251
Weight of water, grams	= 33.7889-14.2251
	= 19.5638
Volume of water, cm^3	= 19.5638
Volume of solid shale, cm^3	= 25.0832-19.5638
	= 5.5194
Density of solid shale, g/cm^3	14.2251
	= 2.5773

(2) Geometric density of raw Antrim shale

$$\text{Geometric density} = \frac{\text{Wt. of shale sample, grams}}{\text{Geometric volume of shale, cm}^3} = \frac{14.4815}{3.14\left(\frac{1.526}{2}\right)^2 3.54}$$

$$= 2.2426\ g/cm^3$$

$$= 139.9\ lb/ft^3$$

(3) Density of organic material in the shale

Basis one cubic foot of shale

(Data taken from Table 4-1)

Weight of organics and inorganics, lb = 140.59

Weight of organics evolved (9.16%), lb = 12.66

Weight of original inorganics, lb = 127.93

Volume of organics and inorganics, ft^3 = 1

Volume of inorganics, ft^3 = $\frac{127.93}{160.82}$

= 0.795

Volume of organics, ft^3 = 0.205

Density of organics, lb/ft^3 = $\frac{12.66}{0.205}$ = 61.75

= 0.99 g/cm^3

(4) Void fraction percent as a result of kerogen decomposition and evolution of vapor product equal to

$$= 100\% \left(1 - \frac{\text{Wt. of spent sample/density of spent sample solids}}{\text{Wt. of raw sample/density of raw sample solids}}\right)$$

$$= 100\% \left(1 - \frac{(1-0.0916)/2.5773}{1/2.2530}\right)$$

= 20%

APPENDIX B

APPENDIX B

Calculation of heat of combustion of kerogen

Basis: one pound of kerogen

The average elemental analysis (by weight) of the organic part of the shale (kerogen) was reported by Leedy (44) as follows:

Carbon	0.70
Hydrogen	0.06
Sulphur	0.06
Oxygen	0.07
Nitrogen	0.02
Iron	0.04
Others	0.05
	1.00

Assume that oxygen is combined with hydrogen, then the amount of hydrogen available for combustion is = $0.06 - 0.07(\frac{2}{16}) = 0.0513$

The heat of combustion of the elements was looked up from Chemical Engineer's Handbook (70).

The possible combustion reactions are:

$C + O_2 \longrightarrow CO_2$,	heat of combustion = 14,000(0.70)	= 9800
$2H_2 + O_2 \longrightarrow 2H_2O$ (l),	heat of combustion* = 61,200(0.0513)	= 3140
$S + O_2 \longrightarrow SO_2$,	heat of combustion = 3990(0.06)	= 239
Heat of combustion of kerogen, Btu/lb of kerogen		= 13,179
(High Heating Value)		

* Heat of combustion of hydrogen gas per pound. However, heat of combustion of combined hydrogen and hydrocarbons gives about the same figure.

APPENDIX C

APPENDIX C

Calculation of world fossil fuel carbon resource based on stoichiometric equivalence between oxygen and carbon

The principal overall oxygen-forming reaction according to geologists was:

$$CO_{2\ (gas)} \longrightarrow C_{(organic)} + O_{2\ (gas)}$$

Then the fossil carbon resource of the world is approximately:

$$\frac{144(14.7)\text{lb}}{\text{ft}^2} \left| \frac{\pi\ (8000)^2\ (5280)^2 \text{ft}^2}{} \right| \frac{0.23}{} \left| \frac{12}{32} \right| \frac{\text{ton}}{2000\ \text{lb}} \left| \frac{\text{trillion}}{10^{12}} \right.$$

= 511 trillion ton

An average barrel of crude oil is equivalent to 5 million Btu (69). The conversion factor between ton of fuel and barrel of crude oil is then equal to:

$$\frac{14{,}000\ \text{Btu}}{\text{lb carbon}} \left| \frac{2000\ \text{lb}}{\text{ton}} \right| \frac{\text{barrel of oil}}{510^6\ \text{Btu}} = 5.6$$

The equivalent barrels of petroleum is then equal to

511 5.6 = 2863 trillion barrels of petroleum

APPENDIX D

APPENDIX D

Synfuel status, 5-17-82

Workers line up to get their last paychecks at the Colony oil-shale project.

Oil-Shale Fiasco: The Death Knell For Synfuels?

Suddenly, one project after another is collapsing under economic and political pressure. Some experts doubt the industry can survive.

America's fledgling synthetic-fuels industry—once hailed as the harbinger of a new industrial era—is teetering on the brink of disaster.

Growing optimism over oil supplies, weak fuel prices, skyrocketing costs and a changing political environment are combining to kill off project after project in infancy.

The biggest setback came in early May when Exxon Corporation halted work on the nation's biggest synthetic-fuels development, the Colony oil-shale project near Grand Junction, Colo. Officials said they ordered the shutdown because estimated costs had zoomed to between 5 and 6 billion dollars, more than double the original projection.

Exxon's pullout forced its partner in the project, Tosco Corporation, to bail out at the same time despite the prospect of a 1.1-billion-dollar federal loan subsidy for its share.

The demise of the Colony project, says John H. Lichtblau, president of the Petroleum Industry Research Foundation, means that "synthetics have been indefinitely postponed, maybe never to get off the ground."

Collapse of the Colony program came on top of these recent synfuels reverses:

- Cancellation of WyCoalGas, Inc., a 2.7-billion-dollar coal-gasification project in Wyoming, by Panhandle Eastern Corporation.
- Cancellation of a 1.6-billion-dollar coal-liquefaction plant in West Virginia sponsored by Gulf Oil and the governments of West Germany and Japan.
- Postponement of the Cathedral Bluff oil-shale project in Colorado by Occidental Petroleum Company and Tenneco, Inc., a 3-billion-dollar deal.
- Delay of an Exxon project in Texas to convert lignite coal to gas.
- Delay in the Rio Blanco oil-shale project near Rifle, Colo., by Gulf Oil and Standard Oil Company (Indiana).
- Slowdown of a Colorado shale-oil development by Mobil Oil, Inc., and Standard Oil Company of California.

Other costly energy ventures also face an uncertain future. Example: A pipeline to transport Alaskan natural gas to the Lower 48 states has been delayed for two years because companies backing the project cannot raise 43 billion dollars needed to complete it.

Synfuel setbacks are not limited to the United States. In Canada, a group of oil firms withdrew from the Alsands project to manufacture oil from tar sands in Alberta, believed to be the world's largest synfuel endeavor. Exxon also has delayed development of heavy-oil deposits at Cold Lake in Alberta and a shale-oil project in Australia.

The rash of cancellations and delays is making a shambles of the Carter administration's plans to produce 2 million barrels of synthetic fuels daily by 1992 by spending 88 billion dollars in revenue from the "windfall profits" tax on oil companies.

That goal began fading with arrival of the Reagan administration, which wants private enterprise to set the pace of synfuel development. The U.S. Synthetic Fuels Corporation, created by Congress for the first round of synfuel plants. The corporation is requiring private firms to foot 40 percent of project costs, and Chairman Edward Noble indicates the final 68 billion will never be spent.

Some in Congress also are questioning the program's expense. Senator William Armstrong (R-Colo.) and Senator William Proxmire (D-Wis.) introduced legislation in early May to abolish the Synthetic Fuels Corporation and replace it with a more modest program without "sugar-daddy subsidies."

At the moment, only two major synfuel plants are under construction. Union Oil Company is working on a 2-billion-dollar oil-shale project in Colorado. Construction continues in North Dakota on the Great Plains coal-gasification plant, a 2.1-billion-dollar project to convert lignite to natural gas.

The Synthetic Fuels Corporation also is weighing loan or price guarantees for five other projects—a Kentucky plant to produce liquid oil from coal, costing 4.2 billion dollars; a 2-billion coal-to-gasoline plant in Wyoming; a Tennessee coal-gasification plant costing 830 million; a 350-million plan to convert peat to methanol in North Carolina, and a project to convert heavy oil in California to liquid fuels at a cost of 40 million.

International Coal Refining, a joint venture between Wheelabrator-Frye and Air Products Company, is planning a synfuel plant in Kentucky that would cost an estimated 3 billion dollars.

However, Exxon's unexpected decision to halt the Colony project has raised doubts about synfuel ventures across the board. Analysts say some proposed enterprises may never get rolling, even with government aid.

Observed Colorado Governor Richard Lamm: "If Exxon, the largest corporation in America, can't handle the overcost, how can smaller companies?"

Major loss. Lamm said cancellation of the Colony project will wipe out 10,000 jobs. Part of the project involved construction of Battlement Mesa, a planned community for 25,000 that now may become the most expensive ghost town in history. Exxon and Tosco had planned to spend 800 million dollars building houses, schools, churches, a golf course and a huge recreation center.

Despite all the gloomy news, some still insist that synthetic fuels will play an important role in the nation's energy future. Vowed Lamm: "When the next oil crisis arises—and it will arise—the day that happens, the oil-shale industry will be back on stage." □

By KENNETH R. SHEETS

APPENDIX E

APPENDIX E

Calculation of crack opening for best interwell communication in Antrim field tests

In August 1981 VanDerPloeg and others (108) reported an extraction trial conducted on "the two wells that had consistently exhibited the best interwell communication of all wells drilled at the Sanilac site." Measurements during the run included upstream and downstream pressure and air and gas flow rates. From these it is possible to estimate the size of the passage between the two wells depending on how the shape of the passage is visualized.

Table E-1 gives the results of calculations assuming (a) a complex passageway with a single bottleneck restriction for which an equivalent orifice diameter, D_o, is calculated, and (b) a uniform crack 40 ft high by 60 ft long for which a crack opening is calculated.

It is apparent from the table that a uniform crack opening of the minute dimension calculated is unlikely and that a larger opening with a restriction equivalent to a 0.14 to 0.48 cm orifice is more likely. The shape and location of the restriction can be visualized in many ways but it seems unlikely that it would provide good distribution of air flow over the entire area of the crack. Also the small calculated crack opening is evidence against distribution of flow through a network of cracks as in the model of Crowl and Piccirelli (18, 20).

The apparent enlarging of the passage by high downstream pressure was described as "gas propping" by VanDerPloeg but could also be

caused by driving water out of the formation when the hydrostatic pressure (580 psig) was reached. The closing of the passageway as the run progressed was attributed to thermal expansion of the rock with heating, but failure to correct for changes in gas viscosity and density at higher temperatures also accounts for much of the observed flow reduction.

Calculation of D_o in the table was made assuming a permanent pressure loss equivalent to 2 velocity heads in the restriction based on the downstream pressure and 68°F. This is equivalent to an orifice coefficient C_o of 0.7. The acoustic velocity limitation is accounted for by setting the downstream pressure equal to 0.5 times the upstream whenever it is less. The flow rate is taken as the arithmetic average of measured upstream and downstream scfm, and points are chosen for calculation only where upstream and downstream pressures have been constant for some time.

Calculations are made as follows:

$$144\ (P_1 - P_2) = \frac{2v^2\rho}{2g_c}$$

$$v = \frac{(w_1+w_2)\ \text{ft}^3\ 528^\circ\text{R}\ 14.7\ \text{psia}\ 4}{2\text{x}60\ \text{sec}\ 492^\circ\text{R}\ P_2\text{psia}\ \pi\ D_o^2\text{ft}^2} = .1674\ \frac{w_1 + w_2\ \text{ft}}{P_2 D_o^2\ \text{sec}}$$

$$\rho = \frac{29\ \text{lb}\ 492^\circ\text{R}\ P_2\ \text{psia}}{359\ \text{ft}^3\ 528^\circ\text{R}\ 14.7\ \text{psia}} = .00512P_2\ \frac{\text{lb}}{\text{ft}^3}$$

$$P_1 - P_2 = \frac{(.1674)\ (.1674)\ (.00512)\ (w_1+w_2)^2}{(32.16)(144)\ P_2 D_o^4} = 3.098\text{x}10^{-8}\ \frac{(w_1+w_2)^2}{P_2 D_o^4}\ \frac{\text{lb}}{\text{in}^2}$$

$$D_o = 0.0133\ \frac{(w_1+w_2)^{0.5}}{(P_1P_2 - P_2^2)^{0.25}}\ \text{ft}$$

Multiply by 12 and by 2.54 to get cm.

Flow through the crack opening is assumed laminar and then verified.

Denoting crack opening with D_c (5)

$$v = -\frac{D_c^2\, dP g_c}{12\,\mu\, dL}$$

$$v = -\frac{(w_1+w_2)\ ft^3\ 14.7\ psia\ 528^oR}{2x60\ \ sec\ \ P\ psia\ \ 492^oR\ 40\ D_c\ ft^2} = .00329\ \frac{w_1+w_2}{PD_c}\ \ \frac{ft}{sec}$$

$$v = -\frac{D_c^2 ft^2 \qquad ft\ sec\ \ 144\ in^2 32.16 ft\ dP\ psia}{12\ .018x.000672\ lb \qquad ft^2\ sec^2\ \ dL\ ft} = 31.9X10^6$$

$$\frac{D_c^2 dP}{dL}\ \ \frac{ft}{sec}$$

Also

$$D_c^3 P dP = -(w_1+w_2)\ \ 103x10^{-12}\ dL$$

$$D_c^3(P_1^2-P_2^2) = (w_1+w_2)\ 2x60x\ 103x10^{-12}$$

$$D_c^3 = 12.36x10^{-9}\ (w_1+w_2)/(P_1^2-P_2^2)$$

$$D_c = 0.00232\ \ [(w_1+w_2)/(P_1^2-P_2^2)]^{1/3}$$

Multiply by 12 and by 2.54 to get cm.

Table E-1

Passage size calculations from date on
Dow field test for best interwell communication

Hours after ignition	p_1 psia	p_2 psia	w_1 scfm	w_2 scfm	D_o cm	Crack opening cm
0	655	115	158	154	0.39	0.0064
0	675	415	156	146	0.39	0.0072
0	685	615	158	135	0.48	0.0104
28	920	420	150	120	0.31	0.0052
86	1095	705	160	100	0.28	0.0050
115	1115	705	145	100	0.27	0.0049
190	1125	705	130	80	0.25	0.0045
230	1165	755	95	50	0.21	0.0040
256	1175	745	40	30	0.14	0.0031

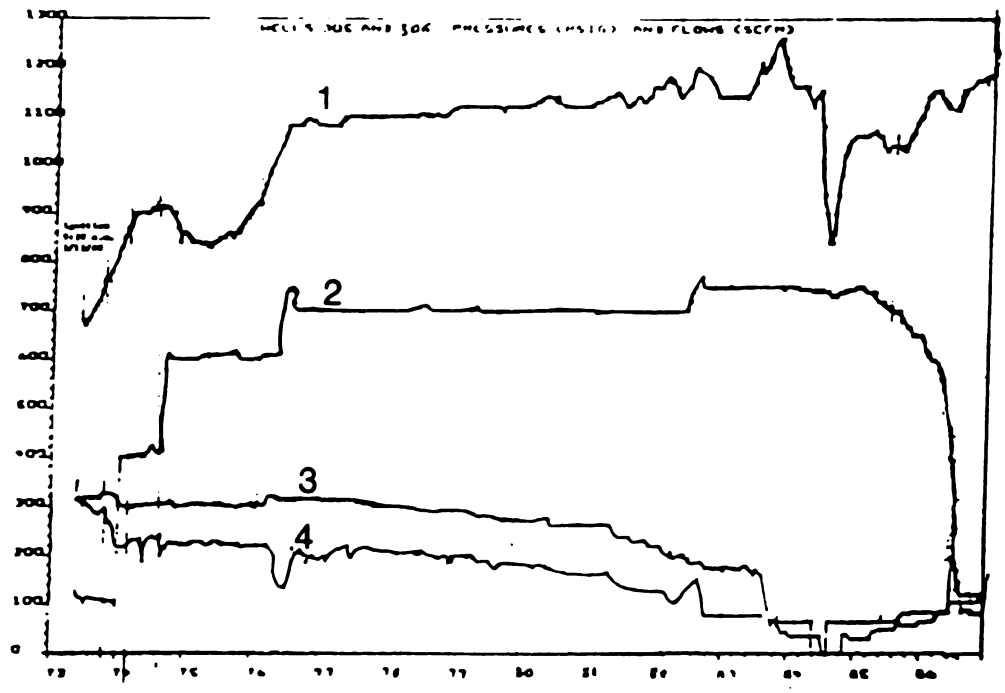

Figure E-1. Pressures and flow rates from Dow extraction trial of March, 1980 (108).

1 305 well pressure, psig
2 306 well pressure, psig
3 305 well injection air rate SCFM x 2
4 306 well injection air rate SCFM x 2

APPENDIX F

APPENDIX F

Jordanian oil shale survey

The following information on Jordanian shale is paraphrased from a book published by the Jordanian Natural Resources Authority (114). Outcrops of the oil shale of the Belqa Series occur in many regions of Jordan, especially in the Yarmouk River, Irbid area in the north, the Nabi Muse area between the Dead Sea and Jerusalem, and in the Central area around Qatrana.

Although the present oil shale investigations are limited to the El-Lajjun area of 24 sq. km. in Central Jordan, it is clear that Jordan has a major resource of fuel in oil shale. This fact is based upon the size of the El-Lajjun deposit where the oil shale occurs in the Chalk-Marl unit and the discovery of oil shale rocks in the underlying Phosphorite Unit while NRA (Natural Resources Authority) was conducting an exploration program for phosphate between Suwaqa and Jurf El-Darawish south of Amman, and occurrences of thick oil shale beds in other areas. About 788 million tons of oil shale were calculated as proved reserves at the El-Lajjun area, and more than 4 billion tons were estimated between Suwaqa and Jurl El-Darawish as indicated reserves.

The investigated area is easily accessible and lies on a hilly area, having an altitude ranging from 675 to 875 meters above sea level.

Oil shale rocks occur in the lower part of the Chalk-Marl unit. This unit covers most of the mapped area at El-Lajjun and attains a thickness of 60 meters. The lower part of this unit is composed of bituminous marl, dark to black in color, often containing a few gypsiferous bands. The deposit is considered to be of Maestrichtian-Danian Age and occurs in the form of elongated lenses.

Oil shale rocks or bituminous rocks are well known in Jordan since ancient times. Outcrops of the oil shales of the Belqa Series occur in many regions of Jordan.

Brownish-black bituminous marl and limestone were quarried near Jericho and have been used for a long time for manufacturing bowls, vases, decorative plates (Dead Sea stones), and were also used on small primitive fire places to produce quick lime.

A total of 53 boreholes were completed in the investigated area with approximately 500 meter distance between each two boreholes as follows:

(a) 38 boreholes came out with positive results.

(b) 9 boreholes were negative.

(c) There was no available data for the rest of the boreholes.

Core samples were collected from the srilled boreholes were send to the NRA laboratories and abroad for analysis, investigation and appraisal of the oil shale deposits in Jordan.

The study of the El-Lajjun deposit came out with the following results:

Proved Reserves	788 million tons
Average mining width	21 meters
Yield of oil shale ranges from 27 to 35 gals/ton	
Average sulphur content in retorted oil	9.8%
Carbon content	79%
Wax	8.9%
Heat of combustion	3650 Btu/lb

The high content of sulphur in the El-Lajjun oil shale and nitrogen content (about 7 wt%) indicate that the deposit does not appear very promising at the time being as an alternate source of liquid fuels, because the total capital cost of mining, crushing, retorting and upgrading prior to processing would be very high. But still there is a possibility of utilizing this deposit for the generation of electricity by direct combustion, for liquid gas products and for the production of sulphur.

Additional information on Jordanian shale was obtained from the Laramie Energy Center by special request from the writer. Fischer assay runs were made on Jordanian shale at the Center. El-Lajjun shale was found to have a richness of 33.2 gallon oil/ton of shale. In addition, Jordanian shale was found to have no tendency for coking.

APPENDIX G

APPENDIX G

Calculation of energy entering formation by oxygen transport compared with heat conduction.

The diffusion coefficient for O_2 gas through a 30 mwt N_2-CO_2 mixture can be estimated from the Chapman-Enskog formula (5).

This gives

$cD = 24.03 \times 10^{-6}$ g mol/cm sec or 5.8×10^{-3} lb mol/ft hr at 1750^{o}F

$cD = 17.28 \times 10^{-6}$ g mol/cm sec or 4.2×10^{-3} lb mol/ft hr at 900^{o}F

Applying Fick's law with an O_2 mol fraction of 0.1 in the cavity and a porosity of 0.2 assumes to be straight open pores.

$J = (0.2)(0.1)\ (5.8 \times 10^{-3})/x$ lb mol/ft^2 hr at 1750^{o}F

$J = (0.2)(0.1)\ (4.2 \times 10^{-3})/x$ lb mol/ft^2 hr at 900^{o}F

and since the heat of combustion is 168,000 Btu per pound mol of oxygen, the heat delivered to the formation at an average temperature between 900 and 1750^{o}F is

$q_o = 16.8/x$, while the heat delivered by thermal conduction

$q_c = (1750-900)(1)/x = 850/x$

Thus, if there are open pores to carry oxygen to the retorting front, the amount of heat transported by that mechanism is only 2% of that transported by thermal conduction. If instead the oxygen burns off residual coke to a front 1/4 of the distance to the retorting front, the energy so produced would be 4x2 or 8% of that brought in by conduction. Such a result would be consitent with the coke representing about 32% of the retorting energy as indicated in some of the experimental work.

However, the assumption of oxygen diffusing freely in straight open pores is not consistent with the appearance of the spent samples nor with the observed effect of overburden pressure in retarding

penetration of pure oxygen. It would seem then that oxygen diffusion has very little effect on carrying energy to the formation.

APPENDIX H

APPENDIX H

Approximation of the high heating value of gases evolved from the well

From Figure 2-5, at zero penetration each pound of shale retorted required 588 Btu of heat input and yields 412 Btu of net energy in the form of gas heating value. If the heat produced by combustion with one pound mol of oxygen is 168,000 Btu, then the 588 Btu represents

588x359/168,000	= 1.26 scf O_2 consumed
	= 1.26 scf CO_2 produced
(1.26)(79.1)/(20.9)	= 4.76 scf N_2
(1.26)(412)/(588)(2)*	= 0.44 scf combustible gas
	6.46 scf
Then, heating value = 412/6.83	= 63.78 Btu/scf at start of retorting
	= 0 Btu/scf at end of retorting

* assuming 1 mol combustible gas consumes 2 mols oxygen.

APPENDIX I

APPENDIX I

Calculation of the weight average temperature for retorting

(1) Based on data from retorting under overburden pressure (Table 4-10), the weight average retorting temperature is equal to:

$$\frac{572(0.96) + 752(0.6) + 932(3.17) + 1112(4.4)}{9.13}$$

$= 969^{o}F$ $(521^{o}C)$

A more accurate value of $932^{o}F$ $(500^{o}C)$ was obtained using the correlation equation of Figure 2-5.

(2) Based on data from retorting without overburden pressure (Table 4-7), the weight average retorting temperature is equal to:

$$\frac{572(1.49) + 752(1.81) + 932(4.64) + 1112(2.67)}{10.61}$$

$= 896^{o}F$ $(480^{o}C)$

APPENDIX J

APPENDIX J

Table of conversion factors: English, CGS, SI

QUANTITY	ENGLISH	CGS	SI
Length	1 ft = 12 inches	30.48 cm	0.3048 m
Volume	1 ft^3 = 7.481 gal = 0.178 bbl	28,320 cm^3	0.0283 m^3
Mass	1 lb_m	453.6 g	0.4536 kg
Temperature difference	1^oF	5/9 ^oC	5/9 ^oK
Temperature absolute	1^oR	5/9 ^oK	5/9 ^oK
Temperature	$^oF = {}^oR-459.58$	$^oC = {}^oK-273.15$	^oK
Density	1 lb_m/ft^3	0.01602 g/cm^3	16.02 kg/m^3
Force	1 lb_f	4.448×10^5 dyn	4.448 N
Pressure	1 psi	6.895×10^4 dyn/cm^2	6.895×10^3 N/m^2
Energy	1 Btu	252 cal	1.056×10^3 J
Power	1 Btu/s	252 cal/s	1.056×10^3 w
Thermal conductivity	1 Btu/hr ft ^oF	0.0041 cal/cm s ^oC	1.73 w/m ^oK
Heat capacity	1 Btu/lb_m ^oF	1 cal/g ^oC	4186 J/kg ^oK
Heat of combustion	1 Btu/lb_m	1.8 cal/g	2326 J/kg
Viscosity	$6.72\ 10^{-4}$ lb_m/ft s	CP	1.10^{-3} N s/m^2

NOTATION

A	Surface area, ft^2
a	Cavity radius, ft
B	Heat input per pound of shale retorted, Btu/lb_m shale
cD	Product of molar concentration and diffusion coefficient, mol/hr ft
c	Heat capacity, $Btu/lb_m {}^oF$
D	Diameter, ft
erf(x)	Error function, $\frac{2}{\sqrt{\pi}} \int_0^x e^{-t^2} dt$
f	Heat flux, $Btu/hr\ ft^2$
g_c	Gravitational conversion factor $lb_m ft/lb_f sec^2$
ΔH_c	Heat of combustion, Btu/lb_m
J	Molar flux of species A, $mol/hr\ ft^2$
Jo(u)	Bessel function of first kind and zero order
k	Thermal conductivity, $Btu/hr\ ft\ {}^oF$
P	Pressure, $lb_f/inch^2$
q_o	Heat delivered by combustion, $Btu/hr\ ft^2$
q_c	Heat delivered by conduction, $Btu/hr\ ft^2$
s	Dimensionless distance, r/a
s_R	Dimensionless retorting distance, r_R/a
r	Radius, ft
r_R	Penetration depth of retorting temperature, ft
Re	Reynolds number, dimensionless

T Temperature, ^{o}F

T_I Initial formation temperature, ^{o}F

T_S Cavity surface temperature, ^{o}F

T_R Retorting temperature, ^{o}F

t Time, hr

u Dummy variable used to evaluate the definite integral

v Velocity, ft/sec

x Distance, feet

x_R Retorting distance, ft

$Yo(u)$ Weber's Bessel function of second kind and zero order

w Gas flow rate, scfm

α Thermal diffusivity, $k/\rho c$, ft^2/hr

ρ Density, lb_m/ft^3

μ Viscosity, $lb_m/ft\ hr$

θ Dimensionless temperature, $\frac{T - T_I}{T_S - T_I}$

θ_R Dimensionless retorting temperature, $\frac{T_R - T_I}{T_S - T_I}$

τ Dimensionless time, $kt/\rho ca^2$

BIBLIOGRAPHY

1. Abubakr, S.; Cooper, C. In situ potentialities of Antrim oil shale. AIChE Summer National Meeting, Detroit, 1981.

2. Allred, V. D. Kinetics of oil shale pyrolysis. Chem. Eng. Prog. 1966, 62(8), 55-60.

3. Barnes, A. L.; Ellington, R. T. A look at in situ oil shale retorting methods based on limited heat transfer contact surface. Oil Shale Symp. Proc. 1968, 5, 827-852.

4. Berry, K. L. Conceptual design of combined in situ and surface retorting of oil shale. Oil Shale Symp. Proc. 1978, 11, 176-183.

5. Bird, R. B.; Stewart, W. E.; Lightfoot, E. N. Transport phenomena, John Wiley, New York, 1960.

6. Braun, R. L.; Chin, R. C. Computer model for in situ oil shale retorting; effect of gas introduced into the retort. Oil Shale Symp. Proc. 1977, 9, 166-179.

7. Burwell, E. L.; Tihen, S. S.; Sohns, H. W. Permeability changes and compaction of broken oil shale during retorting. U.S., Bur. Mines, Rep. Invest. 1979, RI7860.

8. Burwell, E. L.; Sterner, T. E.; Carpenter, H. C. In situ retorting of oil shale. U.S., Bur. Mines, Rep. Invest. 1973, RI7783

9. Campbell, J. H.; Koskinas, G. H.; Stout, N. D. Kinetics of oil generation from Colorado oil shale. Fuel 1978, 57(6), 372-6.

10. Campbell, J. H.; Raley, J. H.; Ackerman, F. J.; Sandholtz, W. A.; Libicki, S. B. Investigation of critical parameters in modified in situ retorting. Oil Shale Symp. Proc. 1980, 13, 73-86.

11. Campbell, J. H.; Koskinas, G. H.; Stout, N. D.; Coburn, T. T. Oil shale retorting: effects of particle size and heating rate on oil evolution and intraparticle oil degradation. In Situ 1978, 2(1), 1-47.

12. Campbell, J. H.; Koskinas, G. H.; Coburn, T. T.; Stout, N. D. Dynamics of oil generation and degradation during retorting of oil shale blocks and powders. Oil Shale Symp. Proc. 1977, 10, 148-165.

13. Campbell, J. H.; Peters, P.; Libicki, S. B.; Gregg, M. L. Analysis of the operation of Occidental's modified in situ Retort 6. Oil Shale Symp. Proc. 1981, 14, 99-117.

14. Carpenter, H. C. Fracturing oil shale for in situ retorting experiments. AIChE Symp. Ser. 1976, 72(155), 1-13.

15. Carpenter, H. C.; Burwell, E. L.; Sohns. H. W. An evaluation of an in situ retorting experiment in Green River oil shale. J. Petrol. Technol. 1972, 21-6.

16. Carpenter, H. C.; Sohns, H. W. Development of technology for in situ oil shale processes. Oil Shale Symp. Proc. 1974, 7, 143-170.

17. Carslaw, H. C.; Jaeger, J. C. Conduction of heat in solids, Oxford University Press, London, 1959.

18. Crowl, D. A.; Piccirelli, R. A. Application of computer models to the retorting of oil shale. Preliminary copy, private communication, 1979.

19. Crowl, D. A.; Hoenle, W. F. The stoichiometry of the pyrolysis of Michigan oil shale. Preliminary copy, private communication, 1979.

20. Crowl, D. A.; Piccirelli, R. A. Transport processes in pyrolysis of Antrim oil shale. Energy Comm. 1979, 5(6), 425-469.

21. Dockter, L. Combustion of oil shale carbon residue. AIChE Symp. Ser. 1976, 72(155), 24-31.

22. Dougan, P. M.; Dockter, L. BX in situ oil shale project. Oil Shale Symp. Proc. 1981, 14, 118-127.

23. Duncan, D. C.; Swanson, V. E. Organic rich shales of the United States and world land areas. U.S., Geol. Surv. Circ. 1965, 523.

24. Duvall, J. J. A laboratory study of true in situ combustion of oil shale using large blocks of oil shale. Oil Shale Symp. Proc. 1980, 13, 149-161.

25. Emerson Apparatus Company, The Emerson fuel calorimeters, operating manual. Melrose, Massachusetts, 1959.

26. Ertl, T. Mining Colorado oil shale. Oil Shale Symp. Proc. 1965, 2, 267-276.

27. Fausett, D. W.; George, J. H.; Carpenter, H. C. Second-order effects in the kinetics of oil shale pyrolysis. U.S., Bur. Mines, Rep. Invest. 1974, RI7889.

28. Fausett, D. W. A mathematical model of an oil shale retort. Oil Shale Symp. Proc. 1975, 8, 273-313.

29. Fiskebackskill, F. L. Method of electro-thermal production of shale oil. U.S., Patent 2,634,961, 1953.

30. Fox, J. P.; Jackson, D. E.; Sakaji, R. H. Potential use of spent shale in the treatment of oil shale retort water. Oil Shale Symp. Proc. 1980, 13, 311-320.

31. Grant, B. F. Retorting shale underground--problems and possibilities. Oil Shale Symp. Proc. 1964, 1, 39-46

32. Grossman, A. P. Economic evaluation of combined in situ and surface retorting of oil shale. Oil Shale Symp. Proc. 1977, 10, 9-15.

33. Harak, A. E.; Dockter, L.; Long, A.; Sohns, H. W. Oil shale retorting in a 150-ton batch-type pilot plant. U.S., Bur. Mines, Rep. Invest. 1974, RI7995.

34. Harak, A. E. Preliminary design and operation of a 150-ton oil shale retort. Oil Shale Symp. Proc. 1970, 6, 41-57.

35. Herman, I. L. Comparative analysis of nine selected oil shale properties. Oil Shale Symp. Proc. 1980, 13, 26-34.

36. Hill, G. R.; Dougan, P. The characteristics of a low temperature in situ shale oil. Oil Shale Symp. Proc. 1967, 4, 641-656.

37. Hite, R. J.; Dyni, J. R. Potential resources of Dawsonite and Nacholite in the Piceance Creek Basin. Oil Shale Symp. Proc. 1967, 4, 591-604.

38. Hockings, W. A. Physical properties of Michigan Antrim shale. U.S., Dept. Energy, 1980, FE-2346-85.

39. Hubbard, A. B.; Robinson, W. E. A thermal decomposition study of Colorado oil shale. U.S., Bur. Mines, Rep. Invest. 1950, RI4744.

40. Hull, W. Q.; Guthrie, B.; Sipprelle, M. Liquid fuel from oil shale. Ind. Eng. Chem. 1951, 43(1), 2-15.

41. Humphrey, J. P. Energy from in situ processing of Antrim oil shale. U.S., Dept. Energy, 1978, FE-2346-25.

42. Independent Petroleum Association of America, Oil producing industry in your state, 1981.

43. Jones, B. J.; Heistard, R. N. Recent Paraho operations. Oil Shale Symp. Proc. 1979, 12, 184-194.

44. Leedy, D. G.; Sandel, V. R.; Swartz, G. L.; Kenny, D. H.; Gulick, W. M.; El Khadem, H. S. Chemical composition of Antrim shale in the Michigan Basin. U.S., Dept. Energy, 1980, FE-2346-89.

45. Leffert, C. B.; Schroeder, R. R. Potential oil yield of the Antrim oil shale of the Michigan Basin. AIChE Summer National Meeting, Detroit, 1981.

46. Lekas, M. A. Progress report on the Geokinetic horizontal in situ retorting process. Oil Shale Symp. Proc. 1979, 12, 228-236.

47. Lekas, M. A. Economics of producing shale oil, the nuclear in situ retorting method. Oil Shale Symp. Proc. 1966, 3, 481-504.

48. Lekas, M. A.; Carpenter. H. C. Fracturing oil shale with nuclear explosives for in situ retorting. Oil Shale Symp. Proc. 1965, 2, 191-214.

49. Lesser, H. A.; Stone, H. L. Conduction heating of oil shale formations. Oil Shale Symp. Proc. 1967, 4, 677-688.

50. Lovell, P. F. Production of Utah shale oils by the Paraho and Union 'B' retorting processes. Oil Shale Symp. Proc. 1978, 11, 184-192.

51. Ludlam, L. L.; Natter, J. F. Perspective on modular demonstration of oil shale technology. Oil Shale Symp. Proc. 1977, 10, 16-22.

52. Mackenzie, R. C. The differential thermal investigation of clays, Mineralogical society, London, 1957.

53. Mallon, R. G.; Braun, R. L. Reactivity of oil shale carbonaceous residue with oxygen and carbon dioxide. Oil Shale Symp. Proc. 1976, 9, 309-334.

54. Marlatt, J. A.; Petty, C. A. A mathematical model for the pyrolysis of oil shale. AIChE Summer National Meeting, Detroit, 1981.

55. Marshall, P. W. The Colony development operation room-and-pillar oil shale mining. Oil Shale Symp. Proc. 1974, 7, 171-184.

56. Matzick, A.; Dannenberg, R. O. Development of the Bureau of Mines gas-combustion oil shale retorting process. U.S., Bur. Mines Bull. 1966, 635.

57. McCarthy, H. E.; Cha, C. Y.; Bartel, W. J. Development of the modified in situ oil shale process. AIChE Symp. Ser. 1976, 72(155), 14-23.

58. McKee, R. H.; Lyder, E. E. The thermal decomposition of oil shales, I. Ind. Eng. Chem. 1921, 13(7), 613-618.

59. McKee, R. H.; Lyder, E. E. The thermal decomposition of oil shales, II. Ind. Eng.Chem. 1921, 13(8), 678-684.

60. McNamara, P. H.; Humphrey, J. P. Hydrocarbons from Eastern oil shale. Chem. Eng. Prog. 1979, 75(9), 87-91.

61. McNamara, P. H.; Piel, C. A.; Washington, L. J. Characterization, fracturing and true in situ retorting in the Antrim shale of Michigan. Oil Shale Symp. Proc. 1979, 12, 353-365.

62. Mehta, P. K.; Persoff, P.; Fox, J. P. Hydraulic cement preparation from Lurgi spent shale. Oil Shale Symp. Proc. 1980, 13, 225-260.

63. Melton, N. M.; Cross, T. S. Fracturing oil shale with electricity. Oil Shale Symp. Proc. 1967, 4, 611-628.

64. Michigan Division of Oil and Gas Association, Oil and Gas News, January, 1982.

65. Miller, J. S.; Howell, W. D. Explosive fracturing tested in oil shale. Oil Shale Symp. Proc. 1967, 4, 629-640.

66. Miller, J. S.; Nicholls, H. R. Methods and evaluation of explosive fracturing in oil shale. U.S., Bur. Mines, Rep. Invest. 1973, RI7729.

67. Miller, R.; Dubow, J.; Fun-Den, W. Mechanical and thermal properties of oil shale at elevated temperatures. Oil Shale Symp. Proc. 1978, 11, 135-146.

68. Musser, W. N. The physical properties and chemical composition of Antrim oil shale. Dow Chem. 1976, FR-310.

69. Nelson, W. L. Petroleum refining engineering, McGraw-Hill, New York, 1958.

70. Perry, R. H.; Chilton, C. H. Chemical engineers' handbook, fifth edition, McGraw-Hill, New York, 1973.

71. Pforzheimer, H. Paraho--new prospects for oil shale. Chem. Eng. Prog. 1974, 70(9), 62-5.

72. Pforzheimer, H. The Paraho oil shale demonstration--a 1975 progress report. AIChE Symp. Ser. 1976, 72(155), 44-5.

73. Piel, C. A.; Humphrey, J. P. Fracturing of the Antrim of Michigan. Oil Shale Symp. Proc. 1978, 11, 227-241.

74. Raley, J. H.; Sandholtz, W. A.; Ackerman, F. G. Results from simulated, modified in situ retorting in pilot retorts. Oil Shale Symp. Proc. 1978, 11, 331-342.

75. Ricketts, T. E. Occidental's Retort 6 rubblizing and rock fragmentation. Oil Shale Symp. Proc. 1980, 13, 46-61.

76. Ridley, R. D. In situ processing of oil shale. Oil Shale Symp. Proc. 1974, 7, 21-24.

77. Ridley, R. D. Progress in Occidental's shale oil activities. Oil Shale Symp. Proc. 1978, 11, 169-175.

78. Robb, W. A.; Smith, J. W. Mineral and organic relationships through Colorado's Green River formation across its Saline depositional center. Oil Shale Symp. Proc. 1977, 10, 136-147.

79. Robinson, W. E.; Lawler, D. L.; Cummins, J. J.; Fester, J. I. Oxidation of Colorado oil shale. U.S., Bur. Mines, Rep. Invest. 1963, RI6166.

80. Robinson, W. E.; Cook, G. L. Compositional variations of the organic material of Green River oil shale. U.S., Bur. Mines, Rep. Invest. 1971, RI7492.

81. Rothman, A. J. Research and development on rubble in situ extraction of oil shale at LLL. Oil Shale Symp. Proc. 1975, 8, 159-178.

82. Ruark, J. R.; Sohns, H. W.; Carpenter, H. C. Gas combustion retorting of oil shale under Anvil Point lease agreement, stage I. U.S., Bur. Mines, Rep. Invest. 1969, RI7303.

83. Ruotsala, A. P. Mineralogy of Antrim shale, Michigan. U.S., Dept. Energy, 1980, FE-2346-79.

84. Sarapuu, E. Underground electrocarbonization of oil shale. Oil Shale Symp. Proc. 1965, 2, 377-384.

85. Schmalfield, P. The use of the Lurgi-Ruhrgas process for the distillation of oil shale. Oil Shale Symp. Proc. 1975, 8, 129-146.

86. Schramm, L. W. Shale oil. Mineral Facts and Problems. U.S., Bur. Mines Bull. 1975, 667, 963-88.

87. Shin, M. S.; Hong, Y. S. A mathematical model for the retorting of a large block of oil shale. Fuel 1978, 57(6), 622-630.

88. Sladek, T. A.; Poulton, P. L.; Davis, W. E.; Robinson, P. A. A technology assessment of oil shale development. Oil Shale Symp. Proc. 1980, 13, 1-25.

89. Smith, J. W. Theoretical relationship between density and yield for oil shale. U.S., Bur. Mines, Rep. Invest. 1970, RI7248.

90. Smith, J. W.; Robb, W. A.; Young, N. B. High temperature reactions of oil shale minerals and their benefit to oil shale processing in place. Oil Shale Symp. Proc. 1978, 11, 100-113.

91. Snyder, G. B.; Pownall, J. R. Union Oil Company's Long Ridge experimental shale oil project. Oil Shale Symp. Proc. 1978, 11, 158-168.

92. Sohn, H. Y.; Braun, R. L. Simultaneous fluid-solid reactions in porous solid: part 1. Reaction between one solid and two fluid reactants. Lawrence Livermore Laboratory, preprint UCRL-81066.

93. Sohns, H. W.; Carpenter, H. C. In situ shale retorting. Chem. Eng. Prog. 1966, 62(8), 75-8.

94. Speers, G. X. El-Lajjun oil shale deposit in Jordan, 1969, British Petroleum. EPR/R 7005.

95. Stanfield, K. E.; Frost, I. C. Method of assaying oil shale by a modified Fischer retort. U.S., Bur. Mines, Rep. Invest. 1949, RI3977.

96. Stone, R. B. Preliminay mining economics for modified in situ process. Oil Shale Symp. Proc. 1977, 10, 1-9.

97. Stout, N. D.; Koskinas, G. H.; Raley, J. H.; Santor, S. D.; Opika, R. L.; Rothman, A. J. Pyrolysis of oil shale: effect of thermal history on oil yield. Oil Shale Symp. Proc. 1976, 9, 153-172.

98. Swartz, G., as reported by L. J. Washington, Jr. U.S., Dept. Energy, 1979, FE-2346-49.

99. Thomas, G. W. A simplified model of conduction heating in systems of limited permeability. J. Petro. Eng. 1964, 231, 335-344.

100. Thomas, G. W. Some effects of overburden pressure on oil shale during underground retorting. J. Petrol. Eng. 1966, 237, 1-8.

101. Thomas, H. E.; Carpenter, H. C.; Sterner, T. E. Hydraulic fracturing of Wyoming Green River oil shale. U.S., Bur. Mines, Rep. Invest. 1972, RI7596.

102. Tisot, P. R. Structural response of propped fractures in Green River oil shale as it relates to underground retorting. U.S., Bur. Mines, Rep. Invest. 1975, RI8021.

103. Tisot, P. R.; Sohns, H. W. Structural deformation of Green River oil shale as it relates to in situ retorting. U.S., Bur. Mines, Rep. Invest. 1971, RI7576.

104. Tisot, P. R.; Murphy, W. R. Physical structure of Green River oil shale from Colorado. U.S., Bur. Mines, Rep. Invest. 1963, RI6184.

105. Tomkuo, M. C.; Park, W. C. Inorganic leaching of spent shale from modified in situ processing. Oil Shale Symp. Proc. 1979, 12, 81-93.

106. Tyner, C. E.; Hommert, P. J. Numerical modeling of a true in situ oil shale retort. U.S., Dept. Energy, Sandia Laboratories, SAND-78-1306.

107. U.S., Dept. Energy, Monthly Energy Review, April, 1982, 87-8.

108. VanDerPloeg, M. L.; Lund, M. M.; Murdick, D. A.; Frost, J. R.; Kinkel, C. G.; Pihlaja, R. K. Energy from true in situ processing of Antrim shale--extraction trials in an explosively fractured site. AIChE Summer National Meeting, Detroit, 1981.

109. Wen, C. Y.; Wang, S. C. Thermal diffusional effects on non-catalytic solid gas reaction. Ind. Eng. Chem. 1970, 62(8), 30-51.

110. Yen, T. F.; Chilingarian, G. V. Oil Shale, Elsevier Scientific Publishing Company, New York, 1976.

111. Young, C.; Harak,A. E.; Trent, B. C.; Maxwell, D. E.; Watson, J. D. Spent shale compaction for void volume generation in in situ oil shale processing. Oil Shale Symp. Proc. 1978, 11, 282-291.

112. Young, D. C. An investigation of the feasibility of recovering energy from Antrim oil shale by in situ processing: a final summary report. U.S., Dept. Energy, 1980, FE-2346-94.

113. Jaeger, J. C. Numerical values for the temperature in radial heat flow. J. Math. Phys. 1956, 34, 316-21.

114. Omary, K. El-Lajjun oil shale deposit. Jordan Natural Resources Authority, 1979.

115. Grissom, M. C. Oil shale and tar sand: a bibliography. U.S., Dept. Energy, 1981, DOE/TIC-3367.

116. Utter, S. Advanced mining technology of oil shale. Oil Shale Symp. Proc. 1976, 9, 177-197.

117. Kaiser, F. J.; Maass, R. H. Commercialization of oil shale. Engineering Symp. 1981, Exxon Research and Engineering Company.